AER/AGS Open File Report 2018-03

Geochronology of Selected Igneous Rocks in the Alberta Rocky Mountains, with an Overview of the Age Constraints on the Host Formations

AER/AGS Open File Report 2018-03

Geochronology of Selected Igneous Rocks in the Alberta Rocky Mountains, with an Overview of the Age Constraints on the Host Formations

D.I. Pană[1], A.S. Rukhlov[2], L.M. Heaman[3] and M. Hamilton[4]

[1] Alberta Energy Regulator / Alberta Geological Survey
[2] Formerly Alberta Energy Regulator / Alberta Geological Survey
(see page ii for current address)
[3] University of Alberta
[4] University of Toronto

March 2018

ISBN 978-1-4601-2690-5

If you use information from this publication in other publications or presentations, please acknowledge the AER/AGS. We recommend the following reference format:

Pană, D.I., Rukhlov, A.S., Heaman, L.M. and Hamilton, M. (2018): Geochronology of selected igneous rocks in the Alberta Rocky Mountains, with an overview of the age constraints on the host formations; Alberta Energy Regulator, AER/AGS Open File Report 2018-03, 60 p.

Publications in this series have undergone only limited review and are released essentially as submitted by the author.

Author addresses:
A.S. Rukhlov
British Columbia Geological Survey
Ministry of Energy and Mines
1810 Blanshard Street,
Victoria, BC V8W 9N3
Canada
250.952.0396
Email: Alexei.Rukhlov@gov.bc.ca

L.M. Heaman
Department of Earth & Atmospheric Sciences
University of Alberta
Edmonton, AB T6G 2E3
Canada
780.492.3265
Email: larry.heaman@ualberta.ca

M. Hamilton
Department of Earth Sciences
University of Toronto
22 Russell Street
Toronto, ON M5S 3B1
Canada
416.946.7424
Email: mahamilton@es.utoronto.ca

Published March 2018 by:
Alberta Energy Regulator
Alberta Geological Survey
4th Floor, Twin Atria Building
4999 – 98th Avenue
Edmonton, AB T6B 2X3
Canada

Tel: 780.638.4491
Fax: 780.422.1459
Email: AGS-Info@aer.ca
Website: www.ags.aer.ca

Contents

Acknowledgements vi
Abstract vii
1 Introduction 1
2 Regional Geology 1
2.1 Tectonics 1
2.2 Tectonostratigraphic Assemblages 3
3 Previous Geochronological Constraints on Igneous Rocks of the Alberta Rocky Mountains and Foothills 5
3.1 Mafic Sills and Lava Flows in the Mesoproterozoic Purcell Supergroup 5
3.1.1 Age of the Belt-Purcell Supergroup 8
3.1.2 Belt-Purcell Supergroup Metamorphism 9
3.1.3 Previous Radiogenic Dating of Mafic Sills Intruding the Belt-Purcell Supergroup 9
3.2 Isolated Dikes and Sills in the Miette Group 11
3.2.1 Age of the Miette Group 11
3.2.2 Miette Group Metamorphism 13
3.2.3 Geikie Dike 13
3.2.4 Crowfoot Dike 13
3.2.5 Blackbear Sill 15
3.3 Cretaceous Alkaline Intrusions 16
3.4 Crowsnest Formation 19
3.4.1 Crowsnest Formation Metamorphism 20
4 Sampling and Analytical Techniques 21
4.1 Mafic Sills and Lava Flows in the Mesoproterozoic Purcell Supergroup, Clark Range 21
4.2 Isolated Dikes and Sills in the Miette Group 23
4.3 Cretaceous Felsic Alkaline Sills and Dikes 23
4.4 Crowsnest Formation 24
4.4.1 Analytical technique 24
5 Results and Geological Significance 25
5.1 Mafic Sills and Lava Flows in the Mesoproterozoic Purcell Supergroup, Clark Range 25
5.1.1 Baddeleyite Age of Mafic Sill 25
5.1.2 SHRIMP Dating of Zircon from Purcell Mafic Sills 25
5.1.3 Preliminary Results of the $^{40}Ar/^{39}Ar$ Dating of the Purcell Mafic Rocks 34
5.1.4 Possible Sources for Inherited Zircon in the Purcell Mafic Sills 37
5.2 Isolated Dikes and Sills in the Miette Group 39
5.3 Cretaceous Sills 40
5.3.1 U-Pb Dating of the Largest Felsic Alkaline Sill in Clark Range 40
5.3.2 $^{40}Ar/^{39}Ar$ Dating of the Crowsnest Lake Trachyte (DP11-26) 41
5.4 Age of Melanite Garnet from the Crowsnest Formation 45
5.5 Contemporaneous and Petrologically Similar Intrusive and Volcanic Rocks in the Southern Canadian Rockies 45
6 Discussion and Conclusions 46
7 References 49

Tables

Table 1. Samples of Purcell mafic sills processed for isotope dating 22
Table 2. Samples of diabase intruded into the Miette Group 23

Table 3. Samples of Cretaceous alkaline sills and dikes processed for mineral separation at the University of Alberta 24
Table 4. U-Pb baddeleyite ID-TIMS data for dolerite sills from the Purcell basin, Clark Range 26
Table 5. Summary of sensitive high-resolution ion microprobe (SHRIMP) data for Purcell mafic sills 28
Table 6. Summary of $^{40}Ar/^{39}Ar$ from mafic rocks in the Purcell Supergroup 35
Table 7. Summary of $^{40}Ar/^{39}Ar$ data from the Crowfoot dike 40
Table 8. Summary of U-Pb data from the titanite trachyte sill DP11-36 at Crowsnest Lake 43
Table 9. Summary of $^{40}Ar/^{39}Ar$ from the Crowsnest Lake trachyte sill 44
Table 10. U-Pb Garnet Results for Crowsnest Volcanics, Alberta 45

Figures

Figure 1. Regional geology of the southern Alberta Rocky Mountains, showing the location of examined igneous rocks 2
Figure 2. Generalized stratigraphic cross-section of the westward-thickening succession in the Western Canada Sedimentary Basin 4
Figure 3. Exposures of mafic rocks in the Belt-Purcell Supergroup in the Clark Range 6
Figure 4. Generalized distribution and stratigraphic correlations of the Belt-Purcell Supergroup 7
Figure 5. Location of the sampled intrusive rocks in the Miette Group 12
Figure 6. Isolated intrusions in the Miette Group 14
Figure 7. Locations of samples collected from Cretaceous alkaline intrusions during this study 17
Figure 8. Outcrops of alkaline intrusions in the southern portion of the Alberta Rocky Mountains 18
Figure 9. a) Representative image of highest quality baddeleyite crystals separated from sample DP11-18 and selected for analysis. b) Concordia diagram showing results for the baddeleyite analyses 27
Figure 10. Cathodoluminescence images of zircon crystals analyzed by sensitive high-resolution ion microprobe from sample AR9-1 29
Figure 11. Cathodoluminescence images of zircon crystals analyzed by sensitive high-resolution ion microprobe from sample AR9-2 30
Figure 12. Cathodoluminescence images of zircon crystals analyzed by sensitive high-resolution ion microprobe from sample AR9-3 31
Figure 13. Cathodoluminescence images of zircon crystals analyzed by sensitive high-resolution ion microprobe from sample AR9-4 32
Figure 14. a) Concordia diagram with all sensitive high-resolution ion microprobe (SHRIMP) analyses on zircon grains from Purcell sills. b) Concordia diagram for the overgrowth rims of zircon grains in sample AR9-2. c) Frequency histogram with all SHRIMP zircon ages from Purcell sills 33
Figure 15. $^{40}Ar/^{39}Ar$ spectra and K/Ca ratios for the samples collected from the Purcell Lava and Yarrow Creek sill 36
Figure 16. $^{40}Ar/^{39}Ar$ data for the Crowfoot dike 40
Figure 17. a) Cathodoluminescence image of zircon grains from the large Cretaceous sill analyzed by laser ablation. b) Tera-Wasserburg plot of zircon overgrowth analyses. c) Weighted average $^{206}Pb/^{238}Pb$ date. d) Probability density plots of the old grains and cores give some sense of the range of inheritance 42
Figure 18. $^{40}Ar/^{39}Ar$ spectrum for the Crowsnest Lake trachyte sill 44

Acknowledgements

We thank P. Smith for the $^{40}Ar/^{39}Ar$ analytical work at the Jack Satterly Geochronology Laboratory (University of Toronto) and our amazing pilot 'Stan' of Bighorn Helicopters in Blairmore for his unreserved support with sample collection in the Clark Range of southern Alberta Rockies. We are grateful to M. Grobe for reading and editing an initial version of this manuscript, and to B. Davie for carefully editing the final version.

Abstract

The Alberta Rocky Mountains expose over 1.4 billion years of stratigraphy from the Mesoproterozoic Purcell Supergroup to Cenozoic strata of the Paskapoo Formation, and encompass a huge area approximately 700 km in length and 50–120 km wide. Occurrences of igneous rocks in the Alberta Rocky Mountains are very limited (except for its southernmost portion, the Clark Range) and their ages poorly constrained. This report presents preliminary results of the first attempt at systematic sampling and dating of igneous rocks cropping out in the Alberta Rocky Mountains and Foothills: from the southern Alberta Rockies, we have sampled selected Purcell mafic sills, felsic alkaline sills, and the Crowsnest alkaline volcanic suite. In addition, we have sampled the three known occurrences of small, isolated, hypabyssal mafic rocks in the northern and central Alberta Rocky Mountains.

The Yarrow Creek mafic sill that intruded along the contact of the Appekunny Formation with the Grinnell Formation of the Purcell Supergroup in the Clark Range yielded a precise baddeleyite crystallization age of 1436.2 ±1.1 Ma. This age, interpreted to represent the emplacement age of the sill, is in the age range of the mafic sills (ca. 1468–1433 Ma) dated elsewhere in the Belt-Purcell basin, outside Alberta. This precise age constrains the deposition of the entire lower Belt-Purcell Supergroup and Appekunny Formation to predate 1436 Ma. The Yarrow Creek sill also yielded a well-defined $^{40}Ar/^{39}Ar$ hornblende plateau age of ca. 700 Ma, which suggests a tectonothermal or hot-fluid migration event during the rifting of the Rodinia Supercontinent that led to the formation of the western Laurentian margin.

The largest trachyte sill that intruded Purcell strata in the Clark Range yielded a zircon overgrowth age of 105.8 ±4.7 Ma, measured by laser-ablation multicollector inductively coupled plasma–mass spectrometry (LA-MC-ICP-MS) from oscillatory zoning rims; a population of titanite from the same sample yielded a U-Pb age of 102.4 ±0.5 Ma, which is interpreted as the most likely emplacement age of the sill. This age is identical with the 102.4 ±1 Ma plateau age of K-feldspar from a megacrystic syenite of the Howell Creek suite, some 45 km to the southwest in British Columbia, and strongly suggests that the ‘Cretaceous’ alkaline swarm in the southern Alberta Rockies is the eastern manifestation of the same alkaline igneous event. A U-Pb age of 102.9 ±1.1 Ma, obtained from the melanite garnet of Crowsnest volcanic rocks, ties the Crowsnest suite to the swarm of alkaline sills in the Clark Range (which includes at least one melanite-analcime phonolite sill) and, further, to the Howell Creek intrusive suite.

Another trachyte sill, which intrudes Paleozoic carbonates near Crowsnest Lake, yielded a $^{40}Ar/^{39}Ar$ plateau age of 69.1 ±0.7 Ma. Because this sill is in a splay of the Lewis Thrust, only about 300 m below the main thrust, and the nearby Crowsnest volcanic rocks have been shown to have experienced low-temperature metamorphism and Na-metasomatism, we tentatively interpret this as the age of maximum burial and albitization of a sill from the same mid-Cretaceous alkaline swarm dated in the Clark Range.

Two dikes and one sill intruding the Miette Group are variably deformed and have not returned minerals that are datable by the U-Pb zircon method. A whole-rock $^{40}Ar/^{39}Ar$ plateau age of ca. 3.87 Ga, obtained from one of the dikes, is anomalously old. These minor and isolated mafic rocks remain a challenge for future geochronological work.

1 Introduction

The genesis of the Cordilleran foreland fold-and-thrust belt is an intrinsic part of the geological history of the western margin of North America, in particular of the Cordilleran tectonics and deposition processes in the Western Canada Sedimentary Basin (WCSB). The Proterozoic and Phanerozoic sedimentary rocks of the WCSB, which overlie crystalline Precambrian basement of the stable interior of the North American continent, extend westwards into the eastern Cordillera, where they were deformed from at least the Late Jurassic to the Eocene to form the Foreland Belt, a stack of thin-skinned, east-verging thrust slices.

The Cordilleran tectonics in the orogenic hinterland are relatively well constrained by stratigraphic and structural relationships, and petrological and geochronological studies of metamorphic and igneous rocks. In contrast, the tectonic evolution the Rocky Mountain fold-and-thrust belt at the eastern margin of the Cordillera is largely derived from stratigraphic and structural studies. Geochronological work is limited to a few provenance studies (Ross et al., 1992; Leier and Gehrels, 2011) and radiometric dating of major thrusts (van der Pluijm et al., 2006; Pană and van der Pluijm, 2015), but none of the igneous occurrences in Alberta have been precisely dated.

Datable igneous rocks are important time markers for deciphering the geological history of the Cordilleran foreland system; volcanic rocks help constrain the age of stratigraphic successions, whereas intrusive rocks provide minimum and maximum ages for the crosscut and the overlying strata, respectively.

This report, derived from work on the *Geological Map of the Alberta Rocky Mountains and Foothills* (Pană and Elgr, 2013), presents preliminary results of the first attempt to systematically sample and date the four categories of igneous rocks, cropping out in the Alberta Rocky Mountains and Foothills, with poorly constrained or unknown ages (Figure 1):

1) undeformed mafic sills in the Mesoproterozoic Purcell Supergroup of the Clark Range, southern Alberta Rocky Mountains;
2) variably deformed and altered mafic dikes intruding the Neoproterozoic Miette Group, central Alberta Rocky Mountains;
3) alkaline sills and dikes intruding various stratigraphic units in the southern Rocky Mountains; and
4) the Crowsnest volcanic suite in the southern Alberta Foothills.

The fine grain size, profound alteration (chloritized, carbonatized), and general mineralogy of most mafic rocks sampled in the Alberta Rocky Mountains and Foothills are not very amenable to U-Pb geochronology. In spite of careful selection of the material in outcrop and the application of multiple radiometric-dating techniques, including sensitive high-resolution ion microprobe (SHRIMP) U-Pb zircon, isotope dilution–thermal ionization mass spectrometry (ID-TIMS), and whole-rock $^{40}Ar/^{39}Ar$, only some rocks could be precisely dated. More effort is required to date other rocks that, for now, proved unsuitable for isotope dating. Throughout the report, samples are identified by their field-site number and by the laboratory identification number, to enable comparison with the original analytical data reported by different laboratories.

2 Regional Geology

2.1 Tectonics

The Cordilleran margin of North America was established by Late Proterozoic breakup and dispersal of the Neoproterozoic supercontinent Rodinia due to the formation of a mantle superswell (or superplume) beneath Rodinia (e.g., Li et al., 2008). Glacial diamictite and associated, ca. 750 Ma volcanic rocks at the

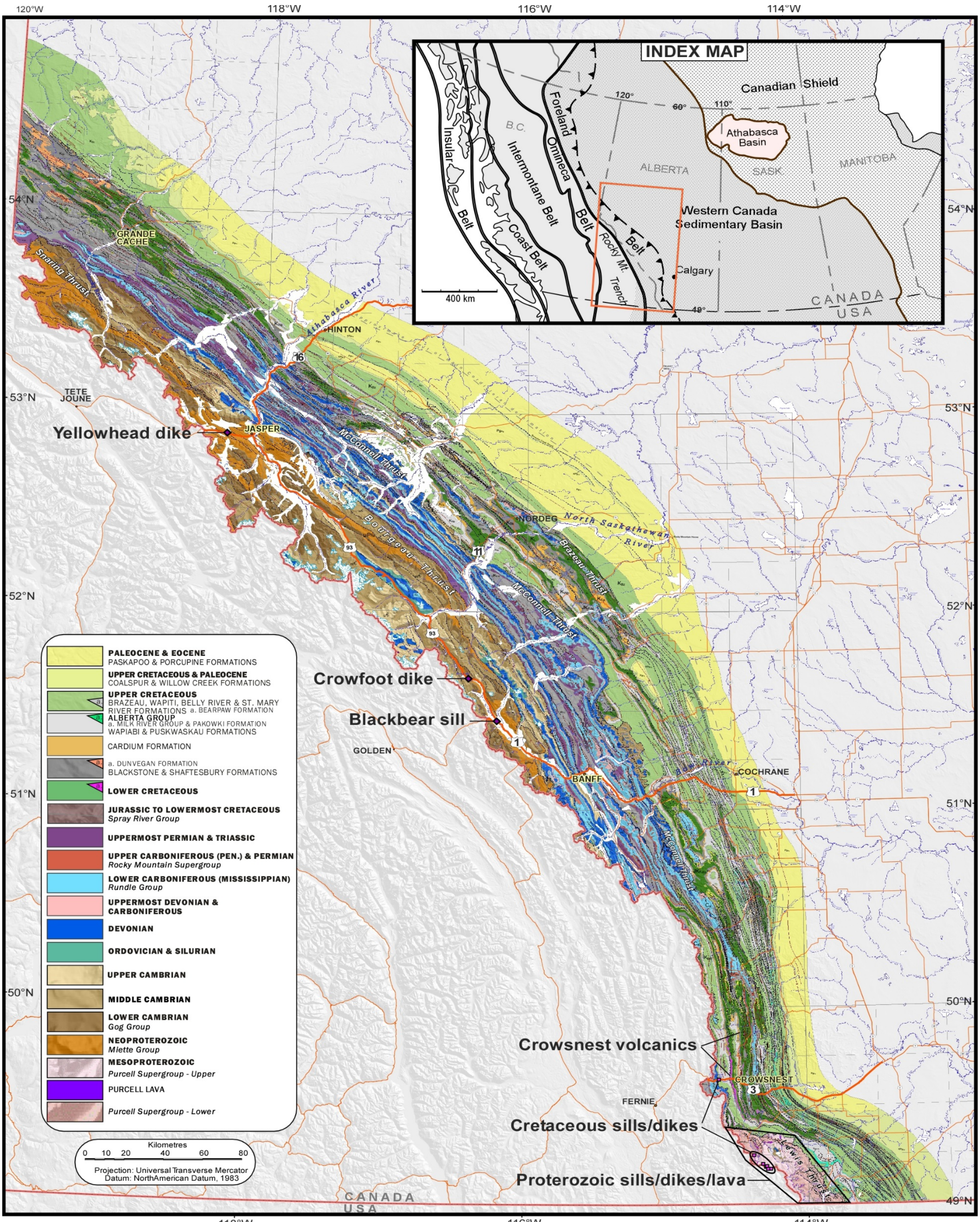

Figure 1. Regional geology of the southern Alberta Rocky Mountains, showing the location of examined igneous rocks (after Pană and Elgr, 2013). For a complete legend see Pana and Elgr (2013).

base of the Windermere Supergroup (which includes the Miette Group) and correlative strata have been interpreted as the initial rift-related deposits of the Cordilleran miogeocline (Gabrielse and Campbell, 1992; Ross et al., 1995; McMechan, 2015). The onset of the hallmark Cordilleran passive-margin subsidence (miogeocline deposition), and therefore the transition from rifting to seafloor-spreading and continental drift, must have begun in the earliest Cambrian (thick, carbonate-dominated, Cambro-Ordovician passive margin succession) or latest Neoproterozoic time.

From Late Proterozoic until Early Jurassic time, the western continent-ocean boundary was largely a passive margin. Farther west in the accreted or suspect Cordilleran terranes, episodes of Paleozoic through Middle Jurassic plate convergence and consumption are evidenced by the development of successive fore- and retro-arc basins, coeval Mesozoic to Cenozoic batholith belts, accretion of oceanic island arcs, and subduction complexes. These events, however, did not markedly affect ancestral North American rocks in Canada.

Events leading to Cordilleran mountain building started in Early Jurassic time (ca. 180 Ma) as a result of the breakup of Pangea and drifting of the North American plate towards subduction zones outboard of its western margin (e.g., Monger et al., 1982; Monger, 1984, 1989; Gabrielse et al., 1992; Monger and Price, 2002). The structural record shows that, between the Early Jurassic and early Eocene, the Cordilleran realm was mainly under compression, accompanied at different times by sinistral and dextral transpression; this was succeeded by dextral transtension and extension during the Eocene (Monger and Price, 2002; Evenchick et al., 2007).

2.2 Tectonostratigraphic Assemblages

The Canadian Rocky Mountain fold-and-thrust belt formed within an easterly-tapering wedge of Upper and locally Middle Proterozoic to Lower Cenozoic sedimentary rocks that form the continental margin (platform, terrace, and ‘miogeocline’) and the foreland basin wedges of the WCSB. A profound unconformity separates the sedimentary cover from the normal thickness or attenuated Proterozoic and older crystalline crust of ancestral North America (Figure 2).

All rocks deposited along the ancestral North American margin are referred to as the ‘continental margin prism’; the term ‘miogeocline’ refers only to those rocks that accumulated during the Neoproterozoic (Windermere Supergroup) and early Paleozoic and are now exposed in the Rocky Mountain fold-and-thrust belt (e.g., Neoproterozoic Miette Group, Cambrian Gog Group), and chronostratigraphic equivalents found now in the Omineca belt (e.g., the Neoproterozoic Horsethief Group the Cambrian Hamill Group, and middle Cambrian to Ordovician Lardeau Group; Thompson et al., 2006).

Deposition was in extensional settings with predominantly cratonic sources until latest Middle Jurassic time, when the region became a foreland basin and received sediments from the rising orogen to the west. Late Jurassic to early Eocene deformation resulted in an enormous stack of east-vergent, downward-younging thrust slices. In general, rocks exposed at surface decrease in age from west to east: Proterozoic strata, locally overprinted by low-grade metamorphism, dominate in western parts of the belt, unmetamorphosed Paleozoic strata in the central and eastern parts, and Mesozoic to Cenozoic rocks in the frontal parts (Price, 1981, 1994; Monger, 1989).

The detached and displaced supracrustal rocks comprise several broad tectonostratigraphic assemblages deposited in distinct tectonic settings:

1) **Pre-Rodinian rift sedimentation:** At intervals along the length of the Canadian Cordillera, thick sedimentary successions were deposited locally within Rodinian intracontinental rift basins, which were later transected by the Neoproterozoic Cordilleran rift trend. In southern Canada, these are represented by the Mesoproterozoic Belt-Purcell Supergroup (1.47–1.40 Ga) that spans the Canada–

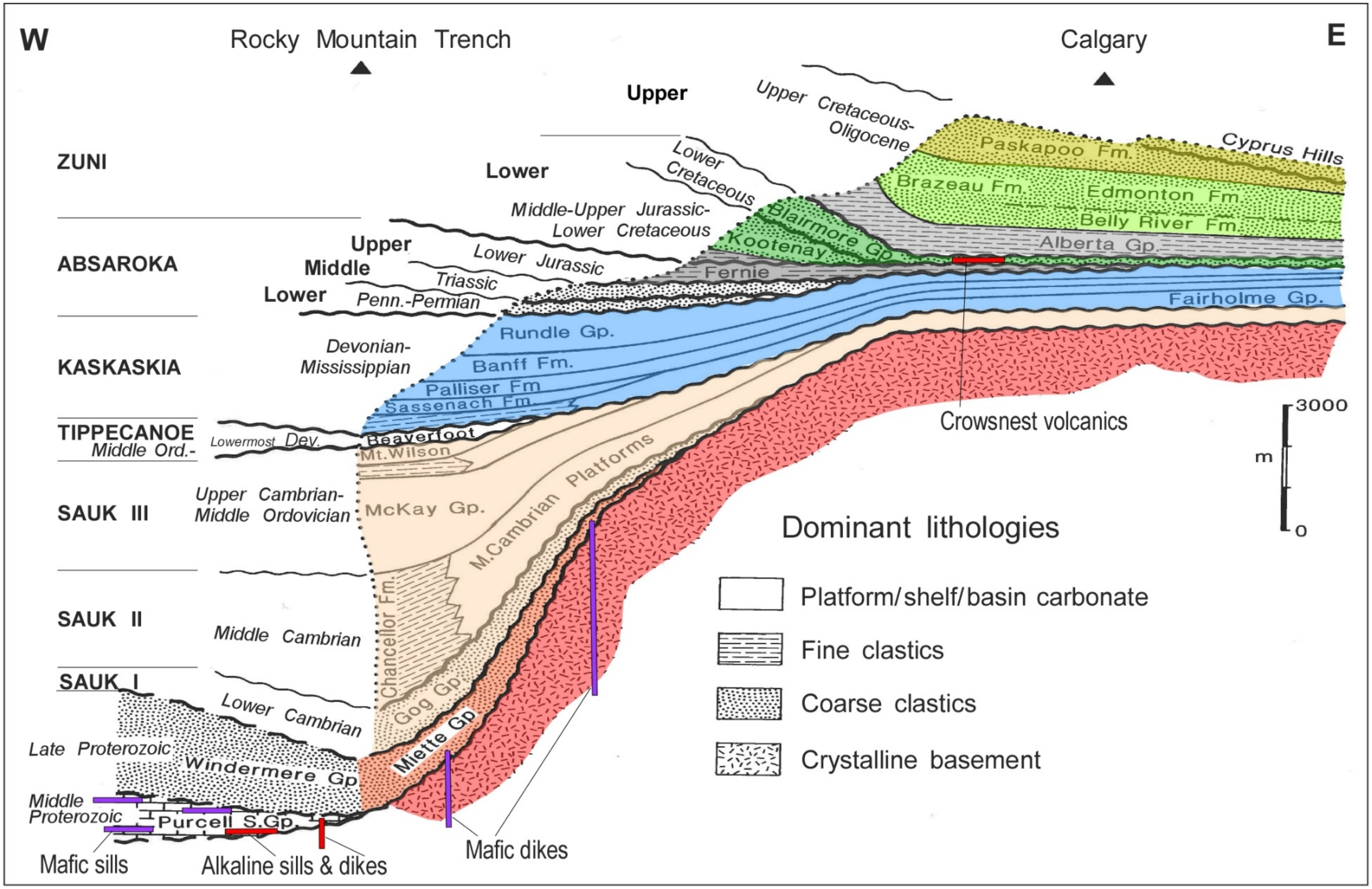

Figure 2. Generalized stratigraphic cross-section of the westward-thickening succession in the Western Canada Sedimentary Basin, with the four categories of igneous rocks, epicontinental-basin (pre-Zuni) and foreland-basin (Zuni) tectonostratigraphic sequences, their bounding unconformities, and lithostratigraphic units (after Price et al., 1985).

United States border (Evans et al., 2000; Sears, 2001; Ross and Villeneuve, 2003; Dickinson, 2004; Lydon, 2007) and encompasses the Clark Range in the southern Alberta Rockies.

2) **Initial rifted-margin sedimentation:** The upper Neoproterozoic (750–600 Ma) Windermere assemblage, consisting of deeper water, fine- and coarse-grained clastic rocks, locally with subordinate carbonate, accumulated to thicknesses of a few kilometres (locally >5 km) in a rift basin that truncated but partly overlapped the Belt-Purcell basin. The eastern margin of the Windermere basin (the proto-Pacific ocean basin) matches most of the eventual early Paleozoic rift-margin configuration of the western margin of Laurentia. The Miette Group, exposed in the Main and Western ranges of the Rocky Mountains, is the only representative of this stage in Alberta (e.g., Arnott and Hein, 1986; Ross et al., 1989; McMechan, 2015).

3) **The continental-terrace wedge:** The lower Paleozoic (uppermost Precambrian?) to Middle Jurassic (600–180 Ma) Cordilleran assemblages formed a westward-prograding, continental-margin terrace wedge (approximately 10–15 km combined maximum thickness), which marked the interface between the lower Paleozoic Laurentia craton and the adjacent proto-Pacific ocean basin. It was deposited mainly above and outboard of the Windermere assemblage but was locally deposited inboard of the Windermere assemblage and over part of the Belt-Purcell assemblage. It is made up of several tectonostratigraphic packages:
   - The lower Paleozoic sequence, consisting predominantly of resistant platform and shelf-carbonate buildups with subordinate shale that pass laterally into finer grained, deeper water facies
   - Middle and upper Paleozoic platform and shelf carbonate rocks and subordinate clastic rocks, which pass laterally into deeper water facies
   - Triassic to Middle Jurassic shale, siltstone, sandstone and carbonate units

4) **The foreland-basin wedge:** The foreland-basin wedge consists of the Upper Jurassic to Eocene Cordilleran foreland-basin assemblage, which overlies the cratonic platform assemblage. The foreland-basin wedge accumulated in front of the northeastward-prograding accretionary wedge as the continental lithosphere subsided isostatically under the weight of the advancing wedge; the wedge was partly incorporated in, and cannibalized by, the encroaching fold-and-thrust belt (e.g., Price, 1973; Beaumont, 1981, McMechan and Thompson, 1989, 1992).

3 Previous Geochronological Constraints on Igneous Rocks of the Alberta Rocky Mountains and Foothills

3.1 Mafic Sills and Lava Flows in the Mesoproterozoic Purcell Supergroup

Mafic sills and a massive lava flow in the Mesoproterozoic Purcell Supergroup, exposed in the Lewis thrust sheet of the Clark Range just north of the Canada–United States border (Figure 1), are the oldest igneous rocks in the Alberta portion of the Rocky Mountains (Figure 3). The tectonic setting of the Belt-Purcell basin has been controversial: rift basin (Höy, 1992; Evans et al., 2000; Lydon, 2007; Sears, 2007), intracratonic lake basin (Winston, 1986), continental-margin delta (Price, 1964; McMechan, 1981; Cressman, 1989), impact basin (Sears and Alt, 1989), trapped ocean basin (Hoffman, 1988), and, finally, extensional basin with a tectonically active western side (Figure 3a; Ross and Villeneuve, 2003). The Belt-Purcell basin is located immediately east of the so-called 'initial strontium line' ($^{87}Sr/^{86}Sr$ [Sri] = 0.706), interpreted to mark the western edge of Laurentia (Figure 4b; Armstrong, 1988). On the basis of paleocurrents, bulk stratigraphic patterns, and Sm-Nd whole-rock geochemistry, dominantly western and southwestern source areas have been proposed for the American portion of the Belt-Purcell basin (Harrison et al., 1974; Winston, 1986; Frost and Winston, 1987; Cressman, 1989). However, the area of this former source region is now underlain by Phanerozoic terranes accreted during the Mesozoic

Figure 3. Exposures of mafic rocks in the Belt-Purcell Supergroup in the Clark Range (see Figure 1): a) approximately 150 m high cliff of Purcell Lava on the east side of Barnaby Ridge; b) pillow basalt at the base of the Purcell Lava, south end of Barnaby Ridge (sample DP11-14); c) diabase sill on Rainy Ridge; d) Yarrow Creek biotite-olivine trachybasalt with typical feldspar star texture (sample DP11-28bt). Exact locations are given in Table 1.

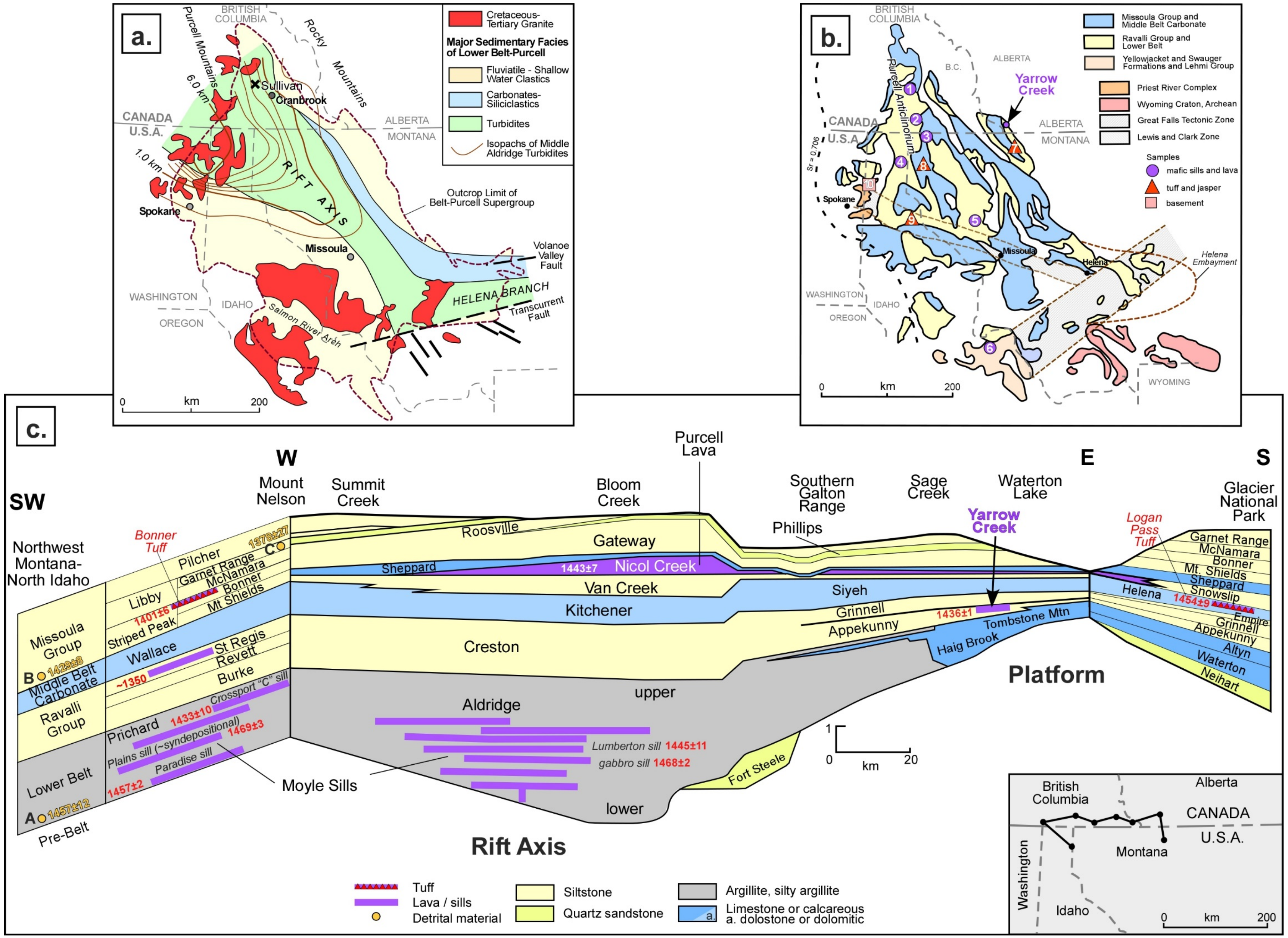

Figure 4. Generalized distribution and stratigraphic correlations of the Belt-Purcell Supergroup: a) facies distribution in the Belt-Purcell basin (after Lydon, 2007); b) distribution of precisely dated sills, lava flows, and tuffs: 1, ca. 1468 ±2 Ma (Anderson and Davies, 1995); 2, ca. 1445 ±11 Ma (Höy, 1989); 3, ca. 1443 ±7 Ma (Evans et al., 2000); 4, 1433 ±10 Ma (Zartman et al., 1982); 5, ca. 1469 ± 2.5Ma and ca. 1457 ±2 Ma (Sears et al., 1998); 6, ca. 1379 ±1 Ma (Doughty and Chamberlain, 1996); 7, ca. 1401 ±6 Ma (Evans et al., 2000); 8, ca. 1454 ±9 Ma (Evans et al., 2000); 9, ca. 1350 Ma (Zartman and Smith, 1995); 10, ca. 1576 ±7 Ma (Evans and Fischer, 1986); c) generalized cross-section in the Belt-Purcell basin with approximate stratigraphic position of precisely dated sills, lava flows, tuffs and detrital material: A, ca. 1452 ±12 Ma detrital zircon; B, ca. 1429 ±8 Ma cobble of feldspar porphyry; C, 1378 ±27 Ma detrital zircon (compiled from Zartman et al., 1982; Evans et al., 2000; Ross and Villeneuve, 2003).

(Burchfiel et al., 1992), so the former source area that fed the Belt basin has been removed, displaced, or otherwise obscured by younger tectonic processes. Dating of detrital minerals (zircon, monazite, xenotime, and muscovite) yielded ages that are widespread in basement blocks of central and eastern Australia, which was interpreted to indicate that, prior to the Neoproterozoic formation of the Panthalassa Ocean, those blocks were joined to the western side of Laurentia, adjacent and with a former fluvial connection to the Belt-Purcell basin (Ross et al., 1992; Ross and Villeneuve, 2003).

The Belt-Purcell Supergroup has been divided into four large groups: Lower Belt, Ravalli Group, Middle Belt Carbonate, and Missoula Group (e.g., Ross and Villeneuve, 2003). Mafic sills were emplaced at all stratigraphic levels and a massive lava flow forms a regional marker (Purcell Lava; Figure 4c). The mafic layers form prominent seismic reflectors within the turbiditic Prichard and Aldridge formations across 5100 km^2 of the Purcell anticlinorium from west-central Montana to British Columbia (Harris 1985; Harrison et al., 1992; van der Velden and Cook, 1994, 1996; Cook and van der Velden, 1995).

3.1.1 Age of the Belt-Purcell Supergroup

As expected, the age of the very thick (15–20 km) Middle Proterozoic Belt-Purcell stratigraphic sequence is poorly constrained paleontologically. Metamorphism has severely degraded the quality of organic remains in the Belt Supergroup in Montana (Walter et al., 1976; Kidder and Awramik, 1990). Carbonaceous algal compressions and acritarchs in the Belt Supergroup do not yet have temporal significance (Walter et al., 1976, 1990; Kidder and Awramik, 1990). *Horodyskia* string-of-beads fossils of uncertain affiliation were found in laminated shales in the lower part of the Appekunny argillite, between very shallow water carbonates with stromatolites of the Altyn and Helena formations (Figure 4c; Retallack et al., 2013). *Horodyskia* is early Mesoproterozoic (Calymmian, 1600–1400 Ma; Gradstein et al., 2012), as suspected from stromatolite biozones of *Collenia* in the Altyn limestone and *Collenia* and *Conophyton* in the Helena Formation (“Siyeh Limestone” of Fenton and Fenton, 1937; Rezak, 1957; Ross, 1959). Assuming uniform sediment accumulation, Retallack et al. (2013) deduced a model age of about 1480 Ma for the *Horodyskia* horizons from correlations with radiometrically dated stratigraphic units in Glacier National Park, Montana.

The age of the Belt-Purcell Supergoup is more precisely constrained by SHRIMP U-Pb zircon ages of volcanic rocks (Evans et al., 2000) from the northern United States (Figure 4b and c):

- ca. 1401 ±6 Ma, tuff in the thin transition zone between the uppermost Bonner Quartzite and the Libby Formation
- ca. 1443 ±7 Ma, porphyritic rhyolite to quartz latite flow within the Purcell Lava in the Snowslip and Shepard formations in the Yaak River region
- ca. 1454 ±9 Ma, tuff in the upper Helena Formation, Glacier National Park, Montana

Detrital zircon grains from the Prichard Formation, dated at 1452 ±12 Ma and 1490 ±17 Ma, are essentially syndepositional, providing a constraint on the maximum age of sedimentation at 1452 ±12 Ma (Ross and Villeneuve, 2003). This is the first stratigraphic level in the Belt-Purcell basin that contains detrital-zircon grains with ages comparable to associated magmatic rocks (Figure 4; see Section 3.1.3). These authors also reported concordant to near-concordant SHRIMP zircon data with weighted-average $^{207}Pb/^{206}Pb$ ages of 1429 ±8 Ma and 1445 ±8 Ma ages on two cobbles of feldspar porphyry from a coarse-grained conglomerate at the base of the Missoula Group (correlative with the Sheppard Formation in Alberta). These ages are comparable to the U-Pb zircon ages of 1443 ±7 Ma for rhyolite in the Purcell Lava obtained by Evans et al. (2000), and are consistent with a local intrabasinal origin for the cobbles.

In the upper part of the Belt-Purcell Supergroup, the Garnet Range Formation (Figure 4c) includes zircon grains with ages between 1436 and 1378 Ma; the youngest grain gave an age of 1378 ±27 Ma (Ross and Villeneuve, 2003). However, sedimentological features (detrital muscovite along bedding planes and the presence of hummocky cross-stratification) uncharacteristic of the Purcell Supergroup have led to the suggestion that the Garnet Range Formation and the overlying Pilcher Formation may not be part of the Belt-Purcell basin (Smith and Barnes, 1966).

Ross and Villeneuve (2003) suggested a ca. 1.47–1.40 Ga time interval for deposition of the 15–20 km thick Belt-Purcell Supergroup.

3.1.2 Belt-Purcell Supergroup Metamorphism

Much of the Belt-Purcell Supergroup is at low metamorphic grade and has undergone limited internal deformation, except for regions in the southern and westernmost parts of the basin. As a result of Mesozoic orogenic activity, virtually the entire basin has been shortened (to various degrees) along thrust faults and high-angle reverse faults (Price and Sears, 2001). In Alberta, strata of the Purcell Supergroup do not appear to be metamorphosed. Nonetheless, alteration of the interlayered igneous rocks suggests very low grade burial metamorphism: 1) geochemical data from the Purcell Lava, which otherwise would have fallen within the field of Purcell sills, are shifted due to chloritization (lower Cs-Pb-Sr-LREE-MREE, coupled with K-Rb-Ba spikes; Goble et al., 1993); and 2) the Rainy Ridge phonolite has altered analcime and pseudomorphs of muscovite on feldspar (Goble et al., 1993).

In Montana, the Appekunny argillite is overprinted by very low grade greenschist-facies metamorphism with fracture cleavage, chlorite, and illitized clay (González-Álvarez and Kerrich, 2012). This metamorphism was inferred to be mainly Grenvillian (ca. 1000 Ma), regional, static thermal metamorphism judging from Grenville-age events reported from various parts of the Belt-Purcell Supergroup (e.g., Anderson and Davis, 1995; Anderson and Parrish, 2000; Aleinikoff et al., 2007; Doughty and Chamberlain, 2008).

In the region of higher grade metamorphism, garnet-bearing rocks from the Belt-Purcell Supergroup or its basement at different localities in northern Idaho yielded diverse Lu-Hf garnet ages (1463 ±24 Ma, 1379 ±8 Ma, and 1151 ±41 Ma) and provide evidence of polymetamorphism. The ca. 1360–1330 Ma titanite ages obtained by Ross et al. (1992) from the Moyie sills were interpreted as metamorphic ages by Schandl et al. (1993) and Anderson and Davis (1995). A suite of younger mafic rocks (and associated augen gneiss) that intrude only up to the level of the Middle Belt Carbonate has been dated at 1370 Ma (Ross and Villeneuve, 2003). These intrusions are associated with local metamorphism and deformation, postdate the 1400 Ma Libby tuff, and are thus considered to postdate Belt-Purcell sedimentation (McMechan and Price, 1982; McFarlane and Pattison, 2000). Alternatively they may represent an episode of renewed rifting (Sears et al., 1998). Cretaceous age event(s) have been also inferred, based on Sr isotopes (Fleck et al., 2002), stable isotopes (Eaton et al., 1995), field relationships (White, 1998, 2000), and U-Pb dates of zircon from jasperoid veins at the Sunshine Mine (Zartman and Smith, 1995, 2009).

3.1.3 Previous Radiogenic Dating of Mafic Sills Intruding the Belt-Purcell Supergroup

Initial K-Ar and $^{40}Ar/^{39}Ar$ ages of the Belt-Purcell Supergroup were imprecise and somewhat misleading, as they grouped in the Neoproterozoic. Thus, Hunt (1961, 1962) obtained K-Ar ages of 1075–1100 Ma for a Siyeh sill (basaltic ‘flow’ on Blakiston Brook at Logan Pass, Glacier National Park, Montana) and the Purcell Lava. Mudge et al. (1968) obtained a K-Ar age of 750 Ma from rocks similar to the Siyeh sills found south of Glacier National Park, Montana. Ghazi (1992) reported K-Ar ages of 796–797 Ma for hornblende from the Siyeh sills and minimum K-Ar and $^{40}Ar/^{39}Ar$ ages of approximately 1000 Ma for the Grinnell dikes on Spionkop Ridge, Alberta. Biotite from the Appekunny sill on Spionkop Ridge yielded K-Ar ages of 1453 Ma (Goble, 1977) and 1500 Ma (Ghazi, 1992), and a $^{40}Ar/^{39}Ar$ age of 1400 Ma (Ghazi, 1992).

These ages, corroborated by field relationships and mineralogical and geochemical differences, were considered by Goble et al. (1999) to be consistent with the emplacement of two older basaltic intrusions.

Although not comagmatic, these intrusions may have shared a common source as a result of repeated rifting in the area, and a younger tholeiitic suite unrelated to either of the two older suites. They are

- a 1500–1400 Ma suite of 'Appekunny-type' glomeroporphyritic alkaline sills and dikes; this suite may be equivalent to the Purcell (ca. 1413 Ma) and Sheppard lavas, which were somewhat fractionated or contaminated during emplacement.

  These rocks from Clark Range appear to be quasicontemporaneous with the Moyie sills, found approximately 125 km to the northwest in the Purcell Mountains and Kootenay Range of British Columbia (Hunt, 1961; Hoy, 1989). The geochemical characteristics are somewhat different: the basaltic rocks in the Clark Range are, with some exceptions, alkaline to transitional and have trace-element concentrations more characteristic of continental basalts, whereas the Moyie sills are alkaline to tholeiitic and show concentrations of elements such as Ti, Zr, and Y that are characteristic of both ocean-floor and continental basalts (Goble et al., 1999).
- a 1000 Ma (minimum age) suite of amygdaloidal, transitional or mildly alkaline, 'Grinnell-type' dikes with TiO_2, Al_2O_3, P_2O_5, and Yb contents of approximately 2.5%, 16%, 0.47%, and 3.3 ppm, respectively.
- an 800 Ma suite of diabasic, tholeiitic, 'Siyeh-type' sills.

The inferred ages for these presumably mafic magmatic suites are similar to those of mafic magmatic events known both within and outside the Belt basin in the United States (hence the age grouping was believed to be more plausible), at approximately 1455–1430 Ma, 1130–1070 Ma, and 760–740 Ma (Wooden et al., 1978).

Precise geochronological ages of mafic sills intruding the Belt-Purcell Supergroup (Figure 4b and c) exist only for occurrences outside Alberta and include U-Pb zircon (ID-TIMS) ages of

- ca. 1433 ±10 Ma for the Crossport 'C' sill in the middle of the Prichard Formation, northern Idaho (Zartman et al., 1982);
- ca. 1445 ±11 Ma for the Lumberton sill, emplaced in the Aldridge Formation in the Kimberley-Cranbrook area, British Columbia (Höy, 1989);
- ca. 1468 ±2 Ma for the syndepositional basaltic Moyie sills that intrude the lower Aldridge Formation in British Columbia, just below the Sullivan horizon (Anderson and Davis, 1995); and
- ca. 1468.8 ±2.5 Ma for medium-grained biotite granophyre 90 m below the top of the Plains sill and ca. 1456.8 ±2.5 Ma for coarse-grained hornblende quartz diorite collected near the centre of the Paradise sill, which intrudes the Prichard Formation in the lower Belt Supergroup in western Montana (Sears et al., 1998).

Ross et al. (1992) reported seven $^{207}Pb/^{206}Pb$ zircon ages for a Moyie sill granophyre from southeastern British Columbia, ranging from ca. 1457 to 1425 Ma, with analytical errors between 2.6 and 7.2 Ma (which overlap with the range of the precisely dated sills), and another age of ca. 1709 ±3.2 Ma. However, these authors preferred an emplacement age of ca. 1350 ±25 Ma, based on five titanite ages that cluster between 1360 and 1330 Ma, and the lower intercept of 1375 +17/–23 Ma for the zircon analyses. This age was probably preferred because it matched the emplacement of granitic plutons in the lower Belt Supergroup of Idaho and British Columbia (see below).

Höy (1989) showed that some of the mafic sills in the Aldridge Formation had intruded wet sediments at shallow depths and hence were almost syndepositional. Sears et al. (1998) suggested that the 'syndepositional' Plains sill dates a rifting episode at 1469 ±3 Ma. Their proposed scenario includes tectonic collapse of the basin that may have generated much of the slump folding, boudinage, and mud diapirism observed in the turbiditic Prichard Formation, which was presumably followed by magma release as a large sill along the rift axis, crosscutting the disrupted beds and boiling water-saturated sediment at some locations. Continued subsidence sheared the sill as it cooled. This important tectonic event may have led to the creation of the world-class Sullivan orebody, and made accommodation space for a large part of the overlying Belt-Purcell Supergroup (Sears et al., 1998).

Chamberlain and Doughty (1993) and Doughty and Chamberlain (1996) reported a ca. 1370 Ma zircon age from intrusions in the Yellowjacket Formation in central Idaho, which was tentatively correlated with part of the Belt Supergroup (Link, 1993) and then assigned to an important period of bimodal magmatism and rifting (Lewis, 1996). Sears et al. (1998) suggested that the ca. 1370 Ma event represents an episode of renewed rifting.

3.2 Isolated Dikes and Sills in the Miette Group

Three isolated occurrences of mafic rocks are known in the Neoproterozoic Miette Group of Alberta (Figure 5):

- a small 'diabase' cropping out beside the old, now totally overgrown, Yellowhead Trail on the north side of the Miette River was described by Charlesworth et al. (1967); for convenience, this igneous occurrence will be called the 'Geikie dike' after the nearby Geikie siding on the CN Rail track (Figure 5a)
- the Crowfoot dike, an approximately 15 m thick massive dike in the roadcut along Highway 93, just southeast of Bow Lake (Figure 5b)
- a highly altered, 0.4–1 m thick sill in the railroad cut just north of the intersection of Highways 1 and 93. Our examination of the outcrop was somewhat delayed by a close encounter with a black bear; hence, this sill will be referred to as 'the Blackbear sill' (Figure 5c).

3.2.1 Age of the Miette Group

There are no strong age constrains for the Miette Group. The Miette Group is part of the Upper Proterozoic Windermere Supergroup, which in the southern Canadian Cordillera unconformably overlies the Middle Proterozoic Purcell Supergroup in the central Purcell and southern Selkirk mountains, and nonconformably overlies the Deserters gneiss (728 + 8/–7 Ma; Evenchick et al., 1984) in the Deserters Range and the Malton and associated gneisses (ca. 2.0 Ga) south of Valemount, British Columbia (B.C.; Murphy, 1990). The Windermere Supergroup was deposited sometime within a 210–230 m.y. interval bracketed by the age of the basal Windermere Supergroup (770–730 Ma; Evenchick et al., 1984; Devlin et al., 1988) and the overlying Lower Cambrian Gog Group (540 Ma). The top of the Windermere is generally eroded and, in parts of the southern Rocky Mountains, approximately 2–3 km of strata are bevelled beneath the sub–Lower Cambrian unconformity (Aitken, 1969; Simony and Aitken, 1990). In the Jasper area, an unconformity-bounded coarse clastic unit, the Jasper Formation, occurs between typical Miette and typical Lower Cambrian lithotypes. It consists of crossbedded, feldspathic to arkosic sandstones and conglomerates with minor argillites and siltstones, and is considered Late Proterozoic to Early Cambrian in age (Charlesworth et al., 1967), or latest Proterozoic, older than the widespread, locally feldspathic sandstones at the base of the Gog Group (Hein and McMechan, 1994).

The Miette Group contains Late Neoproterozoic (Ediacaran) limestones near Jasper (Byng Formation; Hofmann et al., 1985). Correlative units of the Miette Group in the Cariboo Mountains (upper Isaac Formation) contain medusoid forms resembling the Ediacaran fossils (Ferguson and Simony, 1991). Farther north in the Mackenzie and Wernecke mountains, the topmost 2.5 km of the Windermere Supergroup section contains simple trace fossils and Ediacaran megafossils (Narbonne and Hofmann, 1987).

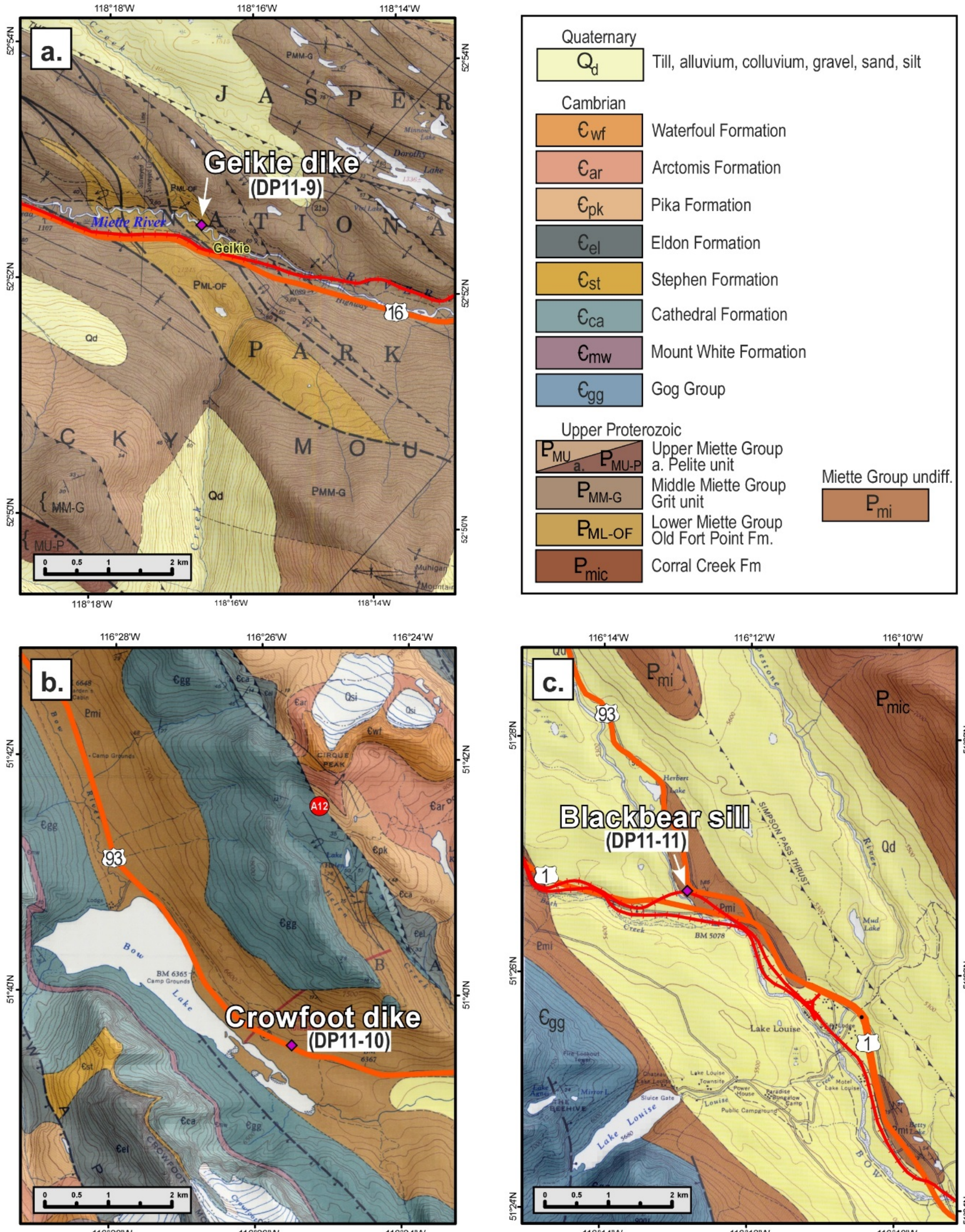

Figure 5. Location of the sampled intrusive rocks in the Miette Group: a) Geikie dike on the north side of Highway 16 (geological base from Mountjoy and Price, 1985); b) Crowfoot dike on the east side of Highway 93; note that the dike trace on the map (geological base from Price and Mountjoy, 1978) is misplaced by about 650 m to the northwest; A12 is the gouge sample collected from the Simpson Pass thrust that yielded an illite $^{40}Ar/^{39}Ar$ age of ca. 162 Ma (Pană and van der Pluijm, 2015); and c) Blackbear sill north of the intersection of Highways 1 and 93 (geological base from Price et al., 1980). Exact locations are given in Table 2.

The youngest detrital zircons in a sample from the upper part of the Miette Group near Jasper, Alberta, are late Paleoproterozoic in age (ca. 1.75 Ga; Pană and Hay, work in progress), so they cannot be used to constrain the minimum age of the Miette Group.

3.2.2 Miette Group Metamorphism

Miette strata are tightly folded, and the folds are associated with various types of axial-plane cleavage. The apparently unfolded nature of the axial surfaces indicates that the folding took place during a single deformation phase; minor departure from parallelism of the axial surface and cleavage in local structures likely reflects a slight variation in the orientation of the stress system with time (Charlesworth et al., 1967). The association of cleavage with metamorphic muscovite and chlorite, particularly in fine-grained rocks where the cleavage surfaces are coated with muscovite and chlorite, indicate deformation under the quartz-albite-chlorite-muscovite subfacies of the greenschist metamorphic facies (Charlesworth et al., 1967). These authors also inferred that the absence of K- and Ca-feldspar, coupled with the abundance of albite, calcite, and white mica, is evidence for the metamorphic alteration of detrital feldspar in the lower part of the sequence at approximately 300°C and 3 kb; this indicates that, for a normal geothermal gradient of 35°C/km, at least this part of the sequence was buried at a depth of approximately 8 km.

The folds and cleavages appear to die out stratigraphically upwards because folds in the unconformably overlying Gog Group are much more open and widely spaced. This would suggest that the intense deformation of the Miette Group strata predates the Early Cambrian deposition of the Gog Group. However, based on whole-rock and muscovite K-Ar dates in the region between Jasper and west of Mount Robson, Charlesworth et al. (1967) inferred a Late Cretaceous tectonometamorphic event propagating from the west. The K-Ar ages range between 1770 Ma (detrital) and 69 Ma (syntectonic), and were interpreted to record ages intermediate between that of the source rocks and that of folding accompanied by cleavage development, low-grade metamorphism, and thrust and strike-slip faulting (Charlesworth et al., 1967). These authors advocated a tectonometamorphic event (‘orogenesis’) younger than 75 Ma, with the intensity of metamorphism increasing west of Mount Robson, where the authors identified younger $^{40}Ar/^{39}Ar$ ages and the biotite-in isograd.

The three isolated mafic intrusions in the Miette Group of Alberta that were examined and sampled for this geochronological study are described below, in sequence from north to south.

3.2.3 Geikie Dike

The Geikie dike is exposed in a 3 m wide by 7 m long by 2 m high outcrop in the roadcut of the old Yellowhead Trail across the Miette River from Highway 16, approcxomately1 km west of the Geiki siding (Figure 5a). It consists of a microdiorite/diabase, with albite (40%), calcite (20%), chlorite (20%), leucoxene (10%), and minor siderite and pyrite (Charlesworth et al., 1967), foliated mainly towards the dike’s periphery (Figure 6a). The foliation varies around 230°/45°; a vague dextral stretching lineation oriented 312°/05° is overprinted locally by normal displacement slickensides. This mafic body appears slightly discordant with the foliated host rock, so its original mode of emplacement (dike or sill) is unknown. Quartz-carbonate veining is locally extensive and can be also found in the host rock. The contacts with the host slates and sandstones of the Miette Group are not exposed. Charlesworth et al. (1967) assigned the host rocks to an informal member ‘B’ of the Old Fort Point Formation, and Mountjoy and Price (1985) assigned them to the undifferentiated middle Miette Group.

Sample DP11-9 was collected from the least sheared and altered portion of this mafic body.

3.2.4 Crowfoot Dike

The Crowfoot dike forms a 25 m wide outcrop in the roadcut of Highway 93 (Figure 5b) about 32 km north of the junction with Highway 1. It intrudes the shales of the Hector Formation (upper Miette

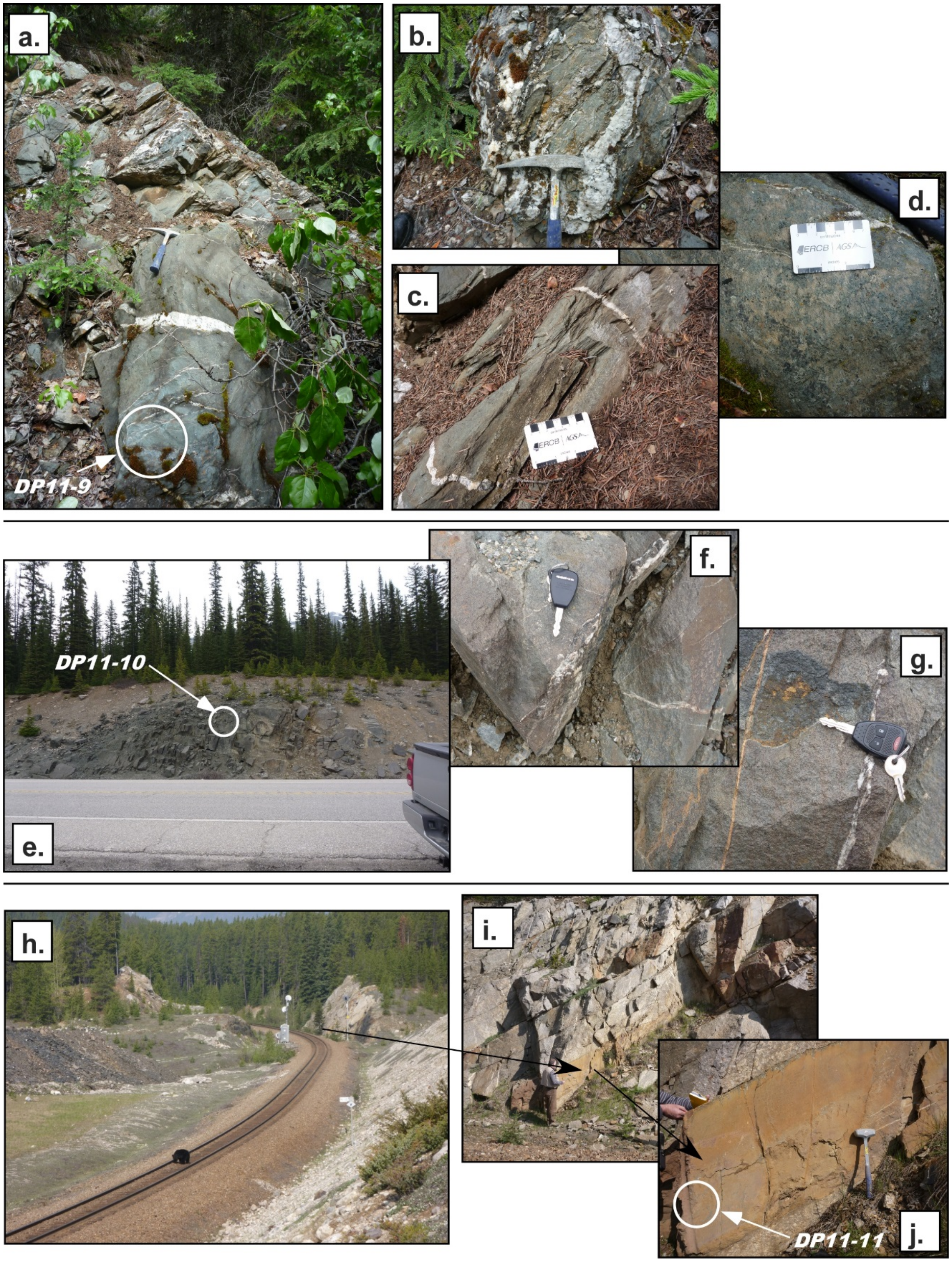

Figure 6. Isolated intrusions in the Miette Group: a) Geikie dike outcrop on the north side of the Miette River; b), c), and d) details of the same outcrop; e) Crowfoot dike outcrop on the east side of Highway 93 at Bow Lake; f) and g) details of the same outcrop; h) Blackbear sill outcrop on the east side of the CN Rail track about 1 km north of the intersection of Highways 1 and 93 (note black bear on the track); i) and j) details of the same outcrop. Exact locations given in Table 2.

Group), but the contacts are not exposed in the roadcut and, as observed from helicopter, the dike does not intrude the overlying massive conglomerates and quartzites of the Jonas Creek Formation (lower Cambrian Gog Group) that form the cliff on the crest of the ridge northeast of the road outcrop. The massive Jonas Creek quartzite grades up into thinner bedded quartzite with dark grey-green argillaceous partings and laminae containing abundant Scolithos tubular borrowing structures.

The dike is a fine- to medium-grained diabase (mass of plagioclase with about 25% augite) with chilled peripheries (glassy matrix that includes grey-green feldspar laths, chlorite and quartz knots, and calcite). On the southeast side of the dike, veins up to 20 cm long consist of calcite, partly replaced by quartz, with pyrite and chalcopyrite, or of magnesite, calcite, and quartz or coarse calcite, asbestos, and quartz (Figure 6b). Apparently, in the sixties, both contacts were exposed and the width of the dike was estimated to be 60 m, with a metamorphic aureole in the Hector Formation that is a few metres wide and characterized by coarser feldspar grains, quartz knots and more slab-like breakage of the bedding planes and laminae towards the dike (Smith, 1963).

Smith (1963) traced the dike upslope for 360 m to the northeast, beyond which it is covered with talus. Observed from helicopter, the dike does not cut the massive quartzite cliffs of the ridge but, according to Smith (1963), it outcrops again below this in Helen Creek, east of the ridge. Small veins of calcite and quartz have also been noted in the adjacent Jonas Creek Formation on the east side of the ridge in Helen Creek.

The dike is overprinted by

- a chlorite-lined foliation (230°/65°; all orientations are dip direction/dip), which conforms to the local structural grain that is associated with a similarly oriented fracture cleavage (220–227°/57–80°), spaced at 20–40 cm, and with a mineral lineation oriented 140°/46°, which is subparallel to the structural grain;
- a chlorite-lined subvertical cleavage (310°/87°), spaced at 10–15 cm, with subhorizontal slickensides (010–040°/10–20°) that locally appear to indicate dextral displacement; this cleavage is not everywhere through-going and, at places, discrete cleavage surfaces merge to form shear zones, spaced at 4–7 cm; and
- subvertical joints (315°/85°), which conform to the orientation of the dike.

The dike is affected by low-grade metamorphism, with chlorite-epidote-actinolite formed on foliation. Assuming that the foliation developed during the regional tectonism responsible for the present structural grain of the Main Ranges (wide, open folds and steeply dipping faults and shear zones), the dike seems to have been emplaced along an ‘ac’ tensional fracture near the crest of the Bow River anticline. The Crowfoot dike is crosscut by foliation but not affected by map-scale folds, suggesting a late-tectonic time of emplacement. Between the Bow River anticline and the syncline to the northeast, there is a high-angle shear zone. Smith (1963), who acknowledged R.E. Folinsbee and H.A.K. Charlesworth of the University of Alberta for information on the geology of the area, proposed that “there was considerable transcurrent movement along the shear zones” in the region. Our orientation measurements of mineral lineations and slickensides are consistent with dextral transpression.

Sample DP11-10 was collected from a more massive portion of the Crowfoot dike exposed in the roadcut.

3.2.5 Blackbear Sill

The Blackbear sill is located about 400 m north of the intersection of Highways 1 and 93 (Figure 5c), exposed on either side of the CN Rail cut (Figure 6h). It has an orientation of 260°/30°, concordant with the thick-bedded sandstone and grits of the upper Miette Group, and reaches a maximum thickness of 0.8 m on the east side of the tracks. The sill is affected by a fracture cleavage oriented 147°/85°, transverse to the structural grain and spaced at 3–10 cm, and a less penetrative cleavage oriented

242°/78°, subparallel to the structural grain. Both cleavages have also been recognized in the country rock. The Miette conglomerate includes quartz clasts 2 cm in diameter and platy to rounded, 2–3 cm diameter, brick red clasts. Approximately 25 m below the sill, the lithology of the Miette changes to 1–15 cm thick beds of dark grey to black shales and silts with spectacularly folded sulphide layers. The orientation of the transposition foliation is 250°/67°, similar to one of the fracture cleavages in the sill (242°/78°), and is consistent with the local structural grain. The locally obvious subhorizontal intersection lineation (335°/15°) is probably associated with some strike-slip displacement.

Sample DP11-11 was collected from the central portion of the sill, near the CN Rail tracks on the north side, where the sill appears to be thickest.

3.3 Cretaceous Alkaline Intrusions

Following a conspicuous Early Cretaceous (ca. 135–125 Ma) lull in magmatism in the North American Cordillera, an episode of widespread mid-Cretaceous (110–90 Ma) felsic magmatism extended from southeastern British Columbia into the southern Alberta Rocky Mountains (Armstrong, 1988). A swarm of ‘Cretaceous’ alkaline sills is emplaced in the Mesoproterozoic Purcell Supergroup of the Clark Range in the Lewis thrust sheet and extends north to Crowsnest Lake, where an alkaline sill intrudes Paleozoic strata in the footwall of the Lewis Thrust (Figure 7). No radiogenic ages and no systematic petrological study of these felsic alkaline sills from Alberta exist. Nonetheless, a detailed petrological study of the Rainy Ridge garnet-analcime phonolite in the Clark Range (Figure 8a; Goble et al., 1993) established its petrological similarities to the mid-Cretaceous Crowsnest volcanic suite, some 20 km to the north. Price (1962) proposed that the feeder of the Crowsnest volcanic suite is represented by the Howell Creek intrusive suite, located approximately 45 km to the southwest in British Columbia (Figure 7).

Because no direct dating of the alkaline swarm of southwestern Alberta exists, age data for the petrologically similar mid-Cretaceous igneous suites in the region are briefly reviewed below, whereas the age of the Crowsnest Formation is discussed in the next section (Section 3.4).

Gordy and Edwards (1962) reported K-Ar ages ranging from 112 to 72 Ma from the Howell Creek alkaline suite of small hypabyssal and intrusive bodies in southeastern British Columbia. A U-Pb zircon date of 98.5 ±5 Ma (with a strong contribution of inherited Early Proterozoic ca. 2347 ±22 Ma zircon), obtained by D. Murphy (Geological Survey of Canada) from a drillcore sample, is cited by Skupinski and Legun (1989). Two single orthoclase ^{40}Ar/^{39}Ar laser microprobe isochron ages of ca. 102.5 ±1 Ma (102.4 ±1 Ma plateau age) and 101.3 ±1 Ma (101.7 ±1 Ma plateau age) were reported by Barnes (2002) from a megacrystic syenite and a foid-syenite, respectively.

The White Creek batholith (Figure 7, inset) yielded Rb/Sr and K-Ar dates ranging from 115 to 71 Ma (Wanless et al., 1968; Archibald et al., 1984) and a ^{207}Pb/^{206}Pb zircon date of ca. 96 Ma (obtained by D. Brown and cited by Larson et al., 2006). This batholith stitches the Hall Lake fault (Reesor, 1958; Foo, 1979) and constrains its displacement to pre–mid-Cenomanian time. The Reade Lake stock, which crosscuts and stitches the St. Mary fault (Figure 7, inset) yielded a lower intercept U-Pb zircon date of ca. 94 Ma (Höy and van der Heyden, 1988) and constrains the displacement on the St. Mary fault and its eastward continuation, the Lussier River fault, to pre–late Cenomanian. Northeast of Cranbrook, B.C., the Mt. Haley and Lussier River stocks (Figure 7, inset) consist of multiphase, K-feldspar–phyric monzonite plutons, which intrude lower Paleozoic miogeoclinal strata near the south end of the western Main Ranges of the southern Canadian Rocky Mountains. Muscovite from the Mt. Haley stock yielded a ^{40}Ar/^{39}Ar plateau age of 108.2 ±0.7 Ma, and a single-crystal, step-heating analysis of muscovite from a skarn in the metamorphic aureole adjacent to the Lussier River stock gave a ^{40}Ar/^{39}Ar plateau age of 108.7 ±0.6 Ma (Larson et al., 2006). Both stocks crosscut and thermally overprint the Lussier River fault and the fold-and-thrust structures in the east flank of the Purcell anticlinorium and the west limb of the Porcupine

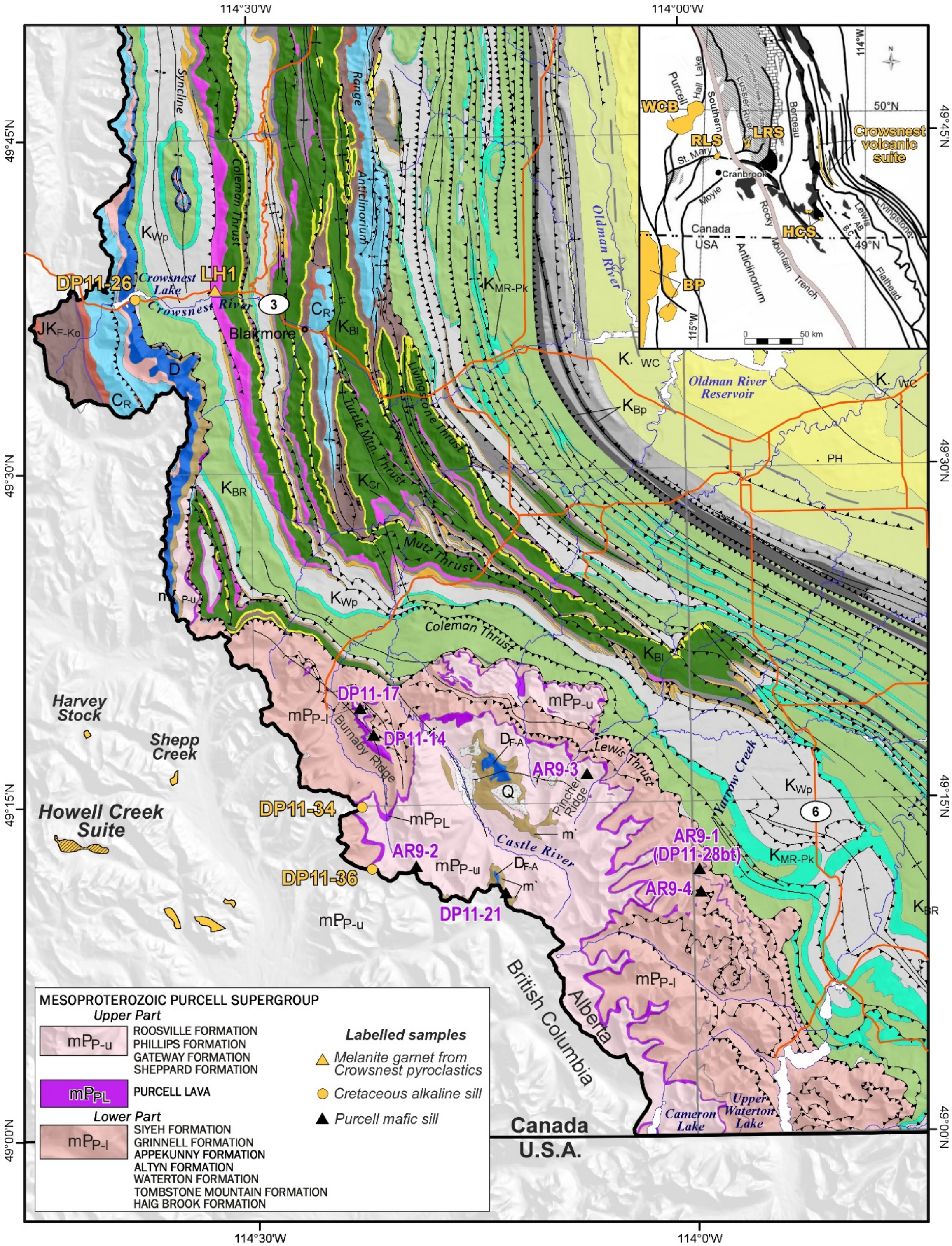

Figure 7. Locations of samples collected from Cretaceous alkaline intrusions during this study, superimposed on the regional geology (after Pană and Elgr, 2013; see Figure 1 for legend). Inset map shows the location of other mid-Cretaceous felsic intrusive rocks in the region: WCB, White Creek batholith; RLS, Reade Lake stock; LRS, Lussier River stocks; HCS, Howell Creek suite; BP, southern segment of the Bayonne plutonic belt. For complete legend see Pană and Elgr (2013). Exact sample locations are included in Tables 1 and 3.

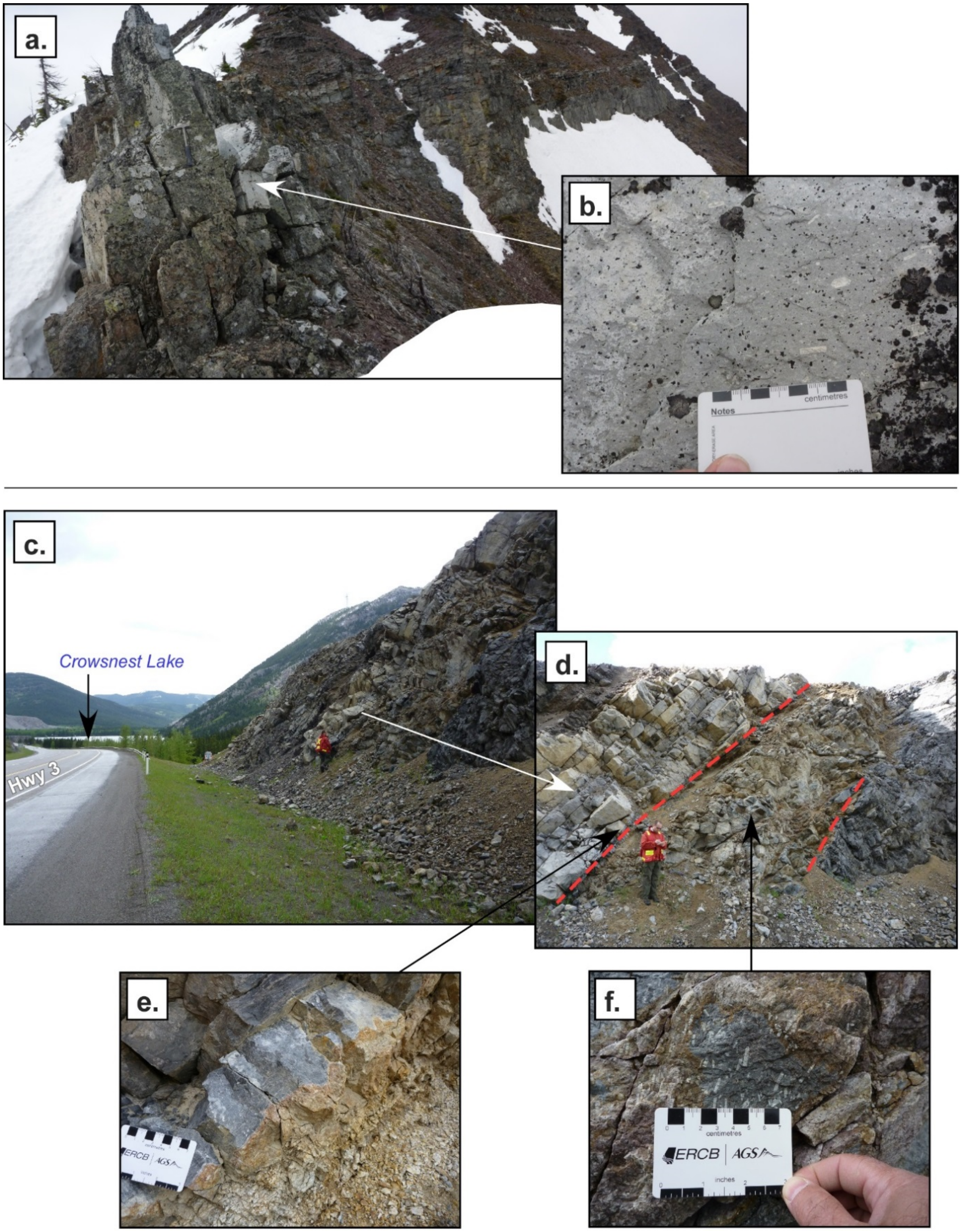

Figure 8. Outcrops of alkaline intrusions in the southern portion of the Alberta Rocky Mountains: a) garnet-analcime phonolite sill emplaced in the middle of the Proterozoic Gateway Formation (Purcell Supergroup) on Rainy Ridge, Clark Range; b) detailed view (sample DP11-34); c) trachyte sill in Paleozoic carbonates cropping out in the roadcut of Highway 3, just east of Crowsnest Lake; d) and e) detailed views; f) exact location of sample DP11-26.

Creek anticlinorial fan structure. These dates constrain the timing of folding and thrusting, and of the displacement along the Lussier River–St. Mary fault, to pre–middle Albian. Farther west, the southern segment of the eastward convex Bayonne plutonic belt (Figure 7, inset) consists of larger plutons with highly variable compositions (with an alkaline granodiorite average composition), textures and colours that yielded radiometric ages in the 130–87 Ma range (Wheeler and McFeely, 1991).

We examined and sampled the Rainy Ridge phonolite (Figure 8a) and the largest trachyte sill found on the Alberta–British Columbia border in the Clark Range, located both in the hangingwall of the Lewis Thrust, and the trachyte in the footwall of the Lewis Thrust exposed in the roadcut of Highway 3 near Crowsnest Lake (Figure 8b).

3.4 Crowsnest Formation

The middle Cretaceous Crowsnest Formation is exposed in a series of en échelon thrust slices in the southern Alberta Foothills, crosscut by Highway 3 (Figure 7). Palinspastic reconstructions place the original location of the Crowsnest Formation approximately 75 km to the west (Norris, 1964). The deposits are resistant to weathering and consequently form prominent northerly-trending ridges in the area. The Crowsnest Formation has a maximum thickness of between 426 and 488 m (Price, 1962; Norris, 1964; Pearce, 1970) in the Coleman thrust sheet. Formation thickness, bed thickness, and clast size generally decrease away from this area (Pearce, 1970) but can be traced up to 35 km north and 20 km south from Highway 3.

The Crowsnest Formation is composed of bedded, subaerial, alkaline pyroclastic deposits (agglomerate, tuff and ash beds, rich in feldspar and analcime with a few thin lava flows) resulting from cyclical eruptions dominated by explosive volcanism during early stages and by effusive volcanism during later stages (Adair and Burwash, 1996). The Crowsnest Formation has been divided into two informal members (Adair, 1986): the lower member, with a distinctive light pink to green colour, is composed of thinly to thickly bedded deposits of heterolithic volcanic rock fragments and abundant crystal fragments; and the upper member is composed of dark green, thickly bedded breccia containing heterolithic rock fragments dominated by volcanic clasts and fewer crystal clasts. Volcanic clasts are up to several metres wide and on Ma Butte may weigh up to 15 (short) tons (Pearce, 1970). Ricketts (1982) described beds with characteristics of laharic breccias (volcanic debris flows) and other beds with primary sedimentary structures that suggest alluvial deposition by short-lived streams. Adair (1986) argued that the structures are similar to volcanic-surge deposits found on modern volcanoes and that plastic deformation structures, suture boundaries, and baked margins suggest that emplacement took place at elevated temperatures.

In order of relative abundance, the crystal clasts in the Crowsnest Formation are sanidine, melanite garnet, analcime, aegirine-augite, plagioclase, titanite, and opaque minerals (ilmenite, pyrite, magnetite, hematite), with epidote, apatite, and clinozoisite as accessory minerals. Individual crystals are euhedral, but some show weak to moderate degrees of abrasion; rounded crystal clasts are rare.

The volcanoes that produced the Crowsnest Formation were on an inland floodplain, centred near Coleman, and were probably of high relief (Glaister, 1959; Norris 1964; Mellon, 1967; Pearce, 1970; Adair, 1986). However, no volcanic edifice and no intrusive rocks associated with the ejecta have been discovered.

The age of the Crowsnest Formation is not fully constrained stratigraphically. Volcanic fragments become progressively more common towards the top of the middle Blairmore Group, with a gradational transition towards the Crowsnest Formation (Norris, 1964). The lower contact of the formation interfingers with clastics of the continental Bruin Creek Member of the Mill Creek Formation (Norris, 1964; Pearce, 1970; Adair, 1986). Black melanite garnet is common in the formation and can be used as an indicator of the lower gradational contact with the Bruin Creek Member. The Bruin Creek Member includes poorly preserved palynological forms that may be of Cenomanian age (Burden and Leckie, 2001).

Subsequent to volcanism and erosion, marine muds of the Cenomanian–Turonian Blackstone Formation onlapped onto the topographically high Crowsnest volcanic pile (Stott, 1963; Norris, 1964). The Vimy and Sunkay members of the Blackstone Formation both thin considerably over the Crowsnest Formation, with the Sunkay Member missing near Coleman (Adair, 1986). Beds containing *Inoceramus labiatus* directly overlie the Crowsnest Formation near Coleman (Glaister, 1959; Mellon, 1967), but away from the Coleman area, to the south and north, the thickness of the interval between the top of the Crowsnest Formation and the first occurrence of *I. labiatus* increases (Burden and Leckie, 2001). Moreover, regional subsurface correlations show that the Fish Scales Formation pinches out westward towards the Crowsnest Pass area. Based on Cenomanian and Turonian dinoflagellates, and relatively evolved pollen and spore taxa, Burden and Leckie (2001) inferred that the Crowsnest Formation may be of latest Albian–Cenomanian age.

Pure sanidine from a sample of the Crowsnest volcanics, collected west of Coleman, yielded a K-Ar age of ca. 96 Ma (Folinsbee et al., 1957, 1961).

We collected a grab sample of melanite garnet from the large outcrop on the north side of Highway 3, near Coleman.

3.4.1 Crowsnest Formation Metamorphism

The volcanic rocks of the Crowsnest Formation have been affected by low-grade burial metamorphism characterized by analcime (veins)–prehnite (amygdules)–laumontite (pore-filling cement) mineral assemblages (Begin et al., 1995b). The matrix contains a mixture of quartz, K-feldspar, albite, and chlorite. Calcite veining and pseudomorphs after igneous minerals are common. Feldspar is variably sericitized and albitized. At H_2O equal to lithostatic pressure, the stability of laumontite+quartz restricts metamorphic temperatures to 180–280°C, whereas that of prehnite+laumontite+quartz constrains the pressure of metamorphism to between 1.5 and 3 kbar. These P-T estimates are consistent with maximum depths of burial of 5–8 km, inferred from structural-stratigraphic reconstruction. The restricted stability of laumontite in the presence of CO_2 suggests that fluids that equilibrated with laumontite were low in CO_2.

To what extent this metamorphism has modified elemental abundances is not clear. In contrast with the Goble et al. (1993) interpretation of analcime ($NaAlSi_2O_6 \cdot H_2O$) in the Rainy Ridge phonolite as a primary hydrous mineral phase, analcime in the Crowsnest volcanics was interpreted to have formed through replacement of primary leucite by analcime via a process of ion exchange with Na-rich fluids, mainly because of the absence of other primary hydrous igneous minerals (Pirsson, 1915; Gupta and Fyfe, 1975; Taylor and MacKenzie, 1975; Wilkinson, 1977; Karlsson and Clayton, 1991). The analcime itself is substituted by muscovite in the greenish blairmorite from the top of the Crowsnest Formation in the Carbondale River area (Goble et al., 1993).

Crook (1962) and Pearce (1970) reported albitization of sanidine in the Crowsnest volcanics. Pearce (1970) noted that albitization was developed best in phenocrysts in the trachytes but poorly developed or absent in the analcime-bearing phonolites. The trachytes have the highest Na_2O contents, consistent with more pronounced albitization in these rocks (Pearce, 1970). Evidence that Na and K may have been mobile during the metamorphism of the Crowsnest volcanic rocks is given by the scattering of analytical data in the K_2O-Na_2O diagrams (Bégin et al., 1995a; Peterson et al., 1997; Bowerman et al., 2006).

It is likely that Na and K were mobilized during the low-grade metamorphism of this suite, so their concentrations are not representative of the original igneous geochemistry. Postemplacement metamorphic alteration of the Crowsnest volcanic rocks may also explain the scatter in the isotopic data noticed by Bégin et al. (1995b) and Peterson et al. (1997). Formational waters from the Western Canada Sedimentary Basin are possible proxies for fluids that interacted with the volcanic rocks. These waters have higher $^{87}Sr/^{86}Sr$ but lower Sr concentrations than the volcanic rocks (Bowerman et al., 2006). The scatter in the data for the volcanic rocks may simply reflect multiple sources of the fluids that interacted with the Crowsnest volcanic rocks. Another possibility is that $^{87}Sr/^{86}Sr$ is increased by precipitation of secondary calcite from different sources of carbonate-saturated fluids during metamorphism.

It is reasonable to assume that the maximum burial, accompanied by low-temperature metamorphism, followed shortly after the ca. 72 Ma emplacement of the huge Lewis Thrust (van der Pluijm et al., 2006) immediately to the west and above the Crowsnest Formation. Subsequent exhumation and uplift in the southern Alberta Rockies is constrained by the apatite fission-track age of ca. 59 Ma, interpreted as post-thrusting rapid denudation of the Lewis thrust sheet (Sears, 2001), and by the 57 Ma potassium metasomatism of bentonite in the footwall of the Lewis Thrust (Hoffman et al., 1976).

4 Sampling and Analytical Techniques

4.1 Mafic Sills and Lava Flows in the Mesoproterozoic Purcell Supergroup, Clark Range

Samples from Mesoproterozoic basaltic intrusions collected in 2008 and 2009 were analyzed for U-Pb zircon dating by sensitive high-resolution ion microprobe (SHRIMP; 10 or 11 points per sample). The sampling locations are shown in Figure 7. Zircon separation and analyses were performed at Activation Laboratories Ltd. (Ancaster, Ontario). The sample processing included crushing, grinding, and Wilfley table, heavy liquids, and Frantz magnetic separation; concentrates were examined under the microscope for datable mineral phases.

Sample AR9-1 (YK-409) is from the middle of the 30 m thick biotite-olivine dolerite sill on the hillslope west of Yarrow Creek (Figure 3d), which intruded along the contact between the Appekunny and Grinnell formations within arenitic quartzite with green argillite rip-up clasts. The submitted material consisted of combined AGS samples 8300 and 8301, and included both uncrushed rock sample and coarse reject fractions from splits of these samples crushed at Bureau Veritas Minerals (Vancouver, B.C.; formerly Acme Analytical Laboratories Ltd.).

Sample AR9-2 (YK-410) is from an olivine-hornblende microgabbro sill within green laminated dolomitic sandstone and siltstone of the Roosville Formation at La Coulotte Peak. The submitted material included combined AGS samples 8275 (695519E, 5453659N; olivine-phyric microgabbro from the lower quenched margin), 8278 (695515E, 5453656N; glomeroporphyritic microgabbro from the middle portion), and 8279 (695516E, 5453649N; amygdaloidal microgabbro from the upper quenched margin). All material consisted of uncrushed rock samples with no reject fractions from other analyses.

Sample AR9-3 (YK-411) is olivine-hornblende microgabbro from a sill emplaced within interbedded green, grey, and pink sandstones of the Gateway Formation on Pincher Ridge. The material included combined AGS samples 8269 (709544E, 5461663N; amygdaloidal basalt with 1–3% Fe-sulphides from the upper quenched margin), 8273 (709545E, 5461668N; altered green and red basalt from the middle portion), and 8274 (709545E, 5461668N; altered green and red basalt from the middle portion). All material consisted of uncrushed rock samples with no reject fractions from other analyses.

Sample AR9-4 (YK-412) is from an olivine-hornblende microgabbro sill within interbedded dolomites and argillites of the Siyeh Formation on Cloudy Ridge. The submitted material included combined AGS samples 8260 (282000E, 5451964N; glomeroporphyritic basalt from the lower quenched margin), 8261 (282006E, 5451969N; glomeroporphyritic basalt from the middle portion with white-pink calcite veins), and 8262 (282072E, 5451951N; glomeroporphyritic basalt from near the upper margin). The material included uncrushed rock sample combined with coarse reject fractions from splits of these samples crushed at Bureau Veritas.

In addition, three samples were collected during 2011 from the Purcell mafic rocks for U-Pb ID-TIMS analyses and three samples for $^{40}Ar/^{39}Ar$ analyses at the Jack Satterly Geochronology Laboratory (JSGL) of the University of Toronto (Table 1). These samples were processed by crushing, grinding, and Wilfley table, heavy liquids, and Frantz magnetic separation; the concentrates were then examined under the microscope to identify datable phases.

Table 1. Samples of Purcell mafic sills processed for isotope dating.

Sample ID	Rock Type	Stratigraphic Position	Location	Easting	Northing	Analytical Technique
AR9-1 (8300 & 8301)	Biotite-olivine dolerite	Contact Appekunny/ Grinnell formations	Yarrow Creek	282012	5453864	SHRIMP
AR9-2 (8278, 8279 & 8275)	Olivine-hornblende microgabbro	Roosville Formation	La Coulotte Peak	695517	5453655	SHRIMP
AR9-3 (8269, 8273 & 8274)	Olivine-hornblende microgabbro	Gateway Formation (?)	Pincher Ridge	709545	5461668	SHRIMP
AR9-4 (8260, 8261 & 8262)	Olivine-hornblende microgabbro	Siyeh Formation,	Cloudy Ridge	282006	5451965	SHRIMP
DP11-14 (8312)	Pillow basalt, aphanitic, aphyric base	Purcell Lava (near base)	Barnaby Ridge	691680	5464409	ID-TIMS & $^{40}Ar/^{39}Ar$
DP11-17 (8313)	Amygdaloidal; abundant chlorite vesicles	Purcell Lava (near top)	Barnaby Ridge	690504	5466701	$^{40}Ar/^{39}Ar$
DP11-21 (8316)	Microgabbro fragments and blocks	Upper Roosville Formation	On saddle	702843	5451431	ID-TIMS
DP11-28bt (8318)	Biotite-olivine basalt, star texture (datable plagioclase and/or baddeleyite)	Contact between Appekunny and Grinnell formations	Yarrow Creek	282012	5453864	ID-TIMS & $^{40}Ar/^{39}Ar$

After extensive mineral separation work, the Yarrow Creek star-texture biotite-olivine dolerite sample DP11-28bt (Figure 3b) yielded a moderate amount of baddeleyite. High-precision isotope dilution–thermal ionization mass spectrometry (ID-TIMS) U-Pb isotopic dating was performed on four selected baddeleyite grains at the JSGL:

- Mineral separation, selection, and preparation were undertaken with the utmost care using an isodynamic magnetic separator, heavy liquids, and air abrasion or ‘chemical abrasion’ (CA) techniques.
- Low-contamination chemical procedures used ultraclean facilities. Lead blanks are routinely <1 pg.
- Isotopic analysis of U and Pb was performed using high-precision mass spectrometry. The JSGL houses two VG354 mass spectrometers equipped with multiple faraday cups, and Daly detectors with digital ion counting.
- Analytical uncertainties on isotopic measurements are routinely within ±0.5% for $^{206}Pb/^{238}U$ and $^{207}Pb/^{235}U$, and ±0.1% for $^{207}Pb/^{206}Pb$ ratios at the 2σ confidence level for samples containing at least 100 pg Pb.

In spite of numerous attempts, no U-Pb datable mineral phase could be recovered from sample DP11-21 of the microgabbro and basalt rubble from the upper Roosville Formation; from sample DP11-17 near the top of the Purcell Lava (Figure 3a) or from sample DP11-14 of very fine grained, chloritized, olivine-phyric (pseudomorphed) alkali pillow basalt collected near the base of the Purcell Lava (Figure 3b). As no U-bearing minerals could be recovered from these fine-grained samples, they were transferred to the $^{40}Ar/^{39}Ar$ facility at the JSGL. The sample from the Yarrow Creek olivine dolerite sill was also submitted for $^{40}Ar/^{39}Ar$ analysis so the results could be compared with the U-Pb baddeleyite age (Table 1).

4.2 Isolated Dikes and Sills in the Miette Group

The freshest portions of the Geikie and Crowfoot dikes, which intrude the Miette Group along the Miette River and near Hector Lake, respectively, were sampled for dating. The Blackbear sill was also sampled for geochronology in spite of its obvious carbonatitic alteration. All samples were submitted to the JSGL for mineral separation and dating (Table 2).

Table 2. Samples of diabase intruded into the Miette Group.

Sample ID	Rock Type	Stratigraphic Position	Location	Easting	Northing	Analytical Technique
DP11-9 (8309)	Geikie dike	Miette Group	Geikie, north of Hwy. 16	414040	5859106	ID-TIMS
DP11-10 (8310)	Crowfoot dike: diabase, fine to medium grained	Miette Group	Hector Lake, Hwy. 93 roadcut	539727	5723285	ID-TIMS $^{40}Ar/^{39}Ar$
DP11-11 (8311)	Blackbear sill	Miette Group	North of Hwy. 1 & Hwy. 93 intersection	554615	5699611	ID-TIMS

The ophitic texture of the dikes indicates rapid cooling at shallow emplacement depths (shallow dikes). The available material for sampling was fine grained and the state of alteration (and shearing, ± carbonatization) quite pervasive; hence, the chances of recovering datable igneous minerals were limited. Indeed, the sheared diabase collected from the Geikie dike (DP11-9) and the completely carbonatized (no relics of mafic minerals) Blackbear sill sample (DP11-11) did not yield U-Pb–datable mineral phases. It is possible that, due to rapid cooling, the magma may not have reached saturation in baddeleyite or zircon (or zirconolite) and all Zr that may have been present in the melt remained tied up in the mesostasis or glass, which is now largely devitrified.

The fine- to medium-grained diabase sample from the Crowfoot dike (DP11-10) yielded a heavy-mineral concentrate that consists almost entirely of euhedral to subhedral pyrite and rare apatite. One of the two grains of zircon found in the concentrate was somewhat rounded and therefore likely xenocrystic, inherited from the country rocks. Zircon was not analyzed; instead, the Crowfoot dike sample was analyzed by $^{40}Ar/^{39}Ar$ at the JSGL (Table 2). Single-grain zircon analyses remain an option for further work using much more material. Dating apatite remains an option for recovering a magmatic age, assuming the dike has never been heated past about 350°C. Otherwise, the apatite may yield a (potentially much) younger age.

4.3 Cretaceous Felsic Alkaline Sills and Dikes

Three samples collected from Cretaceous alkaline sills in the southern Alberta Rockies were submitted to the U-Pb Geochronological Facility of the University of Alberta (Table 3). They were processed for mineral separation by crushing, grinding, and Wilfley table, heavy liquids, and Frantz magnetic separation; the concentrates were then examined under the microscope to identify datable phases.

Table 3. Samples of Cretaceous alkaline sills and dikes processed for mineral separation at the University of Alberta.

Sample ID	Rock Type	Stratigraphic Position	Location	Easting	Northing	Analytical Technique
DP11-26 (8327)	Alkali trachyte sill	Devonian carbonates	Roadcut Hwy. 3, Crowsnest Pass	670982	5500390	$^{40}Ar/^{39}Ar$ ID-TIMS
DP11-34 (8320)	Garnet-analcime phonolite	Gateway Fm.	Rainy Ridge, continental divide Continental Divide	690778	5458684	ID-TIMS
DP11-36 (8322)	Largest alkali syenite in AB	Gateway Fm.	Scarpe Mountain, Clark Range, continental divide	691802	5453390	ID-TIMS

Sample DP11-36, from the largest sill cropping out on the Clark Range divide, yielded abundant zircon with a large variety in colour, shape, and size. A number of these zircon grains are quite rounded and are likely xenocrysts affected by magma resorption. The mineral concentrate also contained abundant large yellow fragments of titanite. Zircon and titanite were analyzed by LA-ICP-MS at the University of Alberta.

Sample DP11-34 from the Rainy Ridge garnet-analcime phonolite yielded a much smaller recovery of mostly resorbed zircon prisms, likely xenocrystic. Most of the concentrate consists of pyrite, apatite, and yellow titanite fragments. This sample has not been analyzed yet but could be targeted in the future after more material is acquired, particularly for garnet dating, which could be directly compared to the dated melanite garnet from the Crowsnest volcanic suite.

The trachyte sill exposed in the roadcut on the north side of Highway 3 (DP11-26) did not yield any zircon and the concentrate included plenty of fluorite. Consequently, the sample was prepared for $^{40}Ar/^{39}Ar$ dating at the JSGL.

4.4 Crowsnest Formation

In the absence of zircon in the mafic Crowsnest volcanic rocks, we analyzed the melanite garnet crystallized from melt. Individual black melanite garnet grains up to 5 mm in diameter, detached from rock by weathering, were collected along the large outcrop north of Highway 3, just west of Coleman (Figure 7). Documenting the potential of garnet in geochronology, Mezger et al. (1989) showed that a) U^{4+} has an ionic radius similar to that of Ca^{2+} and Sm^{3+}, and should therefore substitute for Ca^{2+} in the dodecahedral site of garnet; b) U^{4+}, with a higher charge, may require the substitution of ions with a smaller charge in adjacent sites to maintain charge balance; and c) during diffusion of U^{4+}, such ions would have to diffuse as well. Moreover, the concentrations of U in garnets are on the order of a few hundred parts per billion or less, so metamictization and thus loss associated with alteration should be negligible. The sample was analyzed by isotope dilution–thermal ionization mass spectrometry (ID-TIMS) at the University of Alberta.

4.4.1 Analytical technique

Single selected melanite grains were examined using a stereo-microscope and then washed in warm 4N HNO_3 for ~60 minutes to remove surface contamination. The samples were weighed with a UMT-2 Mettler ultra-microbalance, dissolved in an HF-HNO_3 mixture at 200°C for 72 hours together with a mixed ^{205}Pb-^{235}U tracer solution. The procedure for purifying U and Pb using anion exchange chromatography and analyzing their isotopic compositions on a VG354 solid-source thermal ionization mass spectrometer are identical to those outlined for titanite in Heaman et al. (2002).

5 Results and Geological Significance

5.1 Mafic Sills and Lava Flows in the Mesoproterozoic Purcell Supergroup, Clark Range

5.1.1 Baddeleyite Age of Mafic Sill

Uranium-lead results for four baddeleyite crystals from the Yarrow Creek sill (Table 4) define a tight, linear array through the origin, which yields an upper intercept age of 1436.2 ±1.1 Ma (2σ error; Figure 9). This age is similar to, but much more precise than, the previous K-Ar ages of 1500 and 1453 Ma, and the $^{40}Ar/^{39}Ar$ age of 1400 Ma obtained from biotite of the Appekunny sill on Spionkop Ridge (Goble, 1977; Ghazi, 1992).

The regional extent of the rifting-related igneous events originally documented in the Belt-Purcell basin of the northern United States and southern British Columbia is now also established in the Alberta portion of the basin (Figure 4). The rift-related mafic magma release started at ca. 1469 Ma (Sears et al., 1998; Anderson and Davis, 1995) with the intrusion of the Moyie sills into the lower Purcell turbidites in the rift axis region (Figure 4a). The ca. 1436 Ma Yarrow Creek sill emplacement reflects continued, prolonged rift activity over ~33 m.y. within the developing Belt-Purcell basin. This sill was emplaced at the boundary between the siliciclastic Appekunny and Grinnell formations on the east shoulder of the basin, and sets a minimum depositional age for the lower Belt-Purcell Supergroup up to the Grinnell strata.

5.1.2 SHRIMP Dating of Zircon from Purcell Mafic Sills

Due to the chemical composition of these basaltic/doleritic sills (insufficient silica for the development of magmatic zircons) and to the relatively small sample size (~10 kg), only a small amount of zircon grains was recovered from each sample. The precise emplacement age of the Yarrow Creek sill (ca. 1436.2 ±1.1 Ma) and the consistency of all results obtained by precise U-Pb dating in other parts of the Belt-Purcell basin together provide a reliable reference system (ca. 1.47–1.43 Ga emplacement) for the interpretation of the new SHRIMP data from the Clark Range samples. Ten or eleven spot analyses were performed on the best zircons from each sample (Table 5).

Sample AR9-1 (YK-409) from the Yarrow Creek biotite-olivine dolerite sill yielded 100 zircon grains, of which 30 were isolated and the best 10 were hand-picked and spot analyzed (Figure 10). A 3.06 Ga age (grain 1) and two ages of ca. 2.90 Ga (grains 7 and 10) probably indicate Mesoarchean magmatic events. Ages of 2.66 Ga (grain 8) and 2.55 Ga (grain 9), and several ages between ca. 2.70 Ga and 2.80 Ga (grains 3, 4, and 5) record late Mesoarchean magmatic events, whereas the 2.04 Ga age (grain 2) may be a middle Paleoproterozoic metamorphic event. **Sample AR9-2** (YK-410) from the La Coulotte Peak olivine-hornblende microgabbro sill (Figure 11) yielded a moderate number of zircon grains, from which 30 grains were selected and 11 spot analyses performed on the best 10 grains. The ages of ca. 2.61 Ga (grain 7) and ca. 2.80 Ga (grains 2 and 5) correspond to the clusters identified in the Yarrow Creek sample. More importantly, grains 5 and 6 yielded Mesoarchean core ages of ca. 2.90 Ga, and several grain rims (grains 1, 3, 4 and 6) yielded an overgrowth age of 2716 ±13 Ma. One grain (grain 10) of likely magmatic origin yielded a surprisingly young but well-defined age of ca. 1.60 Ga. The postemplacement ages of 398 Ma and 543 Ma may record subsequent thermal disturbances.

Sample AR9-3 (YK-411) is from the Pincher Ridge olivine-hornblende microgabbro sill (Figure 12). Ten spot analyses from 10 grains yielded one old Mesoarchean age of ca. 3.03 Ga (grain 5), similar to the 3.06 Ga age identified in the Yarrow Creek sill. Two grains with ages of 2.51 Ga (grain 4) and 2.55 Ga (grain 6), and the ca. 2.65 Ga cluster (2.63 Ga, grain 8; 2.65 Ga, grain 7; and 2.67 Ga, grain 3) ages are comparable to similar late Neoarchean ages found in grains from samples AR9-1 and AR9-2; the possibly magmatic age of 2.76 Ga (grain 1) is close to the 2.78 Ga age of grain 5 in sample AR9-1 and comparable

Table 4. U-Pb baddeleyite ID-TIMS data for dolerite sills from the Purcell basin, Clark Range.

Sample/ Fraction	Weight (µg)	U (ppm)	Th/U	Pb_{tot} (pg)	Pb_{Com} (pg)	$^{206}Pb/^{204}Pb$ Measured	$^{207}Pb/^{235}U$	2σ	$^{206}Pb/^{238}U$	2σ	$^{206}Pb/^{238}U$ Age (Ma)	2σ	$^{207}Pb/^{235}U$ Age (Ma)	2σ	$^{207}Pb/^{206}Pb$ Age (Ma)	2σ	% Disc	Error Correlation
Bd-1 (4)	0.15	321	0.10	76.4	0.5	10380	3.07985	0.00754	0.246798	0.000480	1421.9	2.5	1427.7	1.9	1436.3	2.0	1.1	0.9160
Bd-2 (5)	0.18	233	0.13	55.7	0.8	4762	3.07048	0.00837	0.246082	0.000453	1418.2	2.3	1425.4	2.1	1436.0	2.9	1.4	0.8400
Bd-3 (6)	0.20	374	0.09	89.0	1.1	5280	3.09684	0.00816	0.248244	0.000461	1429.4	2.4	1431.9	2.0	1435.6	2.8	0.5	0.8398
Bd-4 (7)	0.20	317	0.12	95.1	0.6	8755	3.05548	0.00737	0.244819	0.000453	1411.7	2.3	1421.6	1.9	1436.5	1.9	1.8	0.9181

Notes:
Bd# (n) is the baddeleyite fraction number, with the number of analyzed grains in the fraction (in brackets)
All fractions consist of pale, medium brown, striated blades and blade fragments
Pbtot is total amount of Pb excluding blank
Pbcom is common Pb, assuming the following isotopic composition of the laboratory blank:
Pb^{206}/Pb^{204}, 18.221; Pb^{207}/Pb^{204}, 15.612; $Pb^{208}/Pb^{20}4$, 39.360 (2σ errors of 2%)
Pb^{206}/Pb^{204} corrected for fractionation and common Pb in the spike; Pb/U ratios also corrected for blank where applicable
Th/U calculated from radiogenic $^{208}Pb/^{206}Pb$ ratio and $^{207}Pb/^{206}Pb$ age, assuming concordance
% Disc. is percent discordance for the given $^{207}Pb/^{206}Pb$ age
Error correlation is given by the correlation coefficients of the X-Y errors on the Concordia diagram

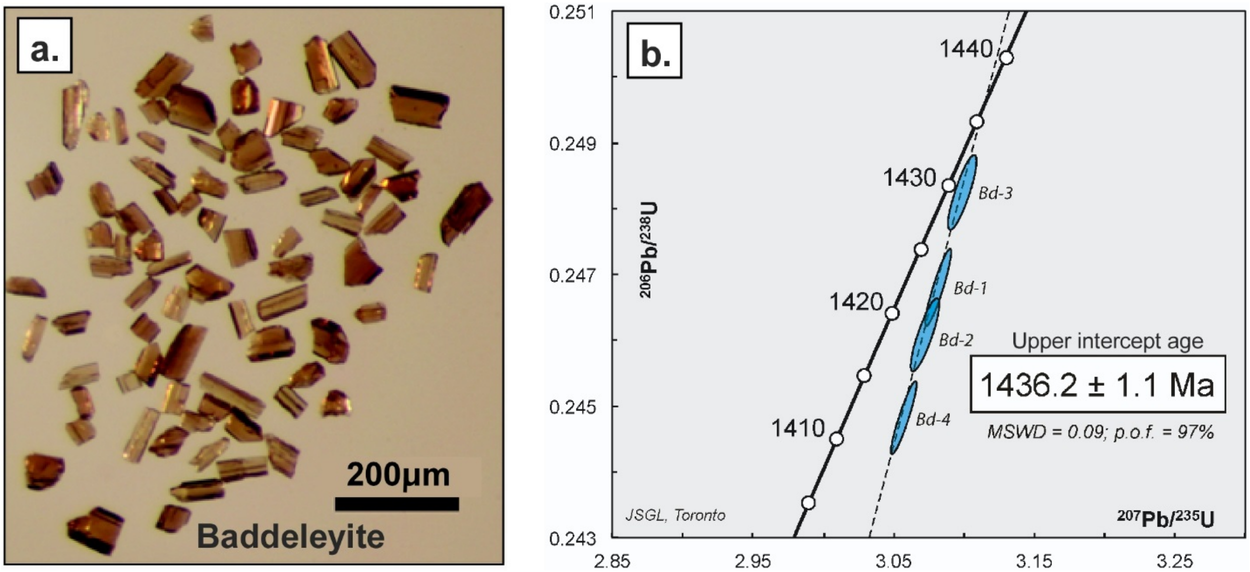

Figure 9. a) Representative image of highest quality baddeleyite crystals separated from sample DP11-18 (8318) and selected for analysis; individual fractions comprised between 4 and 7 grains of baddeleyite. b) Concordia diagram showing results for baddeleyite analyses from sample DP11-18 (8318); the highlighted age represents the upper intercept age of regression anchored through the origin; error ellipses and calculated age uncertainty are shown at the 2σ level.

to the overgrowth age of ca. 2.72 Ga identified in the La Coulotte sill. A 2.05 Ga age (grain 9) is very close to the 2.04 Ga identified in the Yarrow Creek sill. The 791 Ma age likely records a postemplacement thermal disturbance. The 2.43 Ga age of grain 10 is unique.

Sample AR9-4 (YK-412) from the Cloudy Ridge microgabbro (Figure 13), with 10 spot analyses from 9 grains, yielded a very old but perfectly dated Paleoarchean age of 3564±15 Ma (grain 6) and a Mesoarchean date of 3.11 Ga (grain 8), which is similar to the 3.06 Ga from the Yarrow Creek sill and to the 3.03 Ga from the Pincher Ridge sill. An age of 2.81 Ga (grain 5) appears to confirm the Late Mesoarchean magmatic event identified in the Yarrow Creek sill. A small population of 1.70 Ga ages (grains 3 and 9) may be assimilated zircons of detrital origin and represents a range of ages that is uncommon to rare in Precambrian rocks to the immediate east and south, and must therefore be from a western source (Ross et al., 1992). Ages of ca. 2.65 Ga (grain 4) and 2.00 Ga (grain 7) belong to groups found in all other sills. Grain 2 yielded an age of 1.34 Ga, which is the only SHRIMP) zircon age from Clark Range sills that falls in the age range of titanite growth (1.36–1.33 Ga) in the Moyie sills of British Columbia and similar to the ca. 1.37 Ga tectonothermal event related to granitoid intrusions in northern United States. Grain 1 yielded an age of 1.15 Ga and may be the local reflection of the ‘Grenvillian’ thermal metamorphic event.

Most zircon grains have concordant U-Pb ages but appear to be inherited from deep-seated sources or xenocrysts partially assimilated during ascent and emplacement of these magmas (Figure 14). They can be assigned to several age groups (from oldest to youngest):

Table 5. Summary of sensitive high-resolution ion microprobe (SHRIMP) data for Purcell mafic sills.

Spot	^{206}Pbc (%)	U (ppm)	Th (ppm)	^{206}Pb* (ppm)	^{232}Th/^{238}U	Disc. (%)	^{206}Pb/^{238}U age (1)	±%	^{207}Pb/^{206}Pb age (1)	±%	^{238}U/^{206}Pb* (1)	±%	^{207}Pb*/^{206}Pb* (1)	±%	^{207}Pb*/^{235}U (1)	±%	^{206}Pb*/^{238}U	±%	Error Correl.
YK-409_1.1	0.00	405	35	211	0.09	+0	3058	1.0	3058	0.4	1.65	1.3	0.231	0.55	19.3	1.3	0.61	1.3	0.95
YK-409_2.1	0.00	237	75	75.3	0.33	+1	2031	1.2	2042	0.7	2.70	1.3	0.126	0.82	6.4	1.5	0.37	1.3	0.87
YK-409_3.1	0.03	141	60	62.3	0.44	+6	2669	1.2	2796	0.5	1.95	1.5	0.196	0.77	13.9	1.6	0.51	1.5	0.91
YK-409_4.1	0.08	49	72	23.1	1.50	+0	2805	1.6	2813	0.8	1.83	2.0	0.198	1.21	14.9	2.3	0.55	2.0	0.86
YK-409_5.1	0.01	295	167	133	0.59	+2	2720	1.1	2775	0.5	1.90	1.3	0.194	0.63	14.0	1.4	0.53	1.3	0.93
YK-409_6.1	0.00	236	153	104	0.67	+1	2667	1.1	2699	0.6	1.95	1.3	0.185	0.77	13.1	1.5	0.51	1.3	0.89
YK-409_7.1	1.08	264	200	110	0.78	+15	2555	1.1	2926	0.6	2.06	1.3	0.213	0.89	14.3	1.6	0.49	1.3	0.85
YK-409_8.1	0.13	136	88	57	0.67	+5	2560	1.3	2662	0.6	2.05	1.5	0.181	0.88	12.2	1.7	0.49	1.5	0.88
YK-409_9.1	0.22	370	203	150	0.57	+3	2486	1.1	2555	0.6	2.13	1.3	0.170	0.71	11.0	1.4	0.47	1.3	0.90
YK-409_10.1	0.08	140	105	66.7	0.78	+1	2850	1.2	2867	0.5	1.80	1.5	0.205	0.76	15.7	1.6	0.56	1.5	0.91
YK-410_1.1	0.64	55	20	24.8	0.37	+0	2709	1.7	2722	1.1	1.91	2.0	0.188	1.66	13.5	2.5	0.52	2.0	0.78
YK-410_2.1	0.25	180	85	80.6	0.49	+4	2702	0.9	2815	0.7	1.92	1.0	0.199	0.95	14.3	1.3	0.52	1.0	0.73
YK-410_3.1	0.16	248	96	114	0.40	-1	2747	0.9	2720	0.6	1.88	1.1	0.187	0.90	13.7	1.3	0.53	1.1	0.77
YK-410_4.1	0.24	162	221	72.5	1.41	+0	2696	0.9	2707	0.6	1.92	1.0	0.186	0.83	13.3	1.3	0.52	1.0	0.80
YK-410_5.1	0.25	198	186	94.3	0.97	-0	2836	0.8	2834	0.7	1.81	1.0	0.201	1.06	15.3	1.4	0.55	1.0	0.68
YK-410_6.1	0.15	245	191	118	0.81	+1	2870	0.8	2895	0.5	1.78	1.0	0.209	0.69	16.1	1.1	0.56	1.0	0.85
YK-410_6.2	0.19	128	111	57.7	0.90	+0	2716	1.0	2719	0.6	1.91	1.2	0.187	0.88	13.5	1.4	0.52	1.2	0.83
YK-410_7.1	0.36	130	32	52	0.25	+6	2453	0.9	2606	0.9	2.16	1.1	0.175	1.28	11.2	1.7	0.46	1.1	0.63
YK-410_8.1	1.26	605	497	30.7	0.85	+9	366	1.0	398	35.2	17.12	1.0	0.055	6.42	0.4	6.5	0.06	1.0	0.14
YK-410_9.1	0.79	277	249	22.2	0.93	-5	571	1.1	543	22.1	10.79	1.1	0.058	5.42	0.7	5.5	0.09	1.1	0.18
YK-410_10.1	0.54	287	191	70.2	0.69	+1	1604	0.9	1615	2.6	3.54	1.0	0.100	2.24	3.9	2.4	0.28	1.0	0.39
YK-411_1.1	0.02	146	58	66.6	0.41	+1	2749	1.2	2761	2.5	1.88	1.5	0.192	4.21	14.1	4.4	0.53	1.5	0.32
YK-411_2.1	0.00	111	137	6.1	1.28	+51	401	1.5	791	9.1	15.58	1.6	0.066	3.46	0.6	3.8	0.06	1.6	0.41
YK-411_3.1	--	188	115	81.9	0.63	+1	2642	1.1	2671	0.5	1.97	1.3	0.182	0.72	12.7	1.5	0.51	1.3	0.90
YK-411_4.1	0.64	891	220	146	0.25	+60	1128	1.1	2511	4.8	5.23	1.2	0.165	7.20	4.4	7.3	0.19	1.2	0.15
YK-411_5.1	0.00	107	46	55	0.44	-0	3032	1.2	3025	0.5	1.67	1.5	0.226	0.71	18.7	1.6	0.60	1.5	0.92
YK-411_6.1	--	171	122	71.3	0.74	+0	2550	1.2	2552	0.7	2.06	1.4	0.169	0.89	11.3	1.6	0.49	1.4	0.86
YK-411_7.1	0.00	158	388	66.9	2.54	+3	2585	1.1	2651	0.6	2.03	1.4	0.180	0.75	12.2	1.5	0.49	1.4	0.90
YK-411_8.1	0.07	728	554	257	0.79	+19	2219	1.1	2634	0.5	2.43	1.2	0.178	0.56	10.1	1.3	0.41	1.2	0.95
YK-411_9.1	0.00	407	289	131	0.73	+0	2050	1.1	2052	0.7	2.67	1.2	0.127	0.75	6.5	1.4	0.37	1.2	0.88
YK-411_10.1	0.07	781	661	111	0.87	+64	984	20.0	2426	0.6	6.06	21.6	0.157	0.73	3.6	21.6	0.16	[illegible]	1.00
YK-412_1.1	0.00	60	25	9.96	0.43	+1	1136	1.9	1151	0.4	5.19	2.0	0.078	3.11	2.1	3.7	0.19	2.0	0.54
YK-412_2.1	0.11	795	253	101	0.33	+36	889	1.1	1341	1.5	6.76	1.2	0.086	1.07	1.8	1.6	0.15	1.2	0.76
YK-412_3.1	0.12	578	61	72.7	0.11	+53	881	1.1	1733	0.9	6.83	1.1	0.106	0.87	2.1	1.4	0.15	1.1	0.81
YK-412_4.1	0.01	563	312	235	0.57	+4	2555	1.0	2649	0.4	2.06	1.1	0.180	0.52	12.0	1.2	0.49	1.1	0.95
YK-412_5.1	0.00	134	51	62.6	0.39	+0	2807	1.1	2809	0.6	1.83	1.4	0.198	0.87	14.9	1.6	0.55	1.4	0.86
YK-412_6.1	0.05	114	66	70.6	0.60	+2	3506	1.2	3565	0.5	1.38	1.5	0.319	0.77	31.8	1.7	0.72	1.5	0.91
YK-412_6.2	0.00	117	102	74.6	0.91	-1	3591	1.2	3566	0.5	1.34	1.5	0.319	0.68	32.8	1.6	0.75	1.5	0.94
YK-412_7.1	0.06	832	185	252	0.23	+3	1949	1.1	2002	0.6	2.83	1.2	0.123	0.62	6.0	1.3	0.35	1.2	0.92
YK-412_8.1	0.00	192	91	99.4	0.49	+3	3042	1.2	3112	0.5	1.66	1.4	0.239	0.68	19.9	1.5	0.60	1.4	0.93
YK-412_9.1	0.00	104	83	26.7	0.82	+2	1686	1.5	1715	1.9	3.34	1.7	0.105	1.75	4.3	2.4	0.30	1.7	0.69

Note:
Pbc and Pb* indicate the common and radiogenic portions, respectively.
Errors in TEMORA Standard calibration were 0.44% for YK-410 samples and 0.39% for all other samples.
(1) Corrected for common Pb using measured ^{204}Pb. Errors (1 sigma %) include TEMORA standard calibration errors.

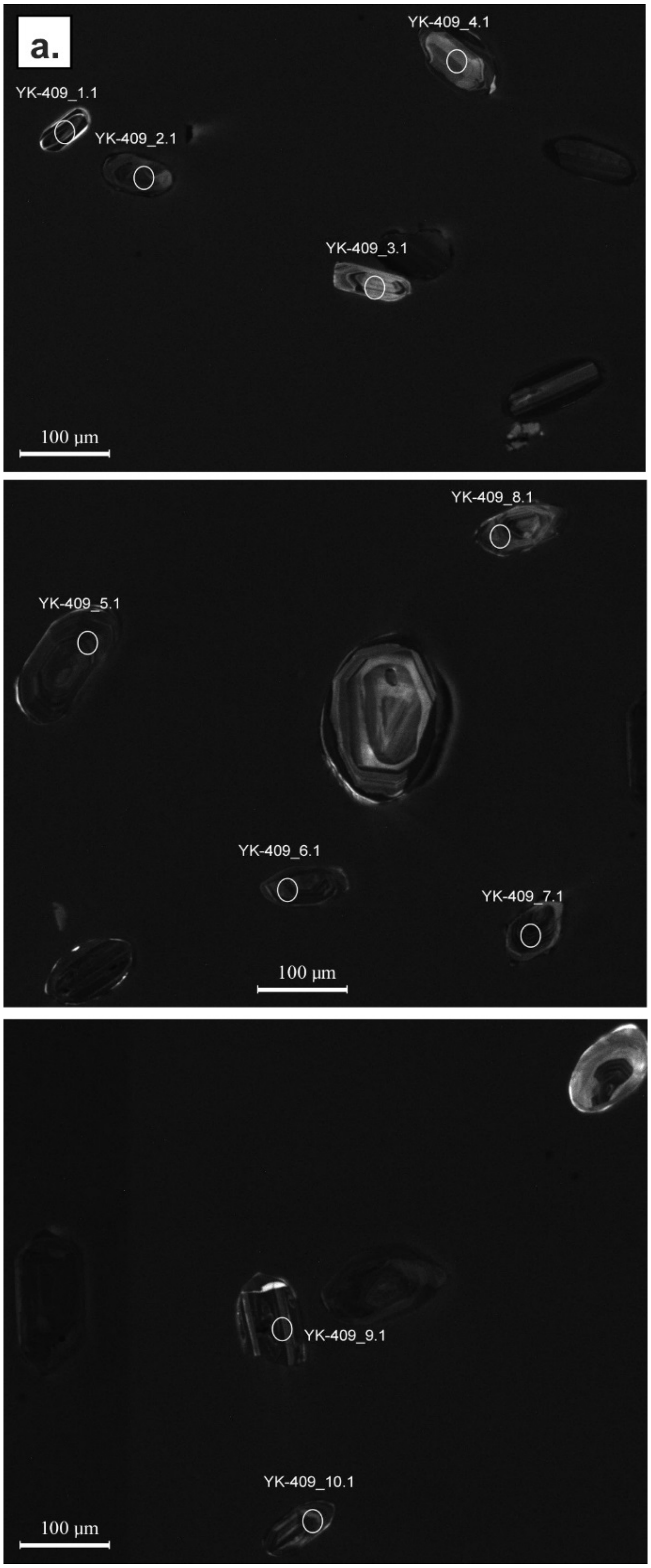

Figure 10. Cathodoluminescence images of zircon crystals analyzed by sensitive high-resolution ion microprobe (SHRIMP) from sample AR9-1 (lab ID YK-409), collected from the middle of the 30 m thick sill of biotite-olivine dolerite emplaced along the contact between the Appekunny and Grinnell formations, west side of Yarrow Creek.

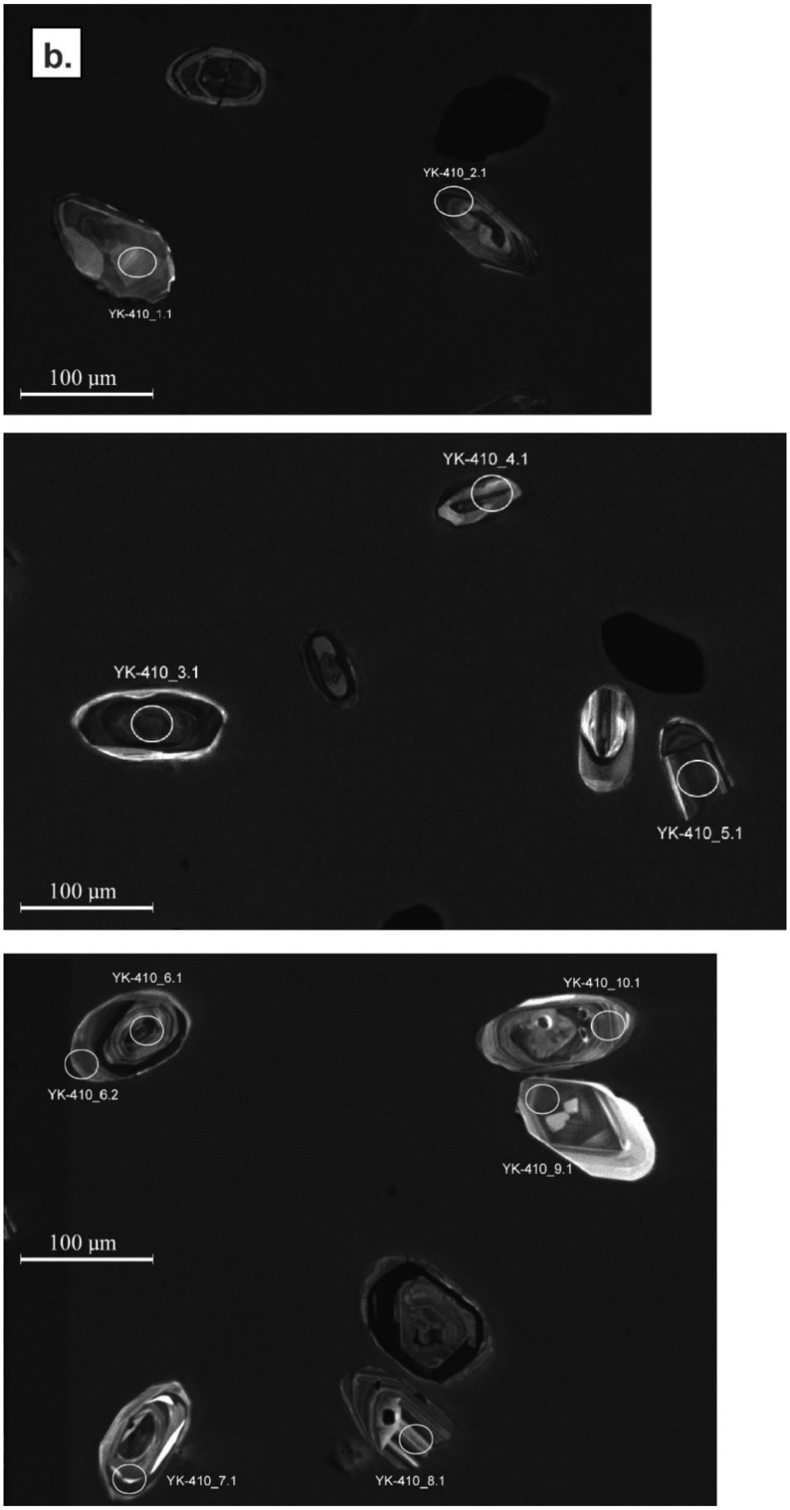

Figure 11. Cathodoluminescence images of zircon crystals analyzed by sensitive high-resolution ion microprobe (SHRIMP) from sample AR9-2 (lab ID YK-410), collected from the olivine-hornblende microgabbro sill that intruded within green-laminated dolomitic sandstone and siltstone units of the Roosville Formation, La Coulotte Peak.

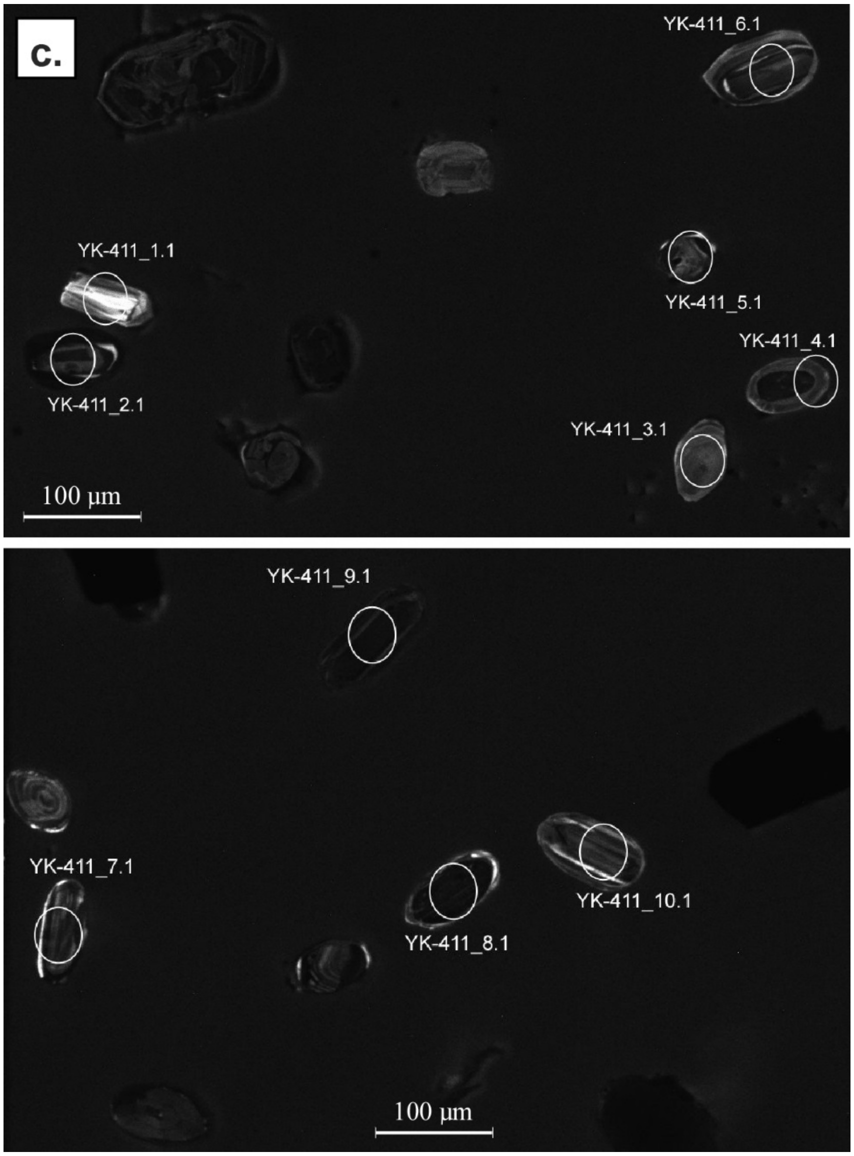

Figure 12. Cathodoluminescence images of zircon crystals analyzed by sensitive high-resolution ion microprobe (SHRIMP) from sample AR9-3 (lab ID YK-411), collected from the olivine-hornblende microgabbro sill intruded within interbedded green, grey and pink sandstones of the Gateway Formation, Pincher Ridge.

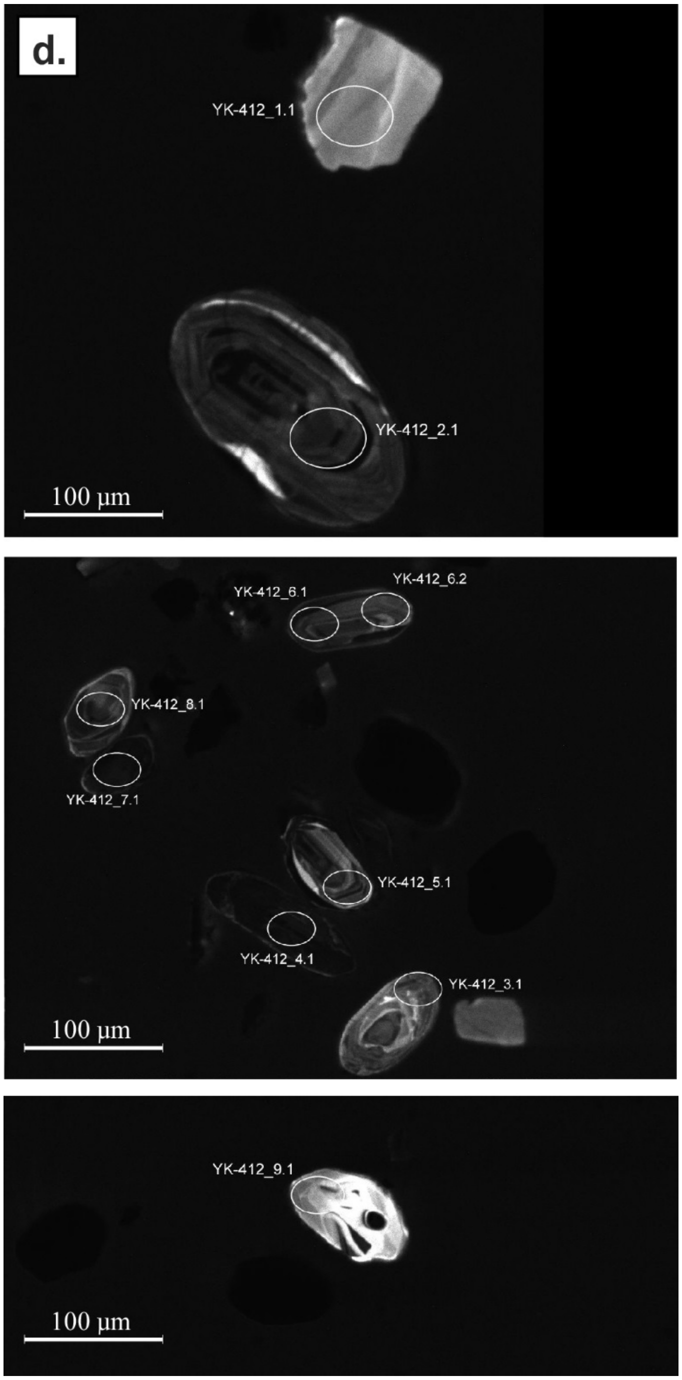

Figure 13. Cathodoluminescence images of zircon crystals analyzed by sensitive high-resolution ion microprobe (SHRIMP) from sample AR9-4 (lab ID YK-412), collected from the olivine-hornblende microgabbro sill intruded within interbedded dolostone and argillite units of the Siyeh Formation, Cloudy Ridge.

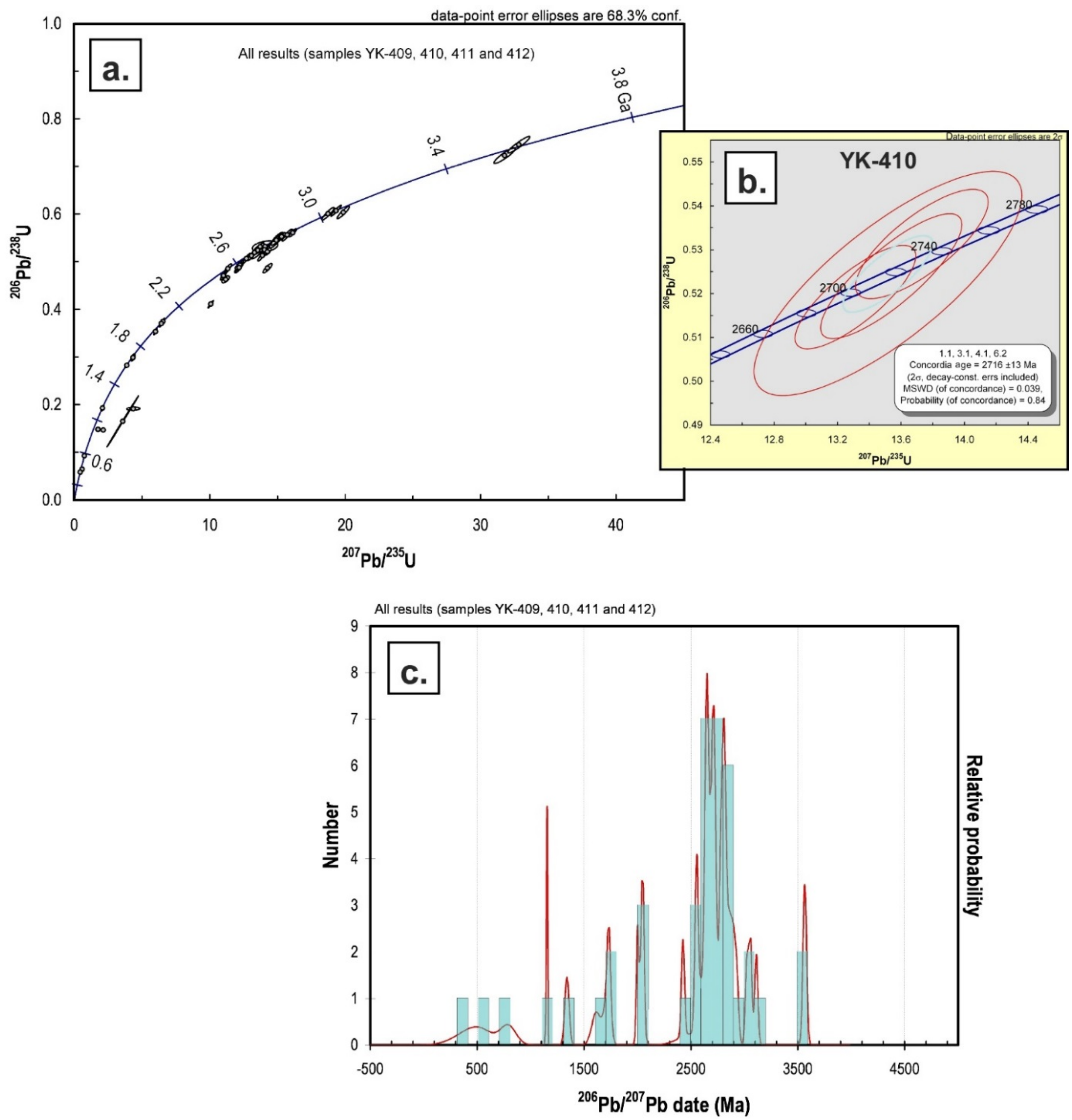

Figure 14. a) Concordia diagram with all sensitive high-resolution ion microprobe (SHRIMP) analyses on zircon grains from Purcell sills. b) Concordia diagram for the overgrowth rims of zircon grains in sample AR9-2 (YK-410). c) Frequency histogram with all SHRIMP zircon ages from Purcell sills.

- Paleoarchean: ca. 3.6 Ga (well-defined 3564±15 Ma, sample AR9-4)
- Mesoarchean:
  a) slightly older than 3.0 Ga (3060 Ma, sample AR9-1; 3030 Ma, sample AR9-3; 3040 Ma, sample AR9-4)
  b) late Mesoarchean, ca. 2.9-2.8 Ga (2926, 2867, and 2813 Ma, sample AR9-1; 2895 Ma core, and 2834 and 2815 Ma, sample AR9-2; 2809 Ma, AR9-4)
- Neoarchean:
  a) early Neoarchean, ca. 2.8-2.6 Ga (2796, 2775, and 2699 Ma, sample AR9-1; 2606 Ma and the 2716 ±13 Ma overgrowth age, sample AR9-2; 2761, 2671, 2651, and 2631 Ma, sample AR9-3; 2649 Ma, sample AR9-4)
  b) late Neoarchean, ca. 2.5 Ga (2555 Ma, sample AR9-1; 2511 and 2552 Ma, sample AR9-3)
- Paleoproterozoic:
  a) middle Paleoproterozoic, ca. 2.0 Ga (2042 Ma, sample AR9-1; 2052 Ma, sample AR9-3; 2002 Ma, sample AR9-4)
  b) latest Paleoproterozoic, ca. 1.7 Ga (1733 and 1715 Ma, sample AR9-4)

The age groups older than the ca. 1.47–1.43 Ga age range of precisely dated Purcell sills (including the 1436 ±1 Ma Yarrow Creek sill) are from inherited/assimilated xenocrysts, whereas the younger ages (from zircon grains with distinctive morphology?) record postemplacement thermal/metasomatic disturbances.

The Archean to Paleoproterozoic zircon xenocrysts (2050 Ma to ca. 3564 Ma) could have been assimilated by the Purcell mafic sills either 1) directly from the autochthonous Laurentian Archean and Proterozoic crust and upper mantle, including gneiss and deep-seated plutonic rocks; and/or 2) from the variously mixed populations of Laurentian-origin detrital zircon in the Mesoproterozoic Purcell platformal strata on the east shoulder of the Belt-Purcell basin. The latest Paleoproterozoic ages of 1733 Ma and 1715 Ma (sample AR9-4) are in an age group characteristic of terrains to the southwest of the present Belt-Purcell Supergroup, which suggests a more distant provenance. Similarly, the 1615 Ma zircon (sample AR9-2) falls near the ca. 1610–1490 Ma North American magmatic gap (van Schmus et al., 1993), so it must have a westerly provenance (from the elusive western shoulder of the Belt basin). See Section 5.1.4 for a detailed discussion of possible sources for the zircon xenocrysts.

The 1341 Ma age (sample AR9-4) falls in the 1370–1300 Ma age range of tectonometamorphic events documented in the Belt-Purcell Supergroup. The 1151 Ma zircon grain identified in the Cloudy Ridge sill (sample AR9-4) may suggest a Grenvillian-age disturbance. The 791 Ma (sample AR9-3) age, and the 543 and 398 Ma (sample AR9-2) ages do not have obvious corresponding events nearby and were obtained from suspiciously fresh zircons, likely of magmatic origin. These isolated occurrences of postemplacement zircon ages are suspect because the host platformal-facies strata of the Mesoproterozoic Purcell Supergroup in Clark Range only record very low grade burial metamorphism. They were identified only in samples for which the mineral separation procedures involved table separation but not in the Yarrow Creek sample, which did not go through table separation. The possibility of contamination cannot be completely ruled out (i.e., alien zircon grains?).

5.1.3 Preliminary Results of the $^{40}Ar/^{39}Ar$ Dating of the Purcell Mafic Rocks

The $^{40}Ar/^{39}Ar$ dating of the Purcell Lava yielded complex spectra with Early Ordovician (DP11-17) and latest Permian (DP11-14) integrated (total gas) ages of unclear (if any) geological significance. The sample from the Yarrow Creek sill yielded a feldspar isochron age of ca. 871 Ma and an amphibole plateau age of ca. 710 Ma. A summary of the results is presented in Table 6.

Table 6. Summary of $^{40}Ar/^{39}Ar$ from mafic rocks in the Purcell Supergroup.

Sample No.	Map Unit	Type of Material#	No. of Steps	Integrated Age (Ma)	Preferred Age (Ma)	Method	Fractions Used	%^{39}Ar	$^{40}Ar/^{36}Ar$	∑S* (n-f)
DP11-14	Purcell Lava-B	w.r.	20	256.3 ±2.0						
DP11-17	Purcell Lava-T	w.r.	17	478.1 ±2.0						
DP11-28bt	Yarrow Creek	K-fsp	17	840.1 ±3.1	871.7 ±4.8	Isochron	5–9	28.4	1140 ±420	0.16
	sill	amph	10	715.2 ±2.9	709.6 ±4.0	Plateau	3–7	69.7		1.06

* Goodness-of-fit parameter; f is degrees of freedom (f = 1 for plateaus, f = 2 for isochrons)
# K-fsp, K-feldspar; amph, amphibole; w.r., whole rock

Sample DP11-14 is fine grained, aphanitic, aphyric pillow basalt from the base of the Purcell Lava in the southeastern part of Barnaby Ridge (Figure 3b). A whole-rock chip (P59-004) run in 20 steps gave an integrated age of 256.3 ±2.0 Ma (uppermost Permian), with an integrated Ca/K ratio of 0.873 ±0.002. The very complex age spectrum (Figure 15) indicates that the pillow basalts experienced a complex history up to the Late Cretaceous and do not retain any memory of their Mesoproterozoic emplacement. Although the significance of the apparent ages from the argon-isotope correlation plot is uncertain, they potentially reflect postcrystallization thermal pulses, which could be tentatively assigned to the late Paleozoic, Early Jurassic and Late Cretaceous.

Sample DP11-17 is from the aphanitic and aphyric basalts at the top of the Purcell Lava. A whole rock (P59-006) run in 17 steps gave an integrated Early Ordovician age of 478.1 ±2.0 Ma, with an integrated Ca/K ratio of 1.472 ±0.008 (Figure 15b).

Sample DP11-28bt is from the Yarrow Creek biotite-olivine trachybasalt sill containing large altered phenocrysts of K-feldspar with star texture (Figure 4). A K-feldspar (P59-018) crystal gave a 17-step integrated age of 840.1 ±3.1 Ma, with an integrated Ca/K ratio of 0.736 ±0.005. The best estimate for the age of points 3–9 (which form a V-shaped array) is given by the isochron for fractions 5–9 (with 28.4% of the total ^{39}Ar, S/[n−2] = 0.16) of 871.7 ±4.8 Ma, with an initial $^{40}Ar/^{36}Ar$ ratio of 1140 ±420. This initial $^{40}Ar/^{36}Ar$ ratio is significantly higher than the modern atmospheric value of 295.5, suggesting a complex history of excess argon in the feldspar. Note that both isochron ages obtained from this feldspar are similar to the previously reported K-Ar ages of ca. 800 Ma (Mudge et al., 1968; Ghazi, 1992), which were believed to date the emplacement of a distinct, late diabasic, tholeiitic suite of 'Siyeh-type' sills (Goble et al., 1999).

Due to the complex nature of the above feldspar result from sample DP11-28bt, a second phase was analyzed from this sample. An amphibole (P59-019) run in 10 steps yielded an integrated age of 715.2 ±2.9 Ma, with an integrated Ca/K ratio of 9.98 ±0.03 (Figure 15c). Its integrated age is significantly younger than the associated K-feldspar, and its age spectrum yields a simpler pattern, with fractions predominantly younger than those of the feldspar. There is an apparent plateau age of 709.6 ±4.0 Ma for fractions 3–7 (with 69.7% of the total ^{39}Ar, S/[n−1] = 1.97]. Following this plateau, the ages rise slightly, then sharply to 938.2 ±9.3 [fraction 9 with 2.6% of the total ^{39}Ar] before settling on an age of 600 ±20 Ma in the final fraction.

The Ca/K spectrum of this amphibole peaks at a high value of 29.0 ±0.2 in fraction 6.

On the argon correlation plot, fractions 3–7 (S/[n−2] = 1.06) yield an isochron age of 703.5 ±4.5 Ma, with initial $^{40}Ar/^{36}Ar$ ratio of 387 ±49.

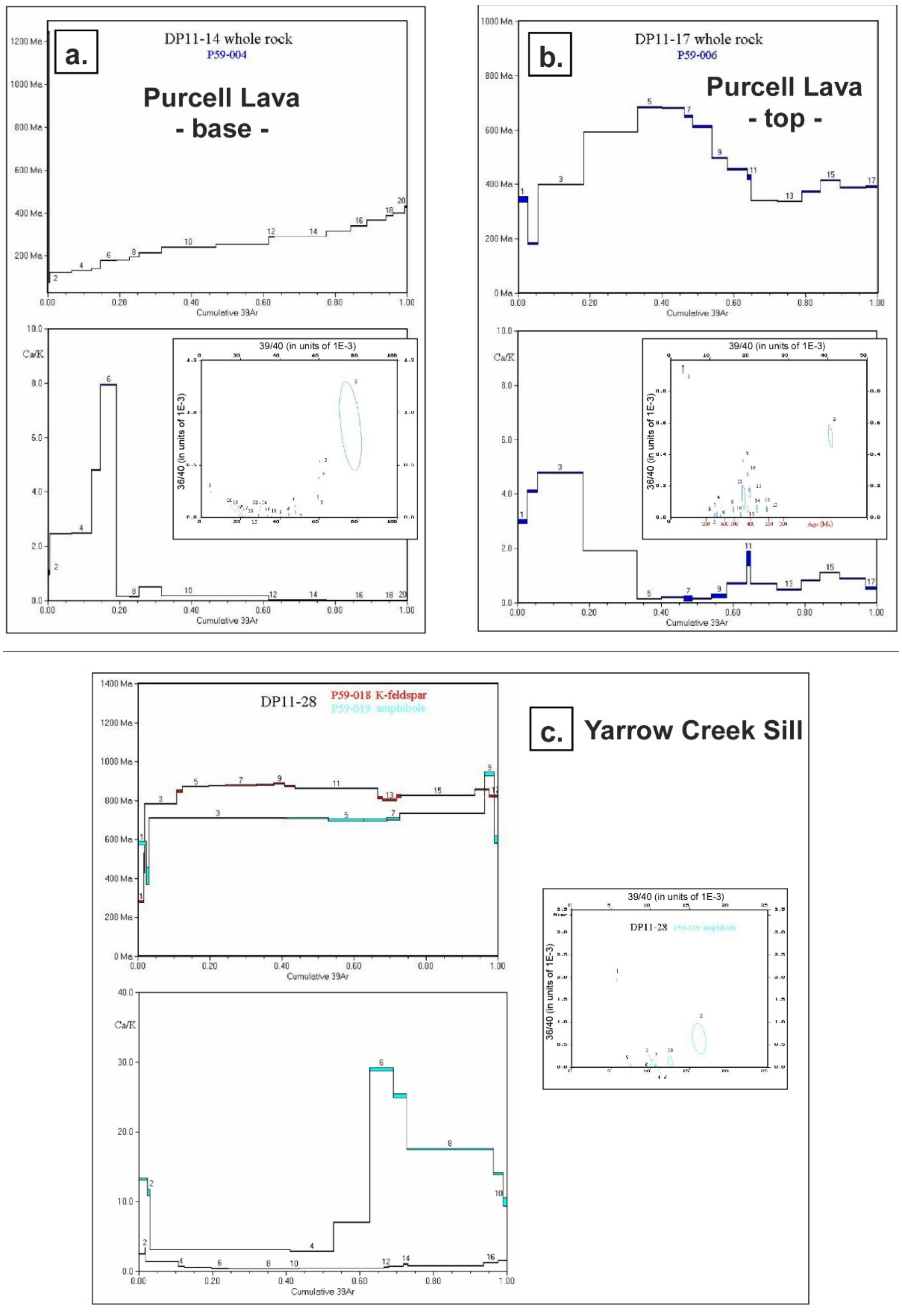

Figure 15. $^{40}Ar/^{39}Ar$ spectra and K/Ca ratios for the samples collected from the Purcell Lava and Yarrow Creek sill: a) whole-rock analysis of sample DP11-14 from pillow basalt at the base of the Purcell Lava on the east side of Barnaby Ridge; b) whole-rock analysis of sample DP11-17 from basalt at the top of the Purcell Lava on the top of Barnaby Ridge; and c) feldspar and amphibole analyses of sample DP11-28bt from the Yarrow Creek sill.

Interpretation of these ages is problematic. If the rock has undergone prolonged slow cooling from high temperature, the amphibole would be expected to yield an older age than the feldspar, given the higher blocking temperature of amphibole compared to K-feldspar. This is opposite to what is seen here, where the best amphibole estimate of 710 ±4 Ma is ~160 m.y. younger than the 872 ±5 Ma K-feldspar age. Although the significance of these ages remains uncertain, we note that hornblende ages (the apparent plateau age of fractions 3–7 is 709.6 ±4.0 Ma and its integrated age is 715.2 ±2.9 Ma) are close to the age range of the granite rocks (740 ±36 Ma to 728 + 8/–7 Ma) that nonconformably underlie the Neoproterozoic Windermere Supergroup (McMechan, 2015). The granites have been related to the Rodinia rifting and break-up, so the hornblende ages may record the same early Cryogenian tectonothermal event, or migration of hot fluids related to such an event.

5.1.4 Possible Sources for Inherited Zircon in the Purcell Mafic Sills

In principle, zircon xenocrysts in the mafic sills could be 1) igneous and metamorphic zircons from the intruded crystalline basement and upper mantle of the Belt-Purcell basin; 2) detrital zircons of igneous and metamorphic origin accumulated in the Belt-Purcell basin at the time of sill emplacement, or 3) zircons from metamorphic events in the early stage of the Belt-Purcell basin development, prior to sill emplacement. These possibilities are discussed in more detail:

1) **The pre-Belt basement** that may have underlain the east and north sides of the basin prior to Cordilleran thrusting is known only from potential-field studies and U-Pb geochronology of drillcore. It includes Archean Wyoming and Proterozoic Great Falls crust of the southwestern Canadian Shield (Villeneuve et al., 1993):

    a) The Wyoming craton consists largely of metaplutonic and metasedimentary rocks with a range of Late Archean U-Pb ages but is dominated by 2.80–2.55 Ga plutonic rocks (Frost et al., 1998). Patterns of Nd residence ages in Upper Archean metasedimentary rocks provide evidence for older crust (older than 3.0 Ga; Frost, 1993), but areas with directly dated old crust are limited to the central and northwestern Wyoming craton (Houston et al., 1993; Aleinikoff et al., 1996, 2015). The Archean Wyoming craton, adjacent to the Great Falls tectonic zone, has been partly overprinted by late Paleoproterozoic thermal events (Catanzaro and Kulp, 1964; Giletti, 1966; O’Neill and Lopez, 1985).

    b) The Great Falls tectonic zone is a northeast-trending geophysical discontinuity that is largely buried by younger cover. Outcrops are known from the Little Belt Mountains near Niehart, Montana, the Highland Mountains, and scattered exposures of basement in southwestern Montana (O’Neill, 1993), and reveal the presence of juvenile Proterozoic plutonic rocks (1.88–1.86 Ga; Mueller et al., 2002). Tectonic events at ca. 1770 Ma that affected the Great Falls tectonic zone include high-grade metamorphism that generated widespread resetting of Ar in minerals, as well as limited magmatism in the northwestern Wyoming craton (Burger et al., 1999).

2) **Detrital zircon in the Belt-Purcell Supergroup** originated, in large part, from a western craton with subordinate input from Laurentian sources to the east and south of the basin (Ross and Villeneuve, 2003; Medig et al., 2014).

    The only detrital zircon data from the Alberta portion of the Purcell Supergroup are from the Grinnell and Siyeh formations, with samples collected from north of Waterton National Park. The 29 grains recovered from the Grinnell sandstone yielded predominantly Proterozoic grains with a few Neoarchean grains, whereas the clean quartz arenite sample from the lower Siyeh Formation yielded 33 grains with a dominant population (23 grains) of Neoarchean ages and fewer Proterozoic grains.

    The dominant Neoarchean population of the Siyeh Formation, with ages between 2756 and 2664 Ma, and the four Neoarchean grains of the Grinnell Formation (2688–2599 Ma) define a range that includes many Neoarchean ages identified in the zircon xenocrysts of the analyzed sills (2671, 2651, and 2631 Ma, sample AR9-3; 2649 Ma, sample AR9-4; and 2606 Ma, sample AR9-2).

A single concordant grain dated at 1995 Ma in the Grinnell sample and two grains in the Siyeh sample with ages of 2016 and 2001 Ma are only slightly younger and partly overlap with the middle Paleoproterozoic ages of 2042 Ma (sample AR9-1), 2052 Ma (sample AR9-3), and 2002 Ma (sample AR9-4) identified in the zircon xenocrysts of the analyzed sills.

The predominant Proterozoic detrital zircons in the Grinnell sample appear to define one group in the 1875–1814 Ma range (12 grains) and another group in the 1798–1749 Ma range (7 grains), whereas the Siyeh sample yielded 6 grains in the 1866–1779 Ma range. Proterozoic zircon ages between 1870 and 1760 Ma could be indicative of derivation from the Trans-Hudson Orogen and the Black Hills (Redden et al., 1990), or from the relatively local Proterozoic rocks of the Great Falls tectonic zone (Mueller et al., 2002). Slightly younger ages identified in zircon xenocrysts from the Purcell sills (1733 and 1715 Ma, sample AR9-4) may belong to this late Paleoproterozoic group.

All other age groups identified in the zircon xenocrysts of the Clark Range sills have been reported from detrital zircons in the Belt-Purcell Supergroup by Ross and Villeneuve (2003):

- Paleoarchean ages similar to the well-defined 3564 ±15 Ma age (sample AR9-4) have been found in the sandstone sheet at the base of the supergroup (3612 Ma, Niehart Quartzite; ca. 3524–3450 Ma, Lower Purcell), and a 3491 Ma age was found towards its top (Garnet Range Formation).
- Mesoarchean ages of 3060 Ma (sample AR9-1), 3030 Ma (sample AR9-3), 3040 Ma (sample AR9-4), and 2926 Ma (AR9-1) are known in the Lower Purcell (2968–2920 Ma); in contrast, the late Mesoarchean cluster around ca. 2.9–2.8 Ga (2926, 2867, and 2813 Ma, sample AR9-1; 2895 Ma core and 2834 and 2815 Ma, sample AR9-2; and 2809 Ma, sample AR9-4) is not common in the detrital zircon populations.
- Neoarchean ages of ca. 2.8–2.6 Ga (2796, 2775, and 2699 Ma, sample AR9-1; 2606 Ma and the 2716±13 Ma overgrowth age, sample AR9-2,; 2761, 2671, 2651, and 2631 Ma, sample AR9-3; 2649 Ma, sample AR9-4; 2555 Ma, sample AR9-1; and 2511 and 2552 Ma, sample AR9-3) are known from the Niehart Quartzite (2700 Ma and 2663 Ma), Fort Steele Formation (2794–2517 Ma) and, farther away, the Lower Purcell sandstones of the Helena embayment (Greyson Formation, 2661–2577 Ma) and the turbidite sequence in the main branch of the basin in the Aldridge (2654–2584 Ma; 4 grains) and Prichard (2551 and 2509 Ma) formations.
- Middle Paleoproterozoic xenocryst ages slightly older than 2.0 Ga (2042, 2052, and 2002 Ma) partly overlap with the detrital zircon reported from the Grinnell and Siyeh formations (2016, 2001, and 1995 Ma) and also from the Aldridge Formation (2064–2037 Ma).
- Xenocrysts ages of 1733 and 1715 Ma from the Cloudy Ridge sill sample (AR9-4) overlap with the 1739–1694 Ma (18 grains) range found in the Garnet Range Formation, which may be sourced in pre-Belt magmatic rocks that are widespread in the southwestern United States (Karlstrom and Bowring, 1993).

Late Proterozoic age ranges of 1876–1744 Ma (10 grains) in the Aldridge Formation and 1818–1740 Ma (6 grains) in the Prichard Formations have not been found in the Clark Range sills emplaced on the east shoulder of the basin. Instead, the late Mesoarchean cluster of xenocrysts in the Clark Range sills is missing from the detrital populations, which indicates a source in the local crust or upper mantle. The fresh ca. 1615 Ma zircon grain from the La Coulotte sill (AR9-2) is close to the 1611–1540 Ma (16 grains) age range identified in the Prichard Formation; these ages fall within the North American magmatic gap (Van Schmus et al., 1993) and therefore may have been assimilated from Purcell strata that received an influx of sediment from the western craton (Ross and Villeneuve, 2003).

3) **Metamorphic zircon** could have been assimilated in the 1.47–1.43 Ga Purcell sills from rocks (both early Belt-Purcell strata and their basement) overprinted by metamorphism during the tectonic events that led to the initiation of the Belt-Purcell basin. There is abundant evidence for Mesoproterozoic events in the earliest history of the Belt-Purcell basin: Zirakparvar et al. (2010) reported diverse Lu-Hf garnet ages of 1463 ±24 Ma from northern Idaho; Ramos and Rosenberg (2012) reported a Sm-Nd isochron age of siderites from 1511 ±45 Ma ore-bearing veins, a Pb-Pb isochron age of carbonates from 1523 ±41 Ma ore-barren veins, and a xenotime-core laser-ablation age of 1420 ±90 Ma, which are similar to the model age of Coeur d'Alene–type Pb mineralization (ca. 1450 Ma). Similar early Mesoproterozoic events were inferred based on Pb isotopes (Leach et al., 1998), $^{40}Ar/^{39}Ar$ ages (Rosenberg and Larson, 2000), and field relationships (Harrison, 1972; Harrison et al., 1974).

   Zircon younger than the 1.47–1.43 Ga Purcell sills could record postemplacement tectonothermal events, particularly if they coincide with metamorphic events already documented elsewhere, such as U-Pb ages of 1360–1330 Ma and 1090–1030 Ma from metamorphic titanites in Moyie sills that intrude the lower Purcell Supergroup in southeastern British Columbia (Ross et al., 1992; Anderson and Davis, 1995).

   In the Alberta portion, the Purcell Supergroup is not metamorphosed. In Montana, lower-greenschist facies metamorphism was inferred to be of Grenvillian age (González-Álvarez and Kerrich, 2012). Elsewhere in the Belt-Purcell Supergroup, Grenvillian-age events (ca. 1000 Ma) have been interpreted as static thermal metamorphism (e.g., Anderson and Davis, 1995; Anderson and Parrish, 2000; Aleinikoff et al., 2007; Doughty and Chamberlain, 2008). The evidence comprises ages of xenotime in quartz veinlets and xenotime overgrowths dated at 990 ±130 Ma in ore-barren carbonate veins (Ramos and Rosenberg, 2012) and mica $^{40}Ar/^{39}Ar$ ages of 1.0 Ga (Leach et al., 1998; Rosenberg and Larson, 2000). Two samples of garnet mica schist collected within the staurolite+kyanite isograd and a gem-grade Idaho star garnet sample from a placer, all from the Wallace Formation of the Belt-Purcell Supergroup near Clarkia, Idaho, yielded Lu-Hf garnet ages of 1064 ±10, 1081 ±20, and 1078 ±17 Ma, respectively (Zirakparvar et al., 2010).

   Cretaceous age event(s) are based on Sr isotopes (Fleck et al., 2002), stable isotopes (Eaton et al., 1993, 1995), field relationships (White, 1998), and U-Pb and Pb/Pb zircon dates of ca. 136 ±2 Ma from jasperoid veins at the Sunshine Mine (Coeur d'Alene mining district in northern Idaho), interpreted as second-generation mineralization (Zartman and Smith, 2009).

5.2 Isolated Dikes and Sills in the Miette Group

As discussed in Section 4.2, the samples from the isolated mafic intrusions in the Miette Group did not yield U-Pb–datable minerals. Analyses by $^{40}Ar/^{39}Ar$ were only performed on the Crowfoot dike sample (DP11-10; Table 7) but not on the highly altered samples from the Geikie and Blackbear intrusions.

A whole rock (P59-002) run in 10 steps gave an integrated age of 3817 ±28 Ma, with a high integrated Ca/K ratio of 226 ±4 (Figure 16). Its age spectrum starts at an apparent age of 6.2 ±0.1 Ga, and then plummets to 2.46 ±0.15 Ga. High-temperature fractions 7–10 yielded an apparent plateau with average age of 3869 ±24 Ma (with 42.9% of the total ^{39}Ar, S/[n−1] = 0.26).

Its Ca/K spectrum starts at 12.9 ±1.3, then climbs to a maximum of 836 ±39 (fraction 7) before falling to a final value of 150.7 ±3.0 (fraction 10).

There are no isochrons apparent on the $^{39}Ar/^{40}Ar$ versus $^{36}Ar/^{40}Ar$ correlation diagram. Also plotted with the whole-rock data is a sample of plagioclase analyzed in two steps (P59-003; see Appendix 1) and

Table 7. Summary of $^{40}Ar/^{39}Ar$ data from the Crowfoot dike.

Sample No.	Type of Material#	No. of Steps	Integrated Age (Ma)	Preferred Age (Ma)	Method	Fractions Used	^{39}Ar (%)	$^{40}Ar/^{36}Ar$	∑S* (n-f)
DP11-10	w.r.	10	3817 ±28	3869 ±24	Plateau	7-10	42.9		0.26

w.r.- whole rock.
* Goodness-of-fit parameter; f is degrees of freedom: f = 1 for plateaus, f = 2 for isochrons

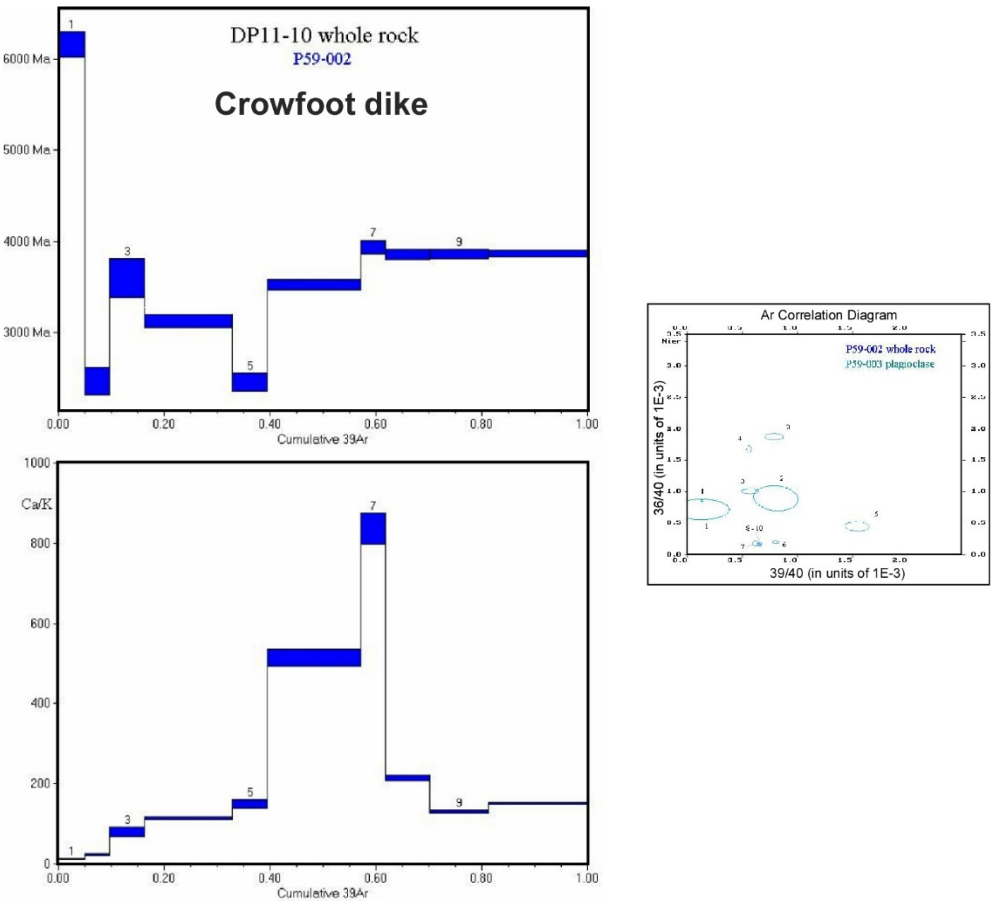

Figure 16. $^{40}Ar/^{39}Ar$ data for the Crowfoot dike.

yielding an integrated age of 4190 ±640 Ma with Ca/K = 91 ±36 (Figure 16, in blue). This analysis is very much depleted in ^{39}Ar and consequently does not provide any more useful information pertaining to the sample's age.

Because the Crowfoot dike intrudes the Neoproterozoic Miette Group, the Archean and Paleoproterozoic whole-rock and plagioclase $^{40}Ar/^{39}Ar$ ages are geologically meaningless.

5.3 Cretaceous Sills

5.3.1 U-Pb Dating of the Largest Felsic Alkaline Sill in Clark Range

Of the three samples from alkaline intrusions of inferred Cretaceous age, only sample DP11-34 provided mineral phases amenable to U-Pb dating. Many zircons had old cores and some grains were entirely xenocrystic. The sources for zircon xenocrysts in the Cretaceous sills include crystalline basement and Mesoproterozoic–Cretaceous strata. Hence, a wide range of detrital zircon could have been incorporated in the alkaline intrusive rocks of the southern Alberta Rockies. The U-Pb ages of detrital zircons that accumulated in the Neoproterozoic–Permian ‘miogeoclinal’ strata along the Canadian Cordilleran margin in British Columbia and Alberta are mainly >1.75 Ga (Gehrels and Ross, 1998). These are interpreted to have been derived from nearby basement provinces, with most grains probably cycled through one or more sedimentary units prior to final deposition. For example, the 2464–2344 Ma age interval corresponds to the ‘Arrowsmith orogeny’ of the western Churchill Province (Berman et al., 2005). Also common in the region are grains in two age intervals that do not correspond to igneous rocks of the western Canadian Shield: ca. 1053–1030 Ma derived from Grenvillian-age sources and 1774–1750 Ma derived from other unrecognized plutons that may be present beneath strata of the Western Canada Sedimentary Basin or from unknown terranes to the west.

Therefore, the focus of the analytical work was on dating zircon overgrowths (Figure 17). Twelve of 34 laser-ablation spot analyses (most from the oscillatory-zoned parts of the grain) give a Tera-Wasserburg plot date of 105.8 ±4.7 Ma (Figure 17a), which is interpreted to be the best age estimate for the sample by this technique. The weighted average date (Figure 17c) is slightly higher, which may be due to slightly older $^{206}Pb/^{238}Pb$ dates in some grains resulting from possible leakage of old radiogenic Pb out from the cores.

The results of ID-TIMS analyses at the University of Alberta on a titanite fraction consisting of 18 crystal fragments are summarized in Table 8.

The U-Pb ages obtained from zircon overgrowths and titanite of this intrusion overlap with the garnet date obtained from the alkaline pyroclastic rocks of the Crowsnest Formation (see Section 5.4). This sill may be part of the mid-Cretaceous igneous suite, one of the subvolcanic channelways that acted as feeders to the Crowsnest volcanic rocks.

5.3.2 $^{40}Ar/^{39}Ar$ Dating of the Crowsnest Lake Trachyte (DP11-26)

Sample DP11-26 (Table 9) is an alkali trachyte with 1–2 mm feldspar phenocrysts that intruded Paleozoic carbonates near Crowsnest Lake. A whole-rock chip (P59-010) run in 14 steps gave an integrated age of 54.9 ±0.3 Ma, with an integrated Ca/K ratio of 0.0830 ±0.0008 (Figure 18).

A sample of fresh K-feldspar (P59-009) run in 9 steps gave an integrated age of 67.9 ±0.3 Ma, with an integrated Ca/K ratio of 0.0129 ±0.0004. Its Ca/K plot shows uniformly low ratios, averaging 0.007 ±0.002 for fractions 1–8. A somewhat elevated ratio of 0.30 ±0.02 is apparent for the final fraction. The age spectrum for this sample is simple and features a plateau averaging 69.1 ±0.7 Ma (Maestrichtian age) for fractions 5–9 (with 56.5% of the total ^{39}Ar, $S/[n-1] = 6.47$). The somewhat high value of $S/(n-1)$ associated with this average reflects the very slight progressive age increase with increasing temperature. Assuming that the slight tilt reflects argon loss, this high-temperature plateau would represent the best estimate of the feldspar crystallization age.

In context, however, the interpretation of this $^{40}Ar/^{39}Ar$ plateau age of 69.1 ±0.7 Ma is less straightforward because the only Late Cretaceous felsic intrusions are far to the west in British Columbia, beyond the western limit of the sketch map in the inset of Figure 7. Also noteworthy is a similar age of 69.3 ±6 Ma reported for authigenic clays in the Lower Cretaceous Luscar shale of the Alberta Foothills in the footwall of the McConnell Thrust (Pană and van der Pluijm, 2015). The Crowsnest Lake trachyte sill is in a similar position in the footwall of the 72.3 ±2.3 Ma Lewis Thrust, so both ages could be related to hot ‘fluids flush’ in the foreland triggered by thrusting/tectonic loading in the approaching fold-and-thrust belt. This interpretation is consistent with the low-grade metamorphism (temperatures in the 180–280°C range and pressures of 0.15–0.3 GPa; Bégin et al., 1995a, b) and metasomatism that overprinted the nearby Crowsnest volcanic rocks (within less than 10 km). Within a sequence a few kilometres thick

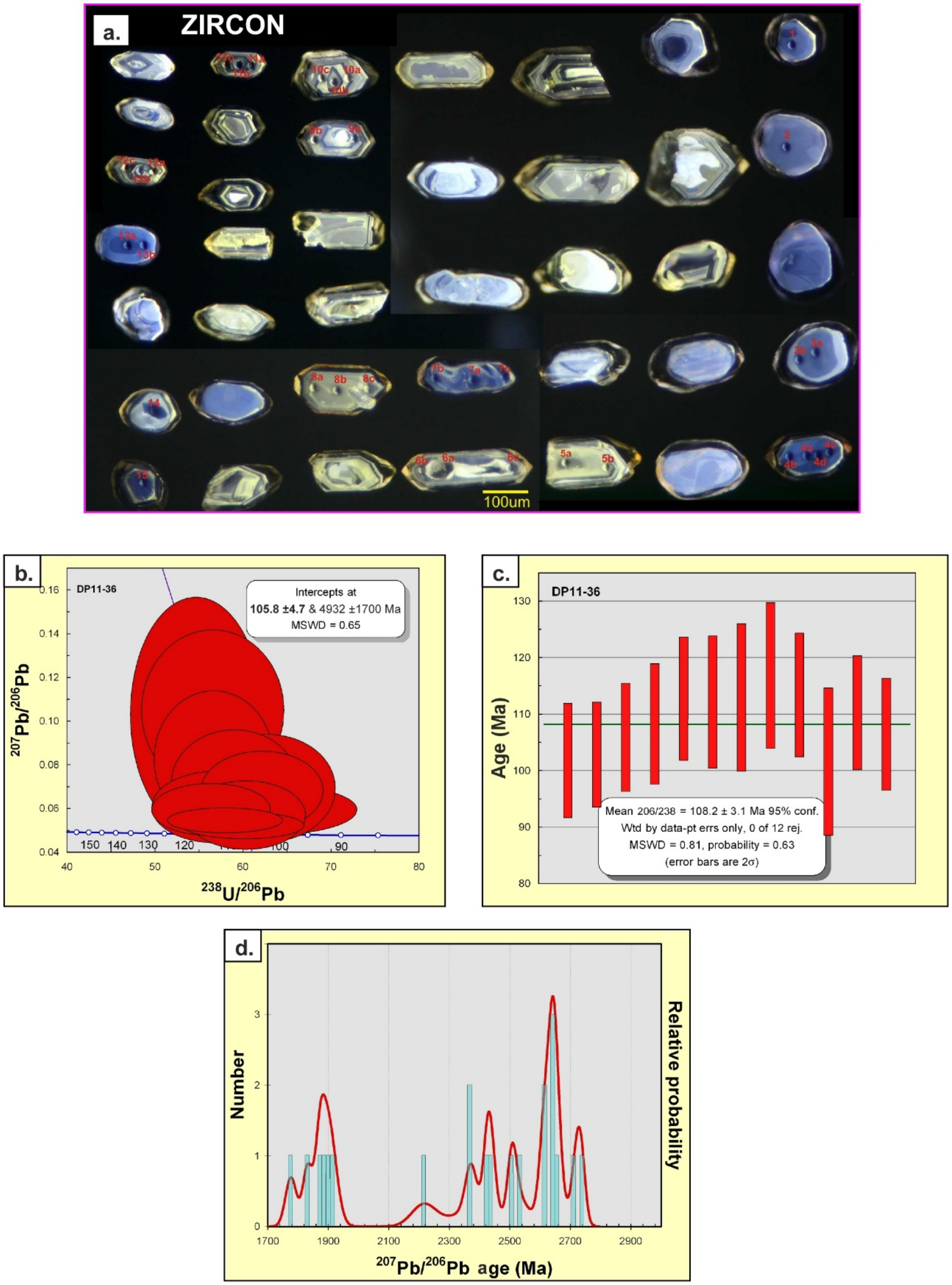

Figure 17. a) Cathodoluminescence image of zircon grains from the large Cretaceous sill analyzed by laser ablation; many zircons have old cores and some grains are entirely xenocrystic; note the oscillatory zoning on the outside of some cores, which we interpret to be igneous growth. b) Tera-Wasserburg plot of zircon overgrowth analyses. c) Weighted average $^{206}Pb/^{238}Pb$ data. d) Probability density plots of the old grains and cores give some sense of the range of inheritance.

Table 8. Summary of U-Pb data from the titanite trachyte sill DP11-36 at Crowsnest Lake.

Descrip-tion	Weight (mg)	U (ppm)	Th (ppm)	Pb (ppm)	Th/U	TCPb (pg)	$^{206}Pb/^{204}Pb$	1σ	$^{238}U/^{204}Pb$	1σ	$^{206}Pb/^{238}U$	1σ	Model Age $^{206}Pb/^{238}U$ (Ma)	1σ
18 yellow fragments	114.5	32	54	2	1.71	97	57.970	0.661	2462.72	40.65	0.01601	0.00008	102.4	0.5

Table 9. Summary of $^{40}Ar/^{39}Ar$ from the Crowsnest Lake trachyte sill.

Sample No.	Type of Material#	No. of Steps	Integrated Age (Ma)	Preferred Age (Ma)	Method	Fractions Used	^{39}Ar (%)	∑S* (n-f)
DP11-26	w.r.	14	54.9 ±0.3	64.0 ±0.7		5-7	6.5	0.37
	K-fsp	9	67.9 ±0.3	69.1 ±0.7	Plateau	5-9	56.5	6.47

* Goodness-of-fit parameter; f is degrees of freedom (f = 1 for plateaus, f = 2 for isochrons)
# K-fsp, K-feldspar; w.r., whole rock.

beneath an ~15 km thick Lewis thrust sheet, temperatures could have reached around 200°C within a few million years after the thrust emplacement (Oxburgh and Turcotte, 1974; Hoffman et al., 1976). Therefore, we tentatively interpret the $^{40}Ar/^{39}Ar$ plateau age of ca. 69 Ma as the time of albitization controlled by burial and hot fluid squeezed from underneath, and migrating in front of, the ca. 72 Ma Lewis Thrust.

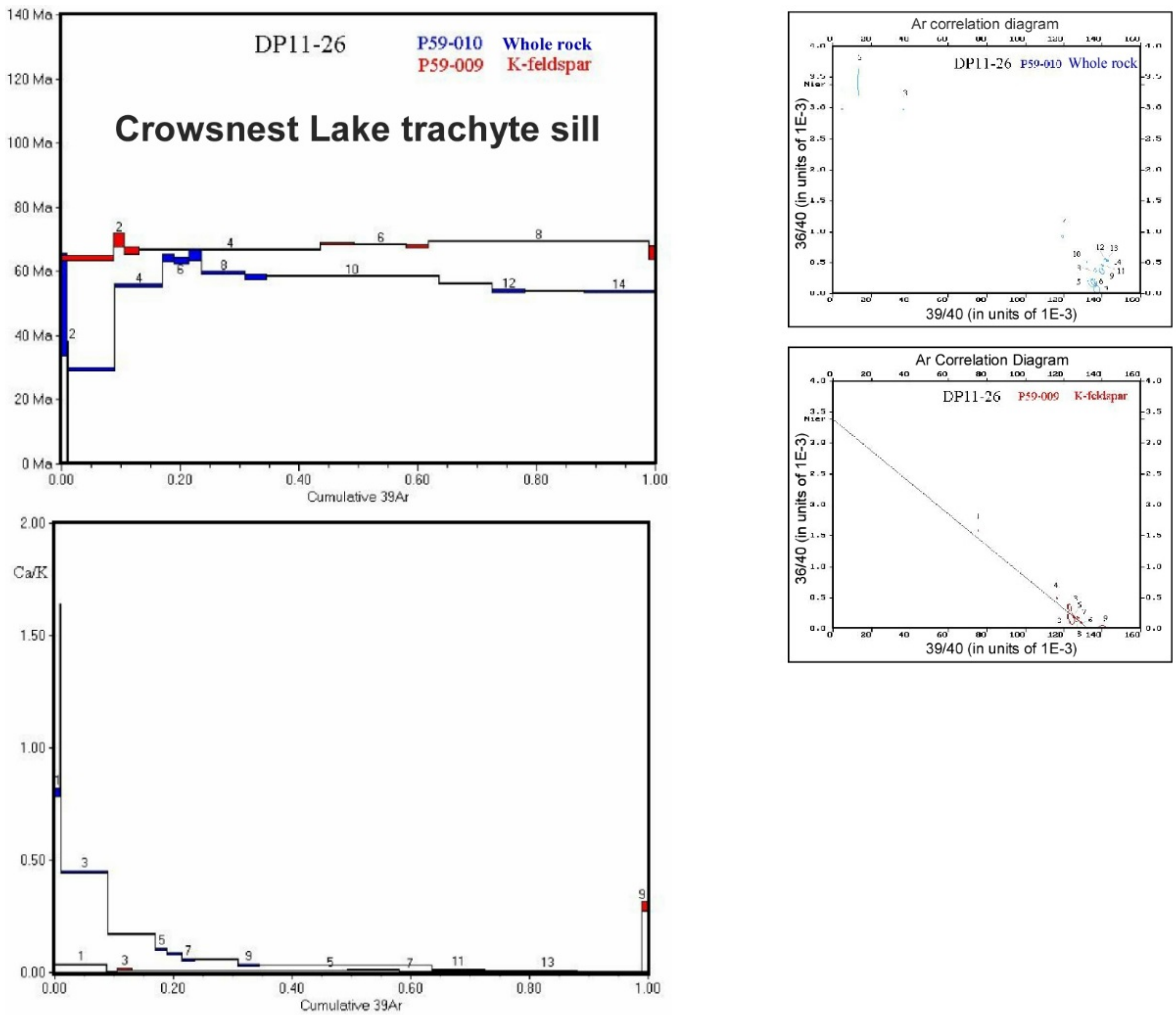

Figure 18. $^{40}Ar/^{39}Ar$ spectrum for the Crowsnest Lake trachyte sill.

5.4 Age of Melanite Garnet from the Crowsnest Formation.

Table 10 includes the summary of U-Pb analytical data for two Crowsnest melanite garnet analyses. The weighted average $^{206}Pb/^{238}U$ age using these two analyses is 102.9 ±1.1 Ma (2σ).

Table 10. U-Pb garnet results for Crowsnest volcanics, Alberta

Description	Weight (µg)	U (ppm)	Th (ppm)	Pb (ppm)	Th/U	TCPb (pg)	$^{206}Pb/^{204}Pb$	$^{206}Pb/^{238}U$	$^{206}Pb/^{238}U$ Age (Ma)
1) dark brown euhedral M@0.2A (20)	390	8.3	11.0	0.5	1.3	122	46.92	0.01601 ±11	102.4 ±0.7
2) dark brown euhedral M@0.2A (20)	302	6.2	2.7	0.4	0.4	89	42.21	0.01624 ±16	103.8 ±1.0
All errors in this table reported at 1σ Abbreviation: M@0.2A (20), magnetic fraction separated at 0.2 A									

Crowsnest eruptions that emplaced the lower member were cyclical, beginning with an explosive phase that destroyed previously emplaced vent-facies effusive rocks. Pyroclastic flow, surge, and fallout deposits were emplaced during these early stages. The eruptions that emplaced the upper member produced pyroclastic flows and the thick, vent-proximal breccia deposits. Vent facies and portions of the previously emplaced pyroclastic material were incorporated in the deposits as fragments, along with juvenile material and xenoliths torn from conduit walls (accidental fragments).

The heterolithic fragments characteristic of these Crowsnest volcanic deposits were incorporated from the destruction of conduit plugs and vent-facies effusive deposits. Clasts of crystal-rich material from the magma chamber and accidental fragments were carried by the rising magma and incorporated as lithic components in the pyroclastic deposits. As the eruptions progressed, they became less gas charged and effusive, emplacing coarsely porphyritic vent-facies plugs, domes, spines, and flows that were subsequently destroyed by the next eruptive cycle.

Because the Crowsnest Formation consists of pyroclastic deposits resulting from cyclical eruptions, the age of deposition must be the same as the age of the pyroclastic material. The melanite garnet is present throughout the pyroclastic deposits, which suggests that it represented a common mineral phase in the magma chamber from which fragments (clasts) were carried by the rising magma and incorporated as lithic components in the pyroclastic deposits. This argues for very similar ages of the melanite xenocrysts and the pyroclastic material, rather than accidental fragments (xenoliths) torn from older conduit walls.

If the age of the pyroclastic material is close to or the same as that of the melanite xenocrysts, then the age of the Crowsnest Formation is ca. 103 Ma. This is slightly older than the 100.5 Ma age of the Albian–Cenomanian boundary (Cohen et al., 2013), which constrains the partly equivalent upper Mill Creek Formation to be upper Albian; hence, it probably does not straddle the Lower–Upper Cretaceous boundary as proposed by Burden and Leckie (2001).

5.5 Contemporaneous and Petrologically Similar Intrusive and Volcanic Rocks in the Southern Canadian Rockies

The titanite crystallization age of ca. 102.4 ±0.5 Ma obtained from the largest trachyte sill in the Clark Range alkaline swarm corresponds within error to the U-Pb age of 102.9 ±1.1 Ma obtained from the melanite garnet of Crowsnest volcanic rocks. The Rainy Ridge melanite-analcime phonolite sill (emplaced in the Proterozoic Gateway Formation), which is part of the alkaline swarm, has mineralogical and chemical characteristics that strongly support a genetic link with the analcime phonolite and blairmorites of the mid-Cretaceous Crowsnest volcanics (Goble et al., 1993). The presence of analcime and melanite garnet in both the blairmorite of the Crowsnest volcanic suite and the Rainy Ridge subvolcanic rock is a striking similarity. Both the sill and the blairmorite show enrichment of Sr, K, Rb, Ba, Th, Ta, Nb, and Ce and depletion of Ti, Y, Yb, and Cr. Chondrite-normalized rare-earth element data for the sill and blairmorite from the Crowsnest Formation are virtually identical and show light rare-earth element enrichment.

The presence of primary analcime phenocrysts, together with amphibole as a primary hydrous phase and hydrogrossular rims on melanite, in the Rainy Ridge sill indicate crystallization from a hydrous magma. In contrast (and possibly in error), analcime in the Crowsnest volcanic suite was interpreted as alteration of leucite because no other hydrous igneous mineral was found (Goble et al., 1993).

The titanite crystallization age of ca. 102.4 ±0.5 Ma of the alkaline sills in the Clark Range is identical to the $^{40}Ar/^{39}Ar$ plateau age of ca. 102.4 ±1.0 Ma and corresponds within error to the 101.7 ±1.0 Ma age of orthoclase phenocrysts reported by Barnes (2002) from two syenite samples of the Howell Creek suite. The contemporaneous emplacement and the relative proximity are strong evidence that the alkaline sills of the Clark Range belong to the Howell Creek suite and likely represent feeders to the Crowsnest volcanic suite.

The Howell Creek plutonic suite consists of numerous small hypabyssal and intrusive bodies, mainly of trachytic-textured syenite and porphyritic trachyte, in southeastern British Columbia, approximately 45 km south-southwest of the outcrops of the Crowsnest volcanic rocks (Figure 7). The Howell Creek suite is deformed and offset by folds and thrust faults and by younger normal faults (Price, 1965; Brown and Cameron, 1998), and its original position was within 100 km to the southwest of its present position. Geochemical data from the Howell Creek suite show that it has not experienced mobilization of the alkali metals, in contrast to the ubiquitous albitization in the Crowsnest volcanics.

Alkaline igneous rocks of the Howell Creek area in southeastern British Columbia have been suggested previously to be cogenetic with the Crowsnest Formation in southwestern Alberta (Price 1959, 1962; Goble et al., 1993, 1999; Peterson et al., 1997; Barnes 2002). The Howell Creek intrusive/subvolcanic rocks and the Crowsnest volcanic rocks are highly potassic, and most are metaluminous rather than peralkaline. Assuming that the whole-rock compositions are reasonable proxies for the liquid compositions, the rocks of both the Crowsnest and Howell Creek suites could have derived from syenitic melts (Bowerman et al., 2006). According to these authors, the petrographic and geochemical (including whole-rock Sr and Nd isotope geochemistry) data from trachyandesite (latites), trachytes, and phonolites from the two areas show similar patterns

- on mantle-normalized trace-element diagrams, being enriched relative to mantle values but depleted in the high-field-strength elements Nb, Ta, and Ti relative to the large-ion lithophile elements;
- on the chondrite-normalized rare-earth element (REE) diagrams, both suites showing enriched light REE, no Eu anomaly, and flat heavy REE;
- in isotope geochemistry, characterized by low initial $^{87}Sr/^{86}Sr$ (Sr^T = 0.704–0.706) and low ε_{Nd}^T (–10 to –16 for the Howell Creek samples and –7 to –12 for the Crowsnest samples); the Howell Creek samples have lower ε_{Nd}^T and higher Sr^T than the Crowsnest samples.

The isotope and trace-element geochemistry of the Crowsnest and Howell Creek suites suggests a common petrogenetic origin; their contemporaneous emplacement is strong evidence that the two suites are genetically related.

6 Discussion and Conclusions

We have attempted to date the four types of igneous rocks known to occur in the Alberta portion of the Rocky Mountains. Although some of our analyses did not constrain the emplacement ages of the rocks, we have produced several precise radiogenic ages for rocks never dated before. Our geochronological work is integrated with the existing time constraints on the approximately 1.4 billion years of geological evolution of the western margin of the North American Craton (Laurentia).

The oldest igneous rocks are the mafic igneous rocks associated with the Belt-Purcell Supergroup. We have precisely dated the emplacement of the Yarrow Creek sill (sample DP11-28bt): this yielded a precise U-Pb baddeleyite age of 1436.2 ±1.1 Ma, within the 1.47–1.43 Ga range of well-constrained U-Pb zircon ages obtained from mafic sills elsewhere in the Belt-Purcell basin. Our new date confirms the equivalence of the mafic intrusions in the Lewis Thrust salient with those in the rest of the Belt-Purcell Supergroup across the Flathead graben that obstructs the establishment direct, mappable relationships of Clark Range sills to Moyie sills in the Purcell Mountains.

The Yarrow Creek sill was emplaced at the lowest stratigraphic level of the known mafic intrusions in the Lewis Thrust salient in the Clark Range. Carbonate platform strata below the Appekunny Formation in the Lewis Thrust salient are shallow equivalents of the Aldridge Formation basinal facies. There are no documented intrusions in these carbonates. However, mafic intrusions are widespread above the Appekunny–Grinnell boundary all the way up to the sub–middle Cambrian unconformity in the Clark Range. The Yarrow Creek sill intruded the platformal facies of the Belt-Purcell basin contemporaneously with the youngest-dated Moyie sill (1433 ±10 Ma) emplaced in the turbidites of the Prichard Formation near the rift axis. Its precise age constrains the deposition of the pre-Appekunny Purcell strata to before ca. 1436 Ma. Previously published structural and geochronological results indicate that the sills in the lower Belt-Purcell basin were emplaced over a period of about 70 million years. An approximately 10 km thick sequence of the Belt-Purcell Supergroup accumulated between 1.47 and 1.43 Ma in a rift environment punctuated by pulses of basin collapse. No time constraints exist for the uppermost ~1700 m of the Belt-Purcell stratigraphic record.

None of the zircon grains from the four Purcell sills analyzed by sensitive high-resolution ion microprobe (SHRIMP) yielded dates indicative of their emplacement age. Instead, several analyses indicate that, during its emplacement, the Purcell magma intruded through old crust and acquired Archean zircon grains. We note a Paleoarchean age (3564±15 Ma) in the Cloudy Ridge microgabbro; several Mesoarchean ages (3040, 3060 and 3030 Ma for the Cloudy Ridge, Yarrow Creek, and Pincher Ridge sills, respectively; and 2900 Ma for zircon cores in La Coulotte Peak); several Neoarchean ages between 2800 and 2700 Ma (2800 Ma for the Yarrow Creek and Cloudy Ridge sills, 2700 Ma for the Pincher Ridge sills, and ca. 2716 Ma for overgrowths in the La Coulotte sill).

Despite a rather exhaustive pursuit of datable phases, none of the three isolated dike and sill occurrences in the Miette Group yielded U-Pb–datable minerals. The $^{40}Ar/^{39}Ar$ date from the Crowfoot dike is anomalously old and geologically meaningless.

The importance of the precise U-Pb ages from the alkaline sill in the Clark Range and from the melanite garnet of the Crowsnest volcanic is threefold:

1) The U-Pb age of 102.9 ±1.1 Ma obtained from the melanite garnet of Crowsnest volcanic rocks ties the Crowsnest suite to the ca. 102.4 ±0.5 Ma trachyte sill in the Clark Range. Mineralogical and chemical similarities strongly support a genetic link between the Rainy Ridge analcime phonolite sill and the analcime phonolite and blairmorites of the mid-Cretaceous Crowsnest volcanics, as first suggested by Goble et al. (1993).
2) The U-Pb titanite crystallization age of ca. 102.4 ±0.5 Ma obtained from the largest trachyte sill in the Clark Range is identical to the $^{40}Ar/^{39}Ar$ plateau age of ca. 102.4 ±1.0 Ma and corresponds, within error, to the 101.7 ±1.0 Ma age of orthoclase phenocrysts reported by Barnes (2002) from two syenite samples of the Howell Creek suite in southeastern British Columbia. These results, and the proximity of the two sites, leave little doubt that the alkaline swarm in the Clark Range is part of the Howell Creek suite.

3) Considering the analytical error in the age of the feeder, the ca. 103 Ma age of the Crowsnest Formation appears to be limited to latest Albian (i.e., geologically younger than the 100.5 Ma age of the Albian/Cenomanian boundary).

Whole-rock elemental geochemistry for the Howell Creek intrusive and Crowsnest volcanic rocks seems to preclude typical subduction and typical rift geodynamic environments, but shows similarities to a continental setting with previously metasomatized mantle (Bowerman et al., 2006). Our new geochronological data are consistent with the petrogenetic model proposed by Bowerman et al. (2006):

I Partial melting, primarily of subcontinental lithospheric mantle that had experienced an ancient metasomatic event characterized by low Sm/Nd and Rb/Sr ratios, producing a parental magma consisting of hydrous alkaline basaltic melt

II A subsequent metasomatic event, possibly related to dehydration of the subducting Farallon Plate; the potassic character of the magmas would thus have resulted from the breakdown of potassic hydrous phases, such as phlogopite and (or) potassic amphibole

III Asthenospheric upwelling that provided the heat source for the mid-Cretaceous partial melting and the ca. 103–102 Ma emplacement of the Howell Creek intrusive and Crowsnest pyroclastic rocks

Thus, the basaltic melt ponded and crystallized at the base of the crust and then was partially melted to produce trachyandesitic to phonolitic melts (consistent with the absence of more mafic rocks in the Howell Creek and Crowsnest rocks). Fractional crystallization then produced the more evolved magmas; such crystallization occurred at high pressures, which is consistent with the presence of analcime as a primary phenocryst phase.

Derivation from a ‘syenitic magma’ and contemporaneous emplacement at ca. 103–102 Ma of the Howell Creek intrusive/subvolcanic suite and of the Clark Range swarm in concert with the Crowsnest volcanic suite are strong arguments for their genetic link. Intra- and intersuite differences in mineralogy and isotope and trace-element geochemistry between the hypabyssal and intrusive Howell Creek feeders in different areas and Crowsnest volcanic products may be explained by their derivation from a heterogeneous source region in the subcontinental lithospheric mantle.

Synchronous mid-Cretaceous tectonic loading in the thrust-and-fault belt (dated thrusts of ca. 103 Ma and ca. 97 Ma; Pană and van der Pluijm, 2015) was accompanied by the major Cenomanian Blackstone transgression. The subsequent Rundle tectonic pulse (ca. 74–72 Ma; van der Pluijm et al., 2006) is responsible for the emplacement of the gigantic Lewis thrust sheet at ca. 72 Ma. In this context, the $^{40}Ar/^{39}Ar$ plateau age of 69.1 ±0.7 Ma obtained from the trachyte sill that intruded Paleozoic carbonates near Crowsnest Lake is tentatively interpreted as the Maastrichtian age of metasomatism (albitization) during the burial metamorphism and metasomatism of a mid-Cretaceous sill (Howell Creek suite), following the thrusting of the ca. 72 Ma Lewis thrust sheet.

7 References

Adair, R.N. (1986): The pyroclastic rocks of the Crowsnest Formation, Alberta; M.Sc. thesis, University of Alberta, 196 p.

Adair, R.N. and Burwash, R.A. (1996): Evidence for pyroclastic emplacement of the Crowsnest Formation, Alberta; Canadian Journal of Earth Sciences, v. 33, p. 715–728.

Aitken, J.D. (1969): Documentation of the sub-Cambrian unconformity, Rocky Mountains, Main Ranges, Alberta; Canadian Journal of Earth Sciences, v. 6, p. 193–200.

Aleinikoff, J.N., Evans, K.V., Fanning, C.M., Obradovich, J.D., Ruppel, E.T., Zia, J.A. and Steinmetz, J.C. (1996): SHRIMP U-Pb ages of felsic igneous rocks, Belt Supergroup, western Montana; Geological Society of America, Abstract with Program, v. 28, no. 7, p. A376.

Aleinikoff, J.N., Evans, K.V., Hayes, T.S., Lowers, H.A. and Fanning, C.M. (2007): Age and geochemistry of multiple generations of xenotime overgrowths from the Belt Supergroup: implications for the origin of the Spar Lake red bed stratabound Cu-Ag deposit; Geological Society of America, Abstracts with Program, v. 39, no. 6, Paper 100-6, p. 275.

Aleinikoff, J.N., Lund, K. and Fanning, C.M. (2015): SHRIMP U-Pb and REE data pertaining to the origins of xenotime in Belt Supergroup rocks: evidence for ages of deposition, hydrothermal alteration, and metamorphism; Canadian Journal of Earth Sciences, v. 52, p. 722–745, doi.org/10.1139/cjes-2014-0239.

Anderson, H.E. and Davis, D.W. (1995): U-Pb geochronology of the Moyie sills, Purcell Supergroup, southeastern British Columbia: implications for the Mesoproterozoic geological history of the Purcell (Belt) basin; Canadian Journal of Earth Sciences, v. 32, p. 1180–1193.

Anderson, H.E. and Parrish, R.R. (2000): U-Pb geochronological evidence for the geological history of the Belt-Purcell Supergroup, southeastern British Columbia; *in* Geological Environment of the Sullivan deposit: British Columbia, J.W. Lydon, T. Hoy, J.F. Slack and M.E. Knapp (ed.), Geological Association of Canada, Mineral Deposits Division, Special Publication 1, p. 113–126.

Archibald, D.A., Krogh, T.E., Armstrong, R.L. and Farrar, E. (1984): Geochronology and tectonic implications of magmatism and metamorphism, southern Kootenay Arc and neighbouring regions, southeastern British Columbia, part II: mid-Cretaceous to Eocene; Canadian Journal of Earth Sciences, v. 21, no. 5, p. 567–583.

Armstrong, R.L. (1988): Mesozoic and early Cenozoic magmatic evolution of the Canadian Cordillera; *in* Processes in Continental Lithospheric Deformation, S.P. Clark Jr., B.C. Burchfiel and J. Suppe (ed.), Geological Society of America, Special Paper 218, p. 55–91.

Arnott, R.W.C. and Hein, F.J. (1986): Submarine canyon fills of the Hector Formation, Lake Louise, Alberta: Late Precambrian syn-rift deposits of the proto-Pacific miogeocline; Bulletin of Canadian Petroleum Geology, v. 34, p. 395-407.

Barnes, E.M. (2002): The Howell Creek suite, southeastern British Columbia – mid-Cretaceous alkalic intrusions and related gold deposition in the Canadian Cordillera; M.Sc. thesis, University of Alberta, 77 p.

Beaumont, C. (1981): Foreland basins; The Geophysical Journal of the Royal Astronomical Society, v. 65, p. 291–329.

Bégin, N.J., Beiersdorfer, R.E. and Ghent, E.D. (1995a): Mineralogical and geochemical analyses and economic potential of the Crowsnest volcanics; *in* Current Research 1995-E, Geological Survey of Canada, p. 11–25.

Bégin, N.J., Ghent, E.D. and Beiersdorfer, R.E. (1995b): Low-temperature metamorphism of the Crowsnest Volcanic Suite, southwestern Alberta; Canadian Mineralogist, v. 33, p. 973–983.

Berman, R.G., Sanborn-Barrie, M., Stern, R.A. and Carson, C.J. (2005): Tectonometamorphism at ca. 2.35 and 1.85 Ga in the Rae Domain, western Churchill Province, Nunavut, Canada: insights from structural, metamorphic and in situ geochronological analysis of the southwestern Committee Bay Belt; Canadian Mineralogist, v. 43, p. 409–442.

Bowerman, M, Christianson, A., Creaser, R.A. and Luth, R.W. (2006): A petrological and geochemical study of the volcanic rocks of the Crowsnest Formation, southwestern Alberta, and of the Howell Creek suite, British Columbia; Canadian Journal of Earth Sciences, v. 43, p. 1621–1637.

Brown D.A. and Cameron, R. (1998): Sediment-hosted, disseminated gold deposits related to alkalic intrusions in the Howell Creek structure, southeastern British Columbia (82G12, 7); *in* Geological Fieldwork 1998, British Columbia Ministry of Energy and Mines, Geological Survey Branch, Paper 1999-1, p. 179–192.

Burchfiel, B.C., Cowan, D.S. and Davis, G.A. (1992): Tectonic overview of the Cordilleran orogen in the western United States; *in* The Cordilleran Orogen: Conterminous U.S., B.C. Burchfiel, P.W. Lipman and M.L. Zoback (ed.), Boulder, Colorado; Geological Society of America, Geology of North America, v. G-3, p. 407–480.

Burden, E.T. and Leckie, D. (2001): Stratigraphy, sedimentology, and palynology of the Cretaceous (Albian) Beaver Mines, Mill Creek, and Crowsnest Formations (Blairmore Group) of southwestern Alberta; Geological Survey of Canada, Bulletin 563, 103 p.

Burger, R., Brady, J., Cheney, J., Harms, T., Mueller, P., Heatherington, A. and Wooden, J. (1999): Evidence for a major, Early Proterozoic orogenic event in the Tobacco Root Mountains of southwestern Montana; Geological Society of America, Abstracts with Program, v. 31, no. 7, p. A177.

Catanzaro, E.J. and Kulp, J.L. (1964): Discordant zircons from the Little Belt (Montana), Beartooth (Montana) and Santa Catalina (Arizona) Mountains; Geochimica et Cosmochimica Acta, v. 28, p. 87–124.

Chamberlain, K.R. and Doughty, P.T. (1993): Middle Proterozoic mafic magmatism, east central Idaho: implications for age of deposition of Belt Supergroup and basin subsidence models; Geological Society of America, Abstracts with Program, v. 25, p. 19.

Charlesworth, H.A.K., Weiner, J.L., Akehurst, A.J., Bielenstein, H.U., Evans, C.R., Griffiths, R.E., Remington, D.B., Stauffer, M.R. and Steiner, J. (1967): Precambrian geology of the Jasper region, Alberta; Research Council of Alberta, Bulletin 23, 74 p.

Cohen, K.M., Finney, S.C., Gibbard, P.L. and Fan, J.X. (2013): The ICS International Chronostratigraphic Chart; Episodes, v. 36, p. 199–204.

Cook, F.A. and van der Velden, A.J. (1995): Three-dimensional crustal structure of the Purcell anticlinorium in the Cordillera of southwestern Canada; Geological Society of America Bulletin, v. 107, p. 642–664.

Cressman, E.R. (1989): Reconnaissance stratigraphy of the Prichard Formation (Middle Proterozoic) and the early development of the Belt basin, Washington, Idaho, and Montana; U.S. Geological Survey Professional Paper 1490, 80 p.

Crook, K.A.W. (1962): Alkali-feldspar from the Crowsnest volcanics, Alberta; Canadian Mineralogist, v. 7, pt. 2, p. 253–263

Devlin, W.J., Brueckner, H.K. and Bond, G.C. (1988): New isotopic data and a preliminary age for volcanics near the base of the Windermere Supergroup, northeastern Washington, U.S.A.; Canadian Journal of Earth Sciences, v. 25, p. 1906–1911.

Dickinson, W.R. (2004): Evolution of the North American Cordillera; Annual Review of Earth Planetary Sciences, v. 32, p. 13–45, doi.org/10.1146/annurev.earth.32.101802.120257.

Doughty, P.T. and Chamberlain, K.R. (1996): Salmon River arch revisited: new evidence for 1370 Ma rifting near the end of deposition in the Middle Proterozoic Belt basin; Canadian Journal of Earth Sciences, v. 33, p. 1037–1052.

Doughty, P.T. and Chamberlain, K.R. (2008): Protolith age and timing of Precambrian magmatic and metamorphic events in the Priest River complex, northern Rockies; Canadian Journal of Earth Sciences, v. 45, p. 99–116.

Eaton, G.F., Criss, R.E. and Fleck, R.J. (1993): Isotopic evidence for timing and mechanism of deposition of the Pb-Ag veins of the Sunshine mine, Coeur d'Alene district Idaho (abstract); Geological Society of America, Abstracts with Program, v. 25, no. 5 , p. A33.

Eaton, G.F., Criss, R.E., Fleck, R.J., Bond, W.D., Cleland, R.W. and Wavra, C.S. (1995): Oxygen, carbon, and strontium isotope geochemistry of the Sunshine mine, Coeur d'Alene mining district, Idaho; Economic Geology, v. 90, p. 2274–2286,

Evans, K.V. and Fisher, L.B. (1986): U-Pb geochronology of two augen gneiss terranes, Idaho new data and tectonic implications; Canadian Journal of Earth Sciences, v. 23, p. 1919–1927.

Evans, K.V., Aleinikoff, J.N., Obradovich, J.O. and Fanning, C.M. (2000): SHRIMP U-Pb geochronology of volcanic rocks, Belt Supergroup, western Montana: evidence for rapid deposition of sedimentary strata; Canadian Journal of Earth Sciences, v. 37, p. 1287–1300.

Evenchick, C.A., McMechan, M.E., McNicoll, V.L. and Carr, S.D. (2007): A synthesis of the Jurassic–Cretaceous tectonic evolution of the central and southern Canadian Cordillera: exploring links across the orogen; *in* Whence the Mountains? Inquiries into the Evolution of Orogenic Systems: A Volume in Honour of Raymond A. Price, J.W., Sears, T.A. Harms and C.A. Evenchick (ed.); Geological Society of America, Special Paper 433; p. 117–145.

Evenchick, C.A., Parrish, R.R. and Gabrielse, H. (1984): Precambrian gneiss and Late Proterozoic sedimentation in north-central British Columbia; Geology, v. 12, p. 233–237.

Fenton C.L. and Fenton, M.A. (1937): Belt Series of the north; stratigraphy, sedimentation, paleontology; Geological Society of America Bulletin, v. 48, p. 1873–1969.

Ferguson, C.A. and Simony, P.S. (1991): Preliminary report on structural evolution and stratigraphic correlations, northern Cariboo Mountains, British Columbia; *in* Current Research, Part A, Geological Survey of Canada, Paper 91-1A, p. 103–110.

Fleck, R.J., Criss, R.E., Eaton, G.F., Cleland, R.W., Wavra, C.S. and Bond, W.D. (2002): Age and origin of base and precious metal veins of the Coeur d’Alene mining district, Idaho; Economic Geology, v. 97, p. 23–42.

Folinsbee, R.E., Ritchie, W.D. and Stransberry, C.F. (1957): The Crowsnest volcanics and Cretaceous geochronology; Alberta Society of Petroleum Geologists, 7th Annual Field Conference, p. 20–26.

Folinsbee, R.E., Baadsgaard, H. and Lipson, J. (1961): Potassium-argon dates of Upper Cretaceous ash falls, Alberta, Canada; New York Academy of Science, Annals, v. 91, no. 2, p. 352–363.

Foo, W.K. (1979): Evolution of transverse structures linking the Purcell Anticlinorium to the western Rocky Mountains near Canal Flats, British Columbia; M.Sc. thesis, Department of Geological Sciences, Queen's University, 146 p.

Frost, C.D. (1993): Nd isotopic evidence for the antiquity of the Wyoming province; Geology, v. 21, p. 351–354.

Frost, C.D. and Winston, D. (1987): Nd isotope systematics from coarse- and fine-grained sediments: examples from the Middle Proterozoic Belt-Purcell Supergroup; Journal of Geology, v. 95, p. 309–327.

Frost, C.D., Frost, B.R., Chamberlain, K.R. and Hulsebosch, T.P. (1998): The Late Archean history of the Wyoming province as recorded by granitic magmatism in the Wind River Range, Wyoming; Precambrian Research, v. 89, no. 3–4, p. 145–173.

Gabrielse, H. and Campbell, R.B. (1992): Upper Proterozoic Assemblages; *in* Geology of the Cordilleran Orogen in Canada, H. Gabrielse and C.J. Yorath (ed.), Geological Survey of Canada, Geology of Canada, no. 4, p. 125–150 (also Geological Society of America, The Geology of North America, v. G-2).

Gabrielse, H., Monger, J.W.H., Wheeler, J.O. and Yorath, C.J. (1992): Morphogeological belts, tectonic assemblages, and terranes; *in* Geology of the Cordilleran Orogen in Canada, H. Gabrielse and C. J. Yorath (ed.), Geological Survey of Canada, Geology of Canada, no. 4, p. 15–28 (also Geological Society of America, The Geology of North America, v. G-2).

Gehrels, G.E. and Ross, G.M. (1998): Detrital zircon geochronology of Neoproterozoic to Permian miogeoclinal strata in British Columbia and Alberta; Canadian Journal of Earth Sciences, v. 35, p. 1380–1401.

Ghazi, A.M. (1992): Geochemistry and geochronology of the igneous rocks of the Belt-Purcell Supergroup of the northern Belt Basin, Alberta and southeastern British Columbia, Canada; Ph.D. thesis, University of Nebraska, 331 p.

Giletti, R.A. (1966): Isotopic ages from southwestern Montana; Journal of Geophysical Research, v. 71, p. 4029–4036.

Glaister, R.P. (1959): Lower Cretaceous of southern Alberta and adjoining areas; American Association of Petroleum Geologists Bulletin, v. 43, p. 590–640.

Goble, R.J. (1977): The mineralogy, composition, and crystal structure of selected copper sulfides from the Belt-Purcell Supergroup, southwest Alberta, Canada; Ph.D. thesis, Queen's University, 602 p.

Goble, R.J., Ghazi, A.M. and Treves, S.B. (1999): Mineralogy and geochemistry of Proterozoic basaltic intrusions, Spionkop Ridge, southwestern Alberta; The Canadian Mineralogist, v. 37, p. 163–175.

Goble, R.J., Treves, S.B. and Ghazi, A.M. (1993): Comparison of the Rainy Ridge analcime phonolite sill and the Crowsnest volcanics, Alberta, Canada; Canadian Journal of Earth Sciences, v. 30, p. 1644–1649.

González-Álvarez, I. and Kerrich, R. (2012): Weathering intensity in the Mesoproterozoic and modern large-river systems: a comparative study in the Belt-Purcell Supergroup, Canada and USA; Precambrian Research, v. 208, p. 174–196.

Gordy, P.L. and Edwards, G. (1962): Age of the Howell Creek intrusives; Journal of the Alberta Society of Petroleum Geologists, v. 10, no. 7, p. 369–372.

Gupta, A.K. and Fyfe, W.S. (1975): Leucite survival: the alteration to analcime; Canadian Mineralogist, v. 13, p. 361–363.

Harris, D.W. (1985): Crustal structure of northwestern Montana; M.Sc. thesis, University of Montana, 63 p.

Harrison, J.E. (1972): Precambrian Belt basin of the northwestern United States, its geometry, sedimentation, and copper occurrences; Geological Society of America Bulletin, v. 83, p. 1215–1240.

Harrison, J.E., Cressman, E.R. and Whipple, J.W. (1992): Geologic and structure maps of the Kalispell 1X2 Quadrangle, Montana, Alberta and British Columbia; United States Geological Survey, Map I-2267.

Harrison, J.E., Griggs, A.B. and Wells, J.D. (1974): Tectonic features of the Precambrian Belt basin and their influence on post-Belt structures; United States Geological Survey, Professional Paper 866, 15 p.

Heaman, L.M., Erdmer, P. and Owen, J.V. (2002): U-Pb geochronologic constraints on the crustal evolution of the Long Range Inlier, Newfoundland; Canadian Journal of Earth Sciences, v. 39, p. 845–865.

Hein, F.J. and McMechan, M.E. (1994): Proterozoic and lower Cambrian Strata of the Western Canada Sedimentary Basin; *in* Geological Atlas of the Western Canada Sedimentary Basin, G.D. Mossop and I. Shetsen (comp.), Canada, Canadian Society of Petroleum Geologists, Calgary, Alberta and Alberta Research Council, Edmonton, Alberta, p. 57–67.

Hoffman, J., Hower, J. and Aronson, J.L. (1976): Radiometric dating of time of thrusting in the disturbed belt of Montana; Geology, v. 4, no. 1, p. 16–20, doi:10.1130/0091-7613(1976)4<16:RDOTOT>2.0.CO;2.

Hoffman, P.F. (1988): Belt basin: a landlocked remnant ocean basin? (analogous to the South Caspian and Black Seas); Geological Society of America, Abstracts with Program, v. 20, p. A50.

Hofmann, H.J., Mountjoy, E.W. and Teitz, M.W. (1985): Ediacaran fossils from the Miette Group, Rocky Mountains, British Columbia, Canada; Geology, v. 13, p. 819–821.

Houston, R.S., Erslev, E.A., Frost, C.D., Karlstrom, K.E., Page, N.J., Zientek, M.L., Reed, J.C., Jr., Snyder, G.L., Worl, R.G., Bryant, B., Reynolds, M.W. and Peterman, Z. (1993): The Wyoming province; *in* Precambrian Conterminous U.S., J.C. Reed Jr., M.E. Bickford, R.S. Houston, P.K. Link, D.W. Rankin, P.K. Sims and W.R. Van Schmus (ed.), Geological Society of America, Boulder, Colorado; Geology of North America, v. C-2, p. 121–170.

Höy, T. (1989): The age, chemistry and tectonic setting of the Middle Proterozoic Moyie sills, Purcell Supergroup, southeastern British Columbia; Canadian Journal of Earth Sciences, v. 26, p. 2305–2317.

Höy, T. (1992): Geology of the Purcell Supergroup in the Fernie west-half map area, southeastern British Columbia: British Columbia, Ministry of Energy, Mines and Petroleum Resources, Geological Survey Branch, Bulletin 84, 157 p.

Höy, T. and van der Heyden, P. (1988): Geochemistry, geochronology, and tectonic implications of two quartz monzonite intrusions, Purcell Mountains, southeastern British Columbia; Canadian Journal of Earth Sciences, v. 25, no. 1, p. 106–115.

Hunt, G.H. (1961): The Purcell eruptive rocks; Ph.D. thesis, University of Alberta, 139 p.

Hunt, G.H. (1962): Time of Purcell eruption in southeastern British Columbia and southwestern Alberta; Journal of Alberta Society of Petroleum Geology, v. 10, p. 438–442.

Karlsson, H.R. and Clayton, R.N. (1991): Analcime phenocrysts in igneous rocks: primary or secondary? – reply; American Mineralogist, v. 78, p. 230–232.

Karlstrom, K.E. and Bowring, S.A. (1993): Proterozoic orogenic history of Arizona; *in* Precambrian Conterminous U.S., J.C. Reed Jr., M.E. Bickford, R.S. Houston, P.K. Link, D.W. Rankin, P.K. Sims and W.R. Van Schmus (ed.), Geological Society of America, Boulder, Colorado; Geology of North America, v. C-2, p. 188–211.

Kidder, D.L. and Awramik, S.M. (1990): Acritarchs in lower greenschist facies argillite of the Middle Proterozoic Libby Formation, upper Belt Supergroup, Montana; Palaios, v. 5, p. 124 133.

Larson, K.P., Price, R.A. and Archibald, D.A. (2006): Tectonic implications of $^{40}Ar/^{39}Ar$ muscovite dates from the Mt. Haley stock and Lussier River stock, near Fort Steele, British Columbia; Canadian Journal of Earth Sciences, v. 43, p. 1673–1684.

Leach, D.L., Hofstra, A.H., Church, S.E., Snee, L.W., Vaughn, R.B. and Zartman, R.E. (1998): Evidence for Proterozoic and Late Cretaceous–Early Tertiary ore-forming events in the Coeur d'Alene district, Idaho and Montana; Economic Geology, v. 93, p. 347–359.

Leier, A.L. and Gehrels, G.E. (2011) Continental-scale detrital zircon provenance signatures in Lower Cretaceous strata, western North America; Geology, v. 39, no. 4, p. 399–402, doi.org/10.1130/G31762.1.

Lewis, R.S. (1996): Proterozoic granite and augen gneiss of central Idaho: a result of rifting during Belt Supergroup deposition? Geological Society of America, Abstracts with Program, v. 28, p. A376.

Li, Z.X., Bogdanova, S.V., Collins, A.S., Davidson, A., De Waele, B., Ernst, R.E., Fitzsimons, I.C.W., Fuck, R.A., Gladkochub, D.P., Jacobs, J., Karlstrom, K.E., Lu, S., Natapov, L.M., Pease, V., Pisarevsky, S.A., Thrane, K. and Vernikovsky, V. (2008): Assembly, configuration, and break-up history of Rodinia: a synthesis; Precambrian Research, v. 160, no. 1–2, p. 179–210.

Link, P.E. (1993): Middle and late Proterozoic stratified rocks of the western U.S. Cordillera, Colorado Plateau, and Basin and Range Province; Chapter 6 *in* Precambrian: Conterminous U.S., J.C. Reed, Jr., M.E. Bickford, R.S. Houston, P.K. Link, D.W. Rankin, P.K. Sims and W.R. Van Schmus (ed.), Geological Society of America, Boulder, Colorado, The Geology of North America, v. C-2, p. 463–595.

Lydon, J.W. (2007): Geology and metallogeny of the Belt-Purcell Basin; *in* Mineral Deposits of Canada: A Synthesis of Major Deposit-Types, District Metallogeny, the Evolution of Geological Provinces, and Exploration Methods, W.D. Goodfellow (ed.), Geological Association of Canada, Mineral Deposits Division, Special Publication 5, p. 581–607.

McFarlane, C.R.M. and Pattison, D.R.M. (2000): Geology of the Matthew Creek metamorphic zone, southeast British Columbia: a window into Middle Proterozoic metamorphism in the Purcell Basin; Canadian Journal of Earth Sciences, v. 37, p. 1073–1092.

McMechan, M.E. (1981): The Middle Proterozoic Purcell Supergroup in the southwestern Rocky and southeastern Purcell Mountains, British Columbia and the initiation of the Cordilleran miogeocline, southern Canada and adjacent United States; Bulletin of Canadian Petroleum Geology, v. 29, p. 583–621.

McMechan, M.E. (2015): The Neoproterozoic succession of the central Rocky Mountains, Canada; Bulletin of Canadian Petroleum Geology, v. 63, no. 3, p. 243–273.

McMechan, M.E. and Price, R.A. (1982): Superimposed low-grade metamorphism in the Mount Fisher area, southeastern British Columbia – implications for the East Kootenay orogeny; Canadian Journal of Earth Sciences, v. 19, p. 476–489.

McMechan, M.E. and Thompson, R.I. (1989): Structural style and history of the Rocky Mountain Fold and Thrust Belt; *in* Western Canada Sedimentary Basin, A Case History, B.D. Ricketts (ed.), Canadian Society of Petroleum Geologists, p. 47–72.

McMechan, M.E. and Thompson, R.I. (1992): The Rocky Mountains; *in* Geology of the Cordilleran Orogen in Canada, H. Gabrielse and C.J. Yorath (ed.), Geological Survey of Canada, Geology of Canada, no. 4, (also Geological Society of America), The Geology of North America, v. G-2, p. 635–642.

Medig, K.P.R., Thorkelson, D.J., Davis, W.J., Rainbird, R.H., Gibson H.D., Turner, E.C. and Marshall, D.D. (2014): Pinning northeastern Australia to northwestern Laurentia in the Mesoproterozoic; Precambrian Research, v. 249, p. 88–99.

Mellon, G.B. (1967): Stratigraphy and petrology of the Lower Cretaceous Blairmore and Mannville groups, Alberta Foothills and Plains; Research Council of Alberta, Bulletin 21, 270 p.

Mezger, K., Hanson, G.N. and Bohlen, S.R. (1989): U-Pb systematics of garnet: dating the growth of garnet in the Late Archean Pikwitonei granulite domain at Cauchon and Natawahunan Lakes, Manitoba, Canada; Contribution to Mineralogy and Petrology, v. 101/2, p. 136–148.

Monger, J.W.H. (1984): Cordilleran tectonics: a Canadian perspective; Bulletin of the Geological Society of France, v. XXXVI-7, p. 255–278.

Monger, J.W.H. (1989): Overview of Cordilleran geology; *in* Western Canada Sedimentary Basin, A Case History, B.D. Ricketts (ed.), Canadian Society of Petroleum Geologists, p. 9–32.

Monger, J.W.H. and Price, R.A. (2002): The Canadian Cordillera: geology and tectonic evolution; Canadian Society of Exploration Geophysicists, Recorder, February 2002, p. 17–36.

Monger, J.W.H., Price, R.A. and Tempelman-Kluit, D.J. (1982): Tectonic accretion and the origin of two major metamorphic and plutonic welts in the Canadian Cordillera; Geology, v. 10, p. 70–75, doi:10.1130/0091-7613(1982)10<70:TAATOO>2.0.CO;2.

Mountjoy, E.W. and Price, R.A. (1985): Geology, Jasper, West of Sixth Meridian, Alberta; Geological Survey of Canada, Map 1611A, scale 1:50 000.

Mudge, M.R., Erickson, R.L. and Kleinkopf, D. (1968): Reconnaissance geology, geophysics, and geochemistry of the southeastern part of the Lewis and Clark Range, Montana; United States Geological Survey, Bulletin 1252-E.

Mueller, P.A., Heatherington, A.L. Kelly, D.M., Wooden, J.L. and Mogk, D.W. (2002): Paleoproterozoic crust within the Great Falls tectonic zone: implications for the assembly of southern Laurentia; Geology, v. 30, p. 127–130.

Murphy, D.C. (1990): Stratigraphy and structure, southern Rocky Mountain Trench to the headwaters of the North Thompson River, Cariboo Mountains, British Columbia; *in* Current Research, Part E, Geological Survey of Canada, Paper 90-1E, p. 71–80.

Narbonne, G.M. and Hofmann, H.J. (1987): Ediacaran biota of the Wernecke Mountains, Yukon, Canada; Paleontology, v. 30, p. 647–676.

Norris, D.K. (1964): The Lower Cretaceous of the southeastern Canadian Cordillera; Bulletin of Canadian Petroleum Geology, v. 12, 14th Annual Field Conference Guidebook Issue (August 1964), p. 512–535.

O'Neill, J.M. (1993): The Great Falls tectonic zone, Montana-Idaho: an Early Proterozoic collisional orogen beneath and south of the Belt basin; *in* Belt Symposium III, R.B. Berg (ed.), Montana Bureau of Mines and Geology, Special Publication 112, p. 222–228.

O'Neill, J.M. and Lopez, D.L. (1985): Character and regional significance of the Great Falls tectonic zone, east-central Idaho and west-central Montana: American Association of Petroleum Geologists Bulletin, v. 69, p. 437–447.

Oxburgh, E.R. and Turcotte, D.L. (1974): Thermal gradients and regional metamorphism in overthrust terrains with special reference to the eastern Alps; Schweizerische Mineralogische und Petrographische Mitteilungen. v. 54, p. 641-662.

Pană, D.I. and Elgr, R. (2013): Geological map of the Alberta Rocky Mountains and Foothills (NTS 82G, 82H, 82J, 82O, 82N, 83B, 83C, 83D, 83F, 83E, and 83L); Energy Resources Conservation Board, ERCB/AGS Map 560, scale 1:500 000.

Pană, D.I. and van der Pluijm, B.A. (2015): Orogenic pulses in the Alberta Rocky Mountains: radiometric dating of major faults and comparison with the regional tectono-stratigraphic record; Geological Society of America Bulletin, v. 127; no. 3/4; p. 480–502, doi:10.1130/B31069.1.

Pearce, T.H. (1970): The analcite-bearing volcanic rocks of the Crowsnest Formation, Alberta; Canadian Journal of Earth Sciences, v. 7, p. 46–66.

Peterson, T.D., Currie, K.L., Ghent, E.D., Bégin, N.J. and Beiersdorfer, R.E. (1997): Petrology and economic geology of the Crowsnest volcanics, Alberta; *in* Exploring for Minerals in Alberta: Geological Survey of Canada Geoscience Contributions, Canada-Alberta Agreement on Mineral Development (1992–1995), R.W. Macqueen (ed.), Geological Survey of Canada, Bulletin 500, p. 163–184.

Pirsson, L.V. (1915): The Crowsnest volcanics; American Journal of Science, v. 39, p. 222–223.

Price, R.A. (1959): Flathead, British Columbia and Alberta; Geological Survey of Canada, Map 1-1959, scale 1: 50 000.

Price, R.A. (1962): Fernie map-area, east half, Alberta and British Columbia, 820E1/2; Geological Survey of Canada, Paper 61-24.

Price, R.A. (1964): The Precambrian Purcell system in the Rocky Mountains of southern Alberta and British Columbia; Bulletin of Canadian Petroleum Geology, v. 12, p. 399–426.

Price, R.A. (1965): Flathead map-area, British Columbia and Alberta; Geological Survey of Canada, Memoir 336.

Price, R.A. (1973): Large-scale gravitational flow of supracrustal rocks, southern Canadian Rocky Mountains; *in* Gravity and Tectonics, K.A. De Jong and R.A. Scholten (ed.), Wiley-Interscience, New York, New York, p. 491–502.

Price, R.A. (1981): The Cordilleran foreland thrust and fold belt in the southern Canadian Rocky Mountains; *in* Thrust and Nappe Tectonics, The Geological Society of London, Special Publications, v. 9, p. 427–448.

Price, R.A. (1994): Cordilleran tectonics and the evolution of the Western Canada Sedimentary Basin; *in* Geological Atlas of the Western Canada Sedimentary Basin, G.D. Mossop and I. Shetsen (comp.), Canadian Society of Petroleum Geologists, Calgary, Alberta and Alberta Research Council, Edmonton, Alberta, p. 13–24.

Price, R.A. and Mountjoy, E.W. (1978): Geology, Hector Lake (west half), West of Fifth Meridian, Alberta–British Columbia; Geological Survey of Canada, Map 1462A, scale 1:50 000.

Price, R.A. and Sears, J.W. (2001): A preliminary palinspastic map of the Mesoproterozoic Belt-Purcell Supergroup, Canada and USA: implications for the tectonic setting and structural evolution of the Purcell anticlinorium and the Sullivan deposit; *in* Geological Environment of the Sullivan Deposit: British Columbia, J.W. Lydon, T. Hoy, J.F. Slack and M.E. Knapp (ed.), Geological Association of Canada, Mineral Deposits Division, Special Publication 1, p. 61–81.

Price, R.A., Cook, D.G., Aitken, J.D. and Mountjoy, E.W. (1980): Geology, Lake Louise (east half), West of Fifth Meridian, Alberta–British Columbia; Geological Survey of Canada, Map 1482A, scale 1:50 000.

Price, R.A., Monger, J.W.H. and Roddick, J.A. (1985): Cordilleran cross-section: Calgary to Vancouver; *in* Field Guides to Geology and Mineral Deposits in the Southern Canadian Cordillera, D. Tempelman-Kluit (ed.), Geological Association of Canada, p. 3-1–3-85.

Rosenberg, P.E. and Larson, P.B. (2000): Isotope geochemistry of ankerite-bearing veins associated with the Coeur d'Alene mining district, Idaho; Economic Geology, v. 95, p. 1689–1700.

Ramos, F.C. and Rosenberg, P.E. (2012): Age and origin of quartz-carbonate veins associated with the Coeur D'Alene mining district, Idaho and western Montana: insights from isotopes and rare-earth elements; Economic Geology, v. 107, p. 1321–1339.

Reesor, J.E. (1958): Dewar Creek map-area with special emphasis on the White Creek Batholith, British Columbia; Geological Survey of Canada, Memoir 292, Map 1053A, scale 1:126 720.

Retallack, G.J., Dunn, K.L. and Saxby, J. (2013): Problematic Mesoproterozoic fossil *Horodyskia* from Glacier National Park, Montana, USA; Precambrian Research, v. 226, p. 125–142, doi:10.1016/j.precamres.2012.12.005.

Rezak, R. (1957): Stromatolites of the Belt Series in Glacier National Park and vicinity, Montana; United States Geological Survey, Professional Paper 294D, 94 p.

Ricketts, B.D. (1982): Laharic breccias from the Crowsnest Formation, southern Alberta; *in* Current Research, Part A, Geological Survey of Canada, Paper 1982-1A, p. 83–87.

Ross, C.P. (1959): Geology of Glacier National Park and the Flathead region, northwestern Montana; United States Geological Survey, Professional Paper 296, p. 1–125.

Ross, G.M. and Villeneuve, M. (2003): Provenance of the Mesoproterozoic (1.45 Ga) Belt basin (western North America): another piece in the pre-Rodinia paleogeographic puzzle; Geological Society of America Bulletin, v. 115; no. 10; p. 1191–1217.

Ross, G.M., Bloch, J.D. and Krouse, R. (1995): Neoproterozoic strata of the southern Canadian Cordillera and the isotopic evolution of seawater sulfate; Precambrian Research, v. 73, p. 71–99.

Ross, G.M., McMechan, M.E. and Hein, F.J. (1989): Proterozoic history: the birth of the miogeocline; *in* Western Canada Sedimentary Basin: A Case History; B.D. Ricketts (ed.), Canadian Society of Petroleum Geologists, p. 79–104.

Ross, G.M., Parrish R.R. and Winston, D. (1992): Provenance and U-Pb geochronology of the Mesoproterozoic Belt Supergroup (northwestern United States): implications for age of deposition and pre-Panthalassa plate reconstructions; Earth and Planetary Science Letters, v. 113, p. 57–76.

Schandl, E.S., Davis, D.W. and Gordon, M.P. (1993): The Pb-Pb age of metamorphic titanite in the chlorite-pyrite altered footwall of the Sullivan Zn-Pb SEDEX deposit, B.C., and its relationship to the ore; Geological Association of Canada, Program with Abstracts, v. 18, p. A93.

Sears, J.W. (2001): Emplacement and denudation history of the Lewis-Eldorado-Hoadley thrust slab in the northern Montana Cordillera, USA: implications for steady-state orogenic processes; American Journal of Science, v. 301, p. 359–373, doi:10.2475/ajs.301.4-5.359.

Sears, J.W. (2007): Belt-Purcell Basin: keystone of the Rocky Mountain fold-and-thrust belt, United States and Canada; *in* Whence the Mountains? Inquiries into the Evolution of Orogenic Systems: A Volume in Honor of Raymond A. Price; J.W., Sears, T.A. Harms and C.A. Evenchick (ed.), Geological Society of America, Special Paper 433; p. 147–166.

Sears, J.W. and Alt, D. (1989): Impact origin of the Belt basin; Geological Society of America, Abstracts with Program, v. 21, no. 5, p. 142.

Sears, J.W., Chamberlain, K.R. and Buckley, S.N. (1998): Structural and U-Pb geochronological evidence for 1.47 Ga rifting in the Belt Basin, western Montana; Canadian Journal of Earth Sciences, v. 35, p. 467–475.

Simony, P.S. and Aitken, J.D. (1990): The Windermere Supergroup and its tectonic context: outline and problems; *in* Late Proterozoic Glaciation, Rifting and Eustasy, as Illustrated by the Windermere Supergroup, J.D. Aitken and D.M.R. McDonough (comp.), Geological Association of Canada, Nuna Research Conference, Invermere and Valemount, British Columbia, Field Trip Guidebook, p. 1–11.

Skupinski, A. and Legun, A. (1989): Geology of alkalic rocks at Twentynine Mile Creek, Flathead River area, southeastern British Columbia; *in* Exploration in British Columbia 1988, British Columbia Ministry of Energy, Mines and Petroleum Resources, p. B29–34.

Smith, J.Y. (1963): The Crowfoot dike; *in* Sunwapta Pass Area, F.A. Campbell (ed.), Edmonton Geological Society, 5th Annual Field Trip Guidebook, p. 65–70.

Smith, A.G. and Barnes, W.C. (1966): Correlation of and facies changes in the carbonaceous, calcareous, and dolomitic formations of the Precambrian Belt-Purcell Supergroup; Geological Society of America Bulletin, v. 77, p. 1399–1426.

Stott, D.F. (1963): The Cretaceous Alberta Group and equivalent rocks, Rocky Mountain foothills, Alberta; Geological Survey of Canada, Memoir 317, p. 22–292.

Taylor, D. and MacKenzie, W.S. (1975): A contribution to the pseudoleucite problem; Contributions to Mineralogy and Petrology, v. 49, p. 321–333.

Thompson, I., Glombick, P., Erdmer, P., Heaman, L.M. and Lemieux, Y. (2006): Evolution of the ancestral Pacific margin, southern Canadian Cordillera: insights from new geologic maps; *in* Paleozoic Evolution and Metallogeny of Pericratonic Terranes at the Ancient Pacific Margin of

North America, Canadian and Alaskan Cordillera, M. Colpron and J. Nelson, J. (ed.), Geological Association of Canada, Special Paper 45, p. 433–481.

van der Pluijm, B.A., Vrolijk, P.J., Pevear, D.R., Hall, C.M. and Solum, J. (2006): Fault dating in the Canadian Rocky Mountains: evidence for Late Cretaceous and early Eocene orogenic pulses; Geology, v. 34, p. 837–840, doi:10.1130/G22610.1.

van der Velden, A.J. and Cook, F.A. (1994): Displacement of the Lewis thrust sheet in southwestern Canada: new evidence from seismic reflection data; Geology, v. 22, p. 819–822.

van der Velden, A.J. and Cook, F.A. (1996): Displacement of the Lewis thrust sheet in southwestern Canada: new evidence from seismic reflection data; Geology, v. 22, p. 819–822.

van Schmus, W.R., Bickford, M.E., Anderson, J.L., Bender, E.E., Anderson, R.R., Bauer, P.W., Robertson, J.M., Bowring, S.A., Condie, K.C., Denison, R.E., Gilbert, M.C., Grambling, J.A., Mawer, C.K., Shearer, C.K., Hinje, W.J., Karlstrom, K.E., Kisvarsanyi, E.B., Lidiak, E.G., Reed, J.C., Jr., Sims, P.K., Tweto, O., Silver, L.T., Treves, S.B., Williams, M.L. and Wooden, J.L. (1993): Transcontinental Proterozoic provinces; *in* Precambrian Conterminous U.S., J.C Reed, Jr., M.E. Bickford, R.S. Houston, P.K. Link, D.W. Rankin, P.K. Sims and W.R. Van Schmus, (ed.), Boulder, Colorado, Geological Society of America, Geology of North America, v. C-2, p. 171–334.

Villeneuve, M.E., Ross, G.M., Parrish, R.R., Theriault, R.J., Miles, W. and Broome, J. (1993): Geophysical subdivision, U-Pb geochronology and Sm-Nd isotope geochemistry of the crystalline basement of the Western Canada Sedimentary Basin, Alberta and northeastern British Columbia; Geological Survey of Canada Bulletin 447, 86 p.

Walter, M.R., Oehler, J.H. and Oehler, D.Z. (1976): Megascopic algae 1300 million years old from the Belt Supergroup, Montana: a reinterpretation of Walcott's *Helminthoidichnites*; Journal of Paleontology v. 50, p. 872–881.

Walter, M.R., Rulin, D. and Horodyski, R.J. (1990) Coiled Carbonaceous megafossils from the Middle Proterozoic of Jixian (Tianjin) and Montana; American Journal of Science, v. 290-A, p. 133–148.

Wanless, R.K., Loveridge, W.D. and Mursky, G. (1968): A geochronological study of the White Creek batholith, southeastern British Columbia; Canadian Journal of Earth Sciences, v. 5, no. 3, p. 375–386.

Wheeler, J.O. and McFeely, P. (1991): Tectonic assemblage map of the Canadian Cordillera and adjacent parts of the Unites States of America; Geological Survey of Canada, Map 1712A, scale 1:2 000 000.

White, B.G. (1998): Diverse tectonism in the Coeur d'Alene Mining District, Idaho; *in* Belt Symposium III 1993, R.B. Berg (ed.) Montana Bureau of Mines and Geology, Special Publication 112, p. 254–265.

White, B.G. (2000): Coeur d'Alene mining district: product of preconcentrated source deposits and tectonism within the Lewis and Clark line; *in* Geologic Field Trips, Western Montana and Adjacent Areas, S. Roberts and D. Winston (ed.); Geological Society of America, p. 95–101.

Wilkinson, J.F.G. (1977): Analcime phenocrysts in a vitrophyric analcimite – primary or secondary? Contributions to Mineralogy and Petrology, v. 64, p. 1–10.

Winston, D. (1986): Middle Proterozoic tectonics of the Belt basin, western Montana and northern Idaho; *in* Belt Supergroup: A Guide to the Proterozoic Rocks of Western Montana and Adjacent Areas, S. Roberts (ed.), Montana Bureau of Mines and Geology, Special Publication 94, p. 245–257.

Wooden, J.L., Vitaliano, C.J., Koehler, S.W. and Ragland, P.C. (1978): The late Precambrian mafic dikes of the southern Tobacco Root Mountains, Montana: geochemistry, Rb-Sr geochronology and relationship to Belt tectonics; Canadian Journal of Earth Sciences, v. 15, p. 467–479.

Zartman, R.E. and Smith, J.V. (1995): Mineralogy and U-Th-Pb ages of a uranium-bearing jasperoid vein from the Sunshine Mine, Coeur d'Alene district, Idaho; *in* Leon T. Silver 70th Birthday Symposium and Celebration, California Institute of Technology, Division of Geological and Planetary Sciences, Pasadena, California, p. 37–41.

Zartman, R.E. and Smith J.V. (2009): Mineralogy and U-Th-Pb age of a uranium-bearing jasperoid vein, Sunshine Mine, Coeur d'Alene district, Idaho, USA; Chemical Geology, v. 261, no. 1–2, p. 185–195.

Zartman, R.E., Peterman, Z.E., Obradovich, J.D., Gallego, M.D. and Bishop, D.T. (1982): Age of the Crossport C sill near Eastport, Idaho; *in* Society of Economic Geologists' Coeur d'Alene Field Conference Idaho 1977, R.R. Reid and G.A. Williams (ed.), Idaho Bureau of Mines and Geology, Bulletin 24, p. 61–69.

Zirakparvar, N.A., Vervoort, J.D., McClelland, W. and R.S. Lewis (2010): Insights into the metamorphic evolution of the Belt-Purcell basin: evidence from Lu-Hf garnet geochronology; Canadian Journal of Earth Sciences, v. 47, p. 161–179, doi.org/10.1139/E10-001.